Involvement of Activin and Follistatin in the Pathogenesis of Chronic Testicular Inflammation in Mice

Inaugural Dissertation
submitted to the
Faculty of Medicine
in partial fulfilment of the requirements
for the Ph.D. Degree
of the Faculty of Medicine
of the Justus Liebig University Giessen

as part of the joint award Ph.D. program
with Monash University

by
Nour NICOLAS
from
Sofia, Bulgaria

Giessen, 2016

From the Institute of Anatomy and Cell Biology

Director/Chairman: Prof. Dr. Eveline Baumgard-Vogt

Biology of Reproduction Group

Head: Prof. Dr. Andreas Meinhardt

Faculty of Medicine

Justus-Liebig-University of Giessen, Germany

First supervisor and committee member: Prof. Dr. Andreas Meinhardt/Dr. Monika Fijak

Second supervisor and committee member: Prof. Dr. Martin Bergmann

Committee Members:

Date of Doctoral defense: 20/03/2017

Contents

CONTENTS

ABBREVIATIONS

Acta2	Actin, alpha 2, smooth muscle, aorta
Actb	Β-actin
Acvr1	Activin A receptor, type I
Acvr2	Activin A receptor, type II
ALK	Activin-like kinase; Anaplastic lymphoma kinase
Akr1c3	Aldo-keto reductase family 1, member C3
APC	Antigen presenting cell
αSMA	Alpha smooth muscle actin
Bp	*Bordetella pertussis*
BSA	Bovine serum albumin
BTB	Blood-testis barrier
$CaCl_2$	Calcium chloride
Ccl2	Chemokine (C-C motif) ligand 2
CCL27	Chemokine (C-C motif) ligand 27
cDNA	Complementary deoxyribonucleic acid
CFA	Complete Freund's adjuvant
Col1a1	Collagen type I, alpha 1
CV	Coefficient of variation
Cyp11a1	Cytochrome P450, family 11, subfamily a, polypeptide 1
Cyp17a1	Cytochrome P450, family 17, subfamily a, polypeptide 1
Cyp21a1	Cytochrome P450, family 21, subfamily a, polypeptide 1
DAB	Diaminobenzidine
DAPI	4',6-diamidino-2-phenylindole
DHEA	Dehydroepiandrosterone
DHT	Dihyrotestosterone
DMEM/F12	Dulbecco's modified Eagle's medium/Nutrient mixture F-12
DNA	Deoxyribonucleic acid
DNase	Deoxyribonuclease
dNTPs	Deoxyribonucleoside triphosphate

EAE	Experimental autoimmune encephalomyelitis
EAEO	Experimental autoimmune epididymo-orchitis
E. Coli	Escherichia coli
EV	Empty vector group
FCS	Fetal calf serum
FSH	Follicle-stimulating hormone
FST	Follistatin
gDNA	Genomic Deoxyribonucleic acid
GnRH	Gonadotropin releasing hormone
H2-Ab1	Histocompatibility 2, Class II antigen A, beta 1
H_2SO_4	Sulfuric acid
HCl	Hydrogen Chloride
HPRT	Hypoxanthine guanine phosphoribosyl transferase
Hsd3b	Hydroxy-delta-5-steroid dehydrogenase, 3 beta- and steroid delta-isomerase cluster
HRP	Horseradish peroxidase
IDO	Indolamine-2,3-dioxygenase
IFA	Incomplete Freund's adjuvant
IL	Interleukin
i.m.	Intramuscular
IFN	Interferon
i.p.	Intraperitoneal
Inha	Inhibin alpha
Inhba	Inhibin beta A subunit
Inhbb	Inhibin beta B subunit
IFNγ	Interferon-gamma
LH	Luteinizing hormone
LPS	Lipopolysaccharide
min	Minutes
MCP-1	Monocyte chemotactic protein 1
$MgCl_2$	Magnesium chloride

MHC	Major histocompatibility complex
NaCl	Sodium chloride
NHS	N-Hydroxysuccinimide
PAMPS	Pathogen-associated molecular patterns
PBS	Phosphate Buffered Saline
PCNA	Proliferating cell nuclear antigen
PCR	Polymerase chain reaction
PFA	Paraformaldehyde
PTC	Peritubular cells
rAAV	Recombinant adenovirus-associated viral vector
RE	Relative expression
RNA	Ribonucleic acid
RNase	Ribonuclease
rpm	Revolutions per minute
RT	Room temperature
RT-PCR	Reverse transcription polymerase chain reaction
SBTI	Soybean trypsin inhibitor
SC	Sertoli cells
s.c.	Subcutaneous
sec	Seconds
Smad	Small body size (SMA, *C. elegans* protein); mothers against decapentaplegic (MAD, *Drosophila* protein)
Sox9	SRY-box 9
SRY	Sex determining region Y
Star	Steroidogenic acute regulatory protein
TBS-T	Tris buffered saline-Tween
TCR	T-cell receptor
TdT	Terminal deoxynucleotidyl transferase
TGC	Testicular germ cells
TH	Testicular homogenate
TLR	Toll-like receptors

TMB	Tetramethylbenzidine
TNF	Tumor necrosis factor
TUNEL	Terminal deoxynucleotidyl transferase (TdT) dUTP nick-end labeling
Tregs	Regulatory T cells
UV	Ultraviolet

LIST OF FIGURES AND TABLES

1. INTRODUCTION

Infertility is a growing public health issue, with the male factor accounting for almost 50% of all cases. Inflammation of the testis and the genital tract represents one of the causes of male infertility. Therefore, in the first part of this study, we examined the development and characteristics of autoimmune orchitis, a chronic testicular inflammation of the testis, in a mouse model. We also determined the expression of activin A and B, regulators of spermatogenesis and steroidogenesis under normal conditions, during the development of this disease as cytokines involved in inflammation and fibrosis. In the second part of this study, we designed a potential therapeutical model of testicular inflammation based on our results from the first part of the study.

1.1. The male reproductive tract

The male reproductive tract comprises the gonads, namely the testes where spermatogenesis and steroidogenesis take place, the rete testis and the efferent ducts that connect the testis to the epididymis, where the sperm mature and acquire their motility and capacity to fertilize the egg, and are stored. Sperm maturation is completed under the influence of the secretions of the accessory glands (seminal vesicles, prostate and bulbo-urethral glands) during ejaculation, when they are propelled into the vas deferens and ejaculated through the urethra (Meniru, 2001).

1.2. The testis: structure and function

The testes are formed from the sex cords, under regulation by the *SRY* gene, located on the Y chromosome (Koopman et al., 1990). Expression of *SRY*, and its downstream target Sox9, is restricted to somatic cell precursors that give rise to the epithelial Sertoli cell lineage (Morais da Silva et al., 1996). This process is critical in testis morphogenesis, as it is considered to regulate all subsequent events of testis development; namely, establishment of the testis vasculature, testis cord formation and differentiation of other male-specific cell lineages, peritubular myoid cells and fetal Leydig cells (Brennan and Capel, 2004). Consequently, the Sertoli cells and peritubular

myoid cells contribute to the deposition of the basal lamina that leads to the separation of the testis into two distinct compartments: (a) the seminiferous epithelium, where Sertoli cells and germ cells are sequestrated within the testis cords, and (b) the mesenchymal compartment (interstitium), where steroidogenesis occurs in Leydig cells synthesizing androgens. Later in fetal development, the testis cords undergo elongation, expansion and coiling to form the seminiferous tubules under the influence of activin A (Archambeault and Yao, 2010). Moreover, during fetal life activin A promotes Sertoli cell proliferation (Archambeault et al., 2011). During pubertal development, Sertoli cells stop proliferation (Orth, 1982), align to the basal lamina of the seminiferous tubules and form inter-Sertoli tight junctions, gap and adherens junctions, which form the blood-testis-barrier (BTB) and contribute to establishment of the immune competence of the testis (detailed description in section 1.4.) During the process of sperm production, Sertoli cells provide numerous structural and functional interactions with the developing germ cells. The Sertoli cells form unique branches from their cytoplasm that surround and provide physical support for germ cell development, spermiation (the process of sperm release) and phagocytosis of the residual germ cell cytoplasm (Lyon et al., 2015). They also express transport proteins and growth factors crucial for germ cell development, such as transferrin, inhibins, activins and many others. Due to these characteristics, Sertoli cells are referred to as "mother cells" or "nursing cells".

1.2.1. Spermato- and spermiogenesis

The testis is the site of production of the male gametes, i.e. spermatozoa, through a complex biological process known as spermatogenesis. Essential to this process is the intimate association between developing germ cells and their somatic nursing cells, the Sertoli cells, which provide structural and nutritional support to germ cells at all stages of their development. In the adult testis, germ cells at different phases of development are constantly interacting with one another (Haverfield et al., 2014). There are three main phases of spermatogenesis: mitosis, meiosis and spermiogenesis; illustrated in **Figure 1**. Adjacent to the basal lamina, the pool of spermatogonial stem cells is maintained by continual mitosis, whereas the most differentiated spermatogonia enter meiosis to produce haploid spermatocytes. These round haploid spermatids undergo a

complex series of morphological changes (without division) to form elongated spermatids. This final phase of spermatogenesis is called spermiogenesis.

During this process, the acrosome is formed from the Golgi apparatus. The acrosome is a membrane-bound lysosome-like structure containing proteins, such as acrosomal hydrolases, that enable the sperm to penetrate through the layers surrounding the oocyte during fertilization (Yanagimachi, 1994). While the acrosome is formed on one side of the nucleus of the round spermatid, the flagellum starts to form on the opposite side by pairing of the centrioles. The flagellum, or sperm tail, largely consists of a microtubular structure known as the axoneme. The mid-piece of the tail is rich in mitochondria that contribute to the motility of the sperm. Towards the end of spermiogenesis, the chromatin material becomes condensed in the sperm nucleus and most of the spermatid cytoplasm becomes sequestrated and compacted in a residual body, remaining attached to the Sertoli cells. Spermatids are then released as individual cells, or spermatozoa. The process of release of these spermatozoa into the tubular lumen is known as spermiation. Each generation of spermatogonia, spermatocytes and spermatids form specific cellular associations with other generations in a cyclic manner and these distinct associations are divided into stages, which collectively represent the cycle of the seminiferous epithelium. In mice, the cycle of the seminiferous tubules has been divided into 12 stages (I-XII) (Oakberg, 1956). Overall, the goal of spermatogenesis is to create the structures that facilitate the spermatozoa in reaching and fertilizing the oocyte.
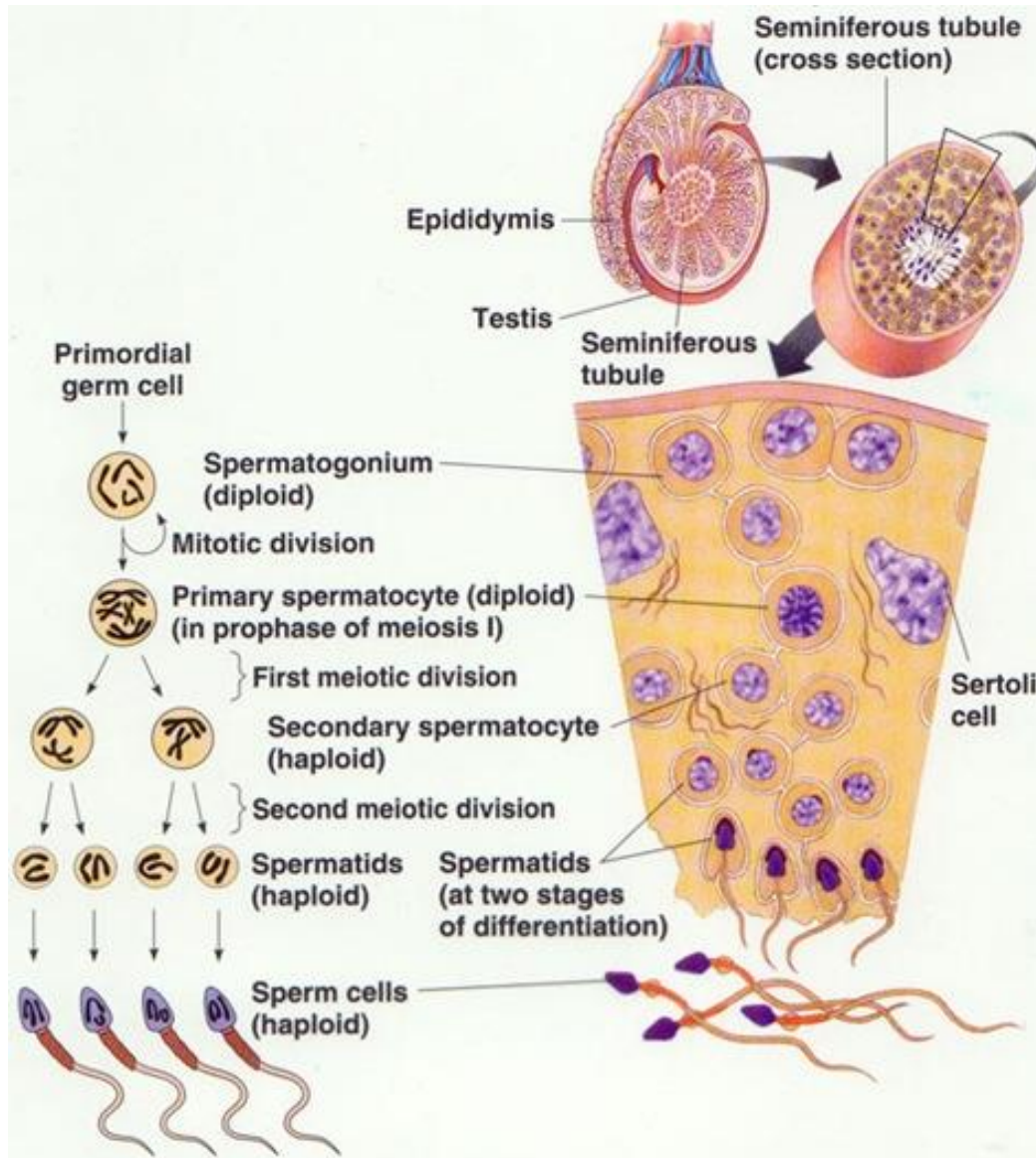
Figure 1: Spermatogenesis: the process of formation of haploid spermatozoa (sperm cells) from undifferentiated diploid spermatogonia.
This process involves a multiplication phase (mitosis), maturation and differentiation phase (meiosis) ending by spermiogenesis which is the transformation of the haploid spermatids into spermatozoa.
(from: http://www.majordifferences.com/2013/06/difference-between-spermatogenesis-and.html#.V7G8Xfl97IU)

1.2.2. Steroidogenesis and the hypothalamic-pituitary-gonadal axis

In the male, spermatogenesis is regulated by a complex interaction between circulating hormones, i.e. gonadotropins, follicle-stimulating hormone (FSH) and luteinizing hormone (LH), and locally produced factors, including activins, inhibins and the sex

steroids produced by the testis, namely androgens and estrogens (Mather et al., 1997, de Kretser et al., 2001). These hormones and factors comprise the hypothalamic-pituitary-gonadal (HPG) axis. Both LH and FSH are glycoprotein hormones produced by the anterior pituitary after stimulation by the gonadotropin releasing hormone (GnRH), which is secreted by the hypothalamus and constitutes the initial step of the HPG axis. Steroidogenesis entails processes by which cholesterol is converted to biologically-active steroid hormones within mitochondria and smooth endoplasmic reticulum (**Figure 2**). The most important steroid hormone produced by the testis is testosterone. Testosterone is part of the androgen family of hormones and is produced by Leydig cells (Zhao et al., 2016). Androgens play a critical role in the development of the male phenotype and sexual behavior. Steroidogenesis in Leydig cells is regulated mainly by LH, while Sertoli cell function is regulated by FSH and testosterone.
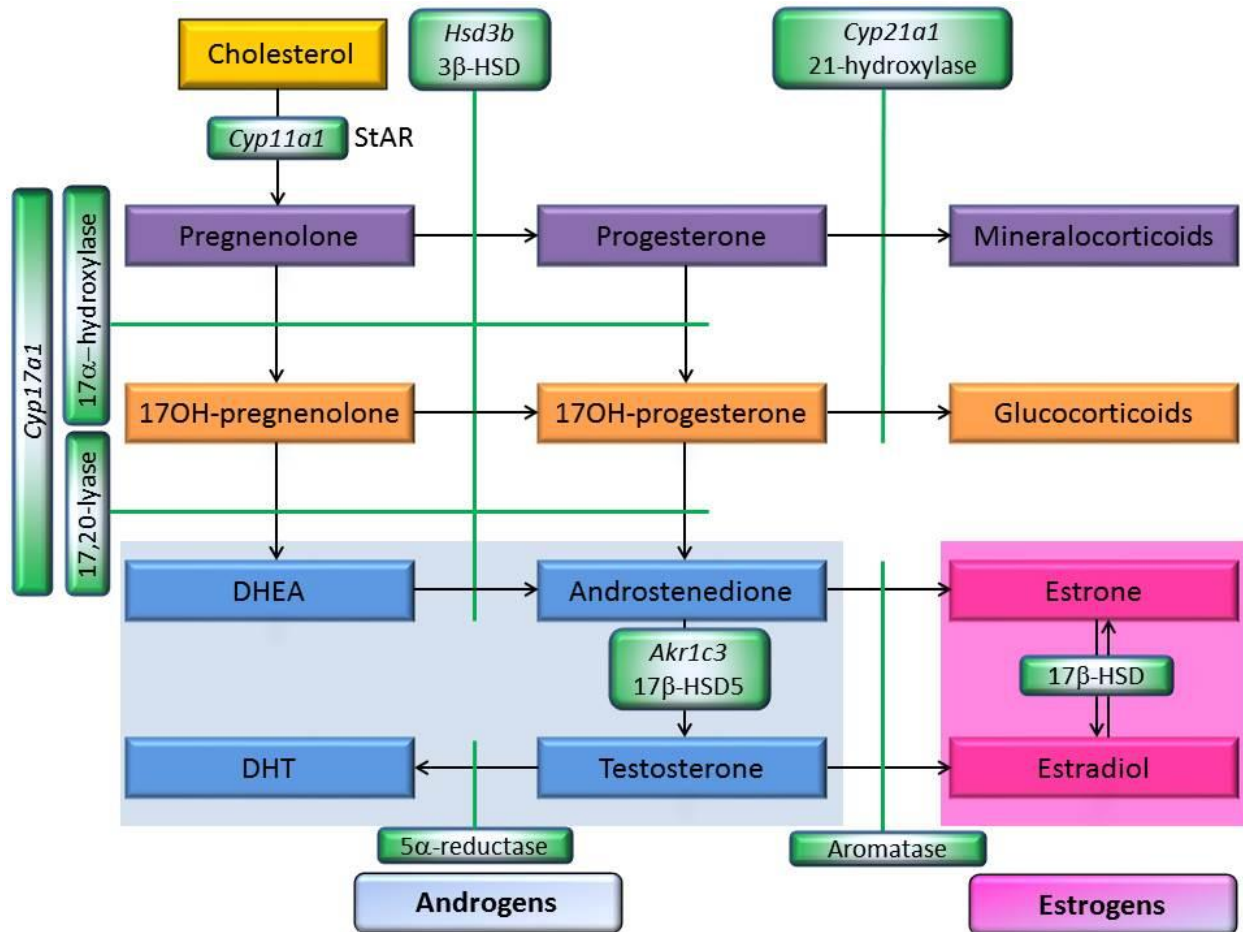
Figure 2: Steroidogenesis.
Steroids are synthesized from cholesterol through a series of enzymatic reactions. StAR (steroidogenic acute regulatory protein) regulates cholesterol transfer into the mitochondria, where it gets converted to pregnenolone by an enzyme called *Cyp11a1* (Cytochrome P450, family 11, subfamily a, polypeptide 1; side chain cleavage enzyme; desmolase). Pregnenolone is the precursor for the synthesis of all steroid hormones after it gets metabolized in the smooth endoplasmic reticulum by *Cyp17a1* (Cytochrome P450, family 17, subfamily a, polypeptide 1) and *Hsd3b1* (Hydroxy-delta-5-steroid dehydrogenase, 3 beta- and steroid delta-isomerase cluster) enzymes. Steroids are divided into five groups of molecules: progestogens, such as progesterone, mineralocorticoids, glucocorticoids, androgens, such as testosterone and estrogens such as estradiol. *Akr1c3*: Aldo-keto reductase family 1, member C3*; Cyp21a1:* Cytochrome P450, family 21, subfamily a, polypeptide 1.

Secretion of both gonadotropins by the pituitary is regulated by circulating testosterone from the testis, and FSH is also regulated by activin, inhibin and follistatin as presented in **Figure 3**. Inhibin from the testis exerts its action at the pituitary to suppress FSH secretion, whereas locally-produced activin stimulates FSH secretion, as discussed in section 1.5.
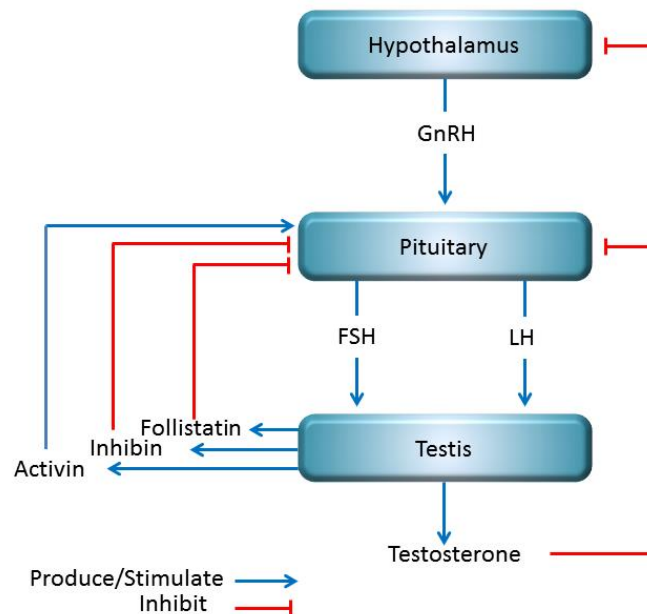
Figure 3: **The hypothalamic-pituitary-testis axis and its hormonal regulation.**
Testosterone, activin, inhibin and follistatin are produced by the testis and/or the pituitary. Gonadotropins are secreted by the pituitary after GnRH and activin stimulation, whereas inhibin and follistatin inhibit their secretion. Testosterone regulates its own secretion through negative feedback at the hypothalamus and the pituitary. GnRH: gonadotropin releasing hormone, FSH: follicle stimulating hormone, LH: luteinizing hormone.

1.3. The immune system

The immune system is the collection of cells, tissues and molecules that protect the body from pathogens. The cells of the immune system are called leukocytes and are produced in the bone marrow by a process called hematopoiesis. They circulate in the blood and lymph and their role is profoundly influenced by the tissue in which they are located at any particular time (Janeway, 2001). The protection against pathogens by the immune system can be divided into innate and adaptive immune responses (also called

antigen-specific immune response). A simplified scheme of the innate and adaptive immune responses is shown in **Figure 4**.
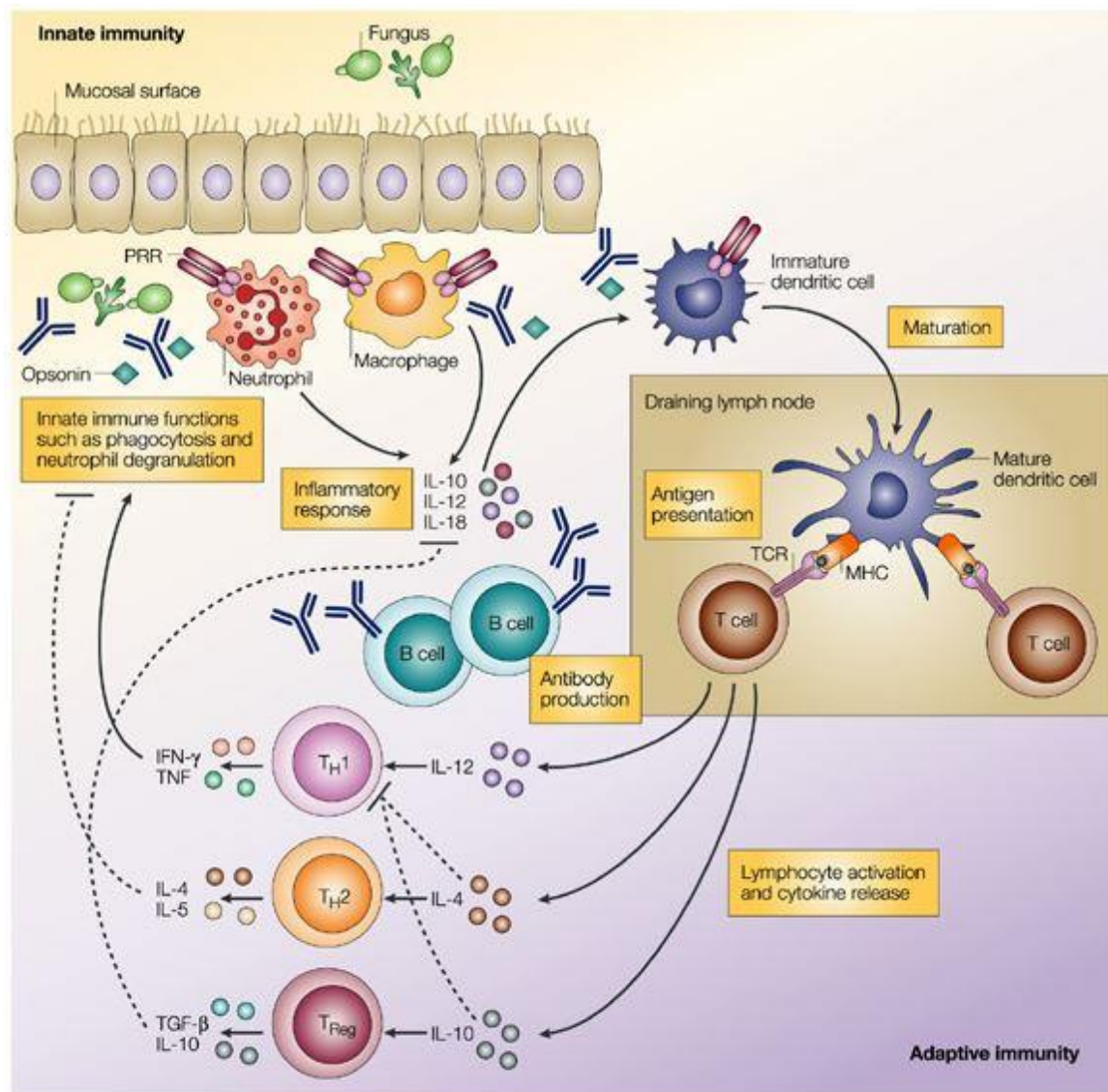
Figure 4: Simplified schematic representation of the innate and adaptive immune responses.
Effectors of innate immunity (neutrophils and macrophages) are activated after invasion of a foreign organism, such as bacteria or fungi, through biological barriers and surfaces of the body. They start secreting cytokines and contribute to the maturation of dendritic cells. Mature dendritic cells constitute the first step of adaptive immunity as they present the foreign antigens to T cells. In turn, differentiated T cells (TH1, TH2, Treg) become activated and secrete specific cytokines (tumor necrosis factor [TNF], interferon-γ [IFN-γ], interleukin-4 [IL-4], IL-5, IL-10 and IL-12) and activated B cells secrete antigen-specific antibodies and cytokines (IL-10, IL-12 and IL-18) (from (Romani, 2004).

In brief, the innate immune response is the first line of defense against many common microorganisms. Circulating monocytes rapidly differentiate into macrophages once they are out of circulation, and enter tissues. Once the pathogen enters the tissues, usually through an epithelial barrier, it gets recognized by Toll-like receptors (TLRs) or other pattern recognition receptors present on the immune cells through its pathogen-associated molecular patterns, or PAMPs, which are small molecule patterns conserved within a class of pathogens. For example, bacterial lipopolysaccharides (LPS) found on the cell membranes of bacteria are PAMPS that get recognized by TLR4 of immune cells of the innate immune system. The pathogen then gets phagocytosed by tissue resident macrophages that start secreting cytokines and chemokines in order to attract neutrophils and monocytes from the bloodstream. The cytokines and chemokines released by macrophages in response to bacterial constituents initiate the process known as inflammation. In this regard, it is important to mention here the macrophage dichotomy, which means that macrophages are divided into two different phenotypes depending on their stimuli. More specifically, tissue resident macrophages generally have an M2 anti-inflammatory phenotype, while activated macrophages possess an M1 pro-inflammatory phenotype (Martinez and Gordon, 2014). Accumulation of neutrophils and mast cells in a tissue is also a sign of inflammation. Neutrophils, together with the activated macrophages, provide rapid and effective phagocytosis of microorganisms and cell debris, while mast cells promote the development of the inflammatory response through secretion of leukotactic agents, and promote fibrosis and scarring through degranulation and secretion of tryptase (Wilgus and Wulff, 2014). The innate immune response subsequently contributes to activation of the adaptive immune response. More precisely, tissue-residing immature dendritic cells phagocytose pathogen antigens in the infected tissue, get activated and undergo maturation into antigen-presenting cells (APC) that migrate to the nearest lymph node and present the pathogenic antigen via the major histocompatibility complex (MHC) to naïve T lymphocytes, which are the main regulators of adaptive immunity. T cells recognize the antigen bound to the MHC through their T-cell receptor (TCR). This leads to recruitment, activation and proliferation of the antigen-specific lymphocytes, both T cells and B cells, which mediate adaptive immunity. B cells are activated by antigen-specific T cells and exposure to

soluble antigen, and start secreting antibodies directed against the antigen, while different T cell subtypes are activated after recognition of their antigen presented on MHC class I or II molecules. Namely, CD8+ cytotoxic T cells recognize antigens on the MHC class I present on somatic cells, and therefore play an important role in protection against viral infections and transformed tumorigenic cells, while CD4+ "helper" T cells recognize antigens on the MHC class II existing on APC, as shown in **Figure 5** (Hedger, 1997).
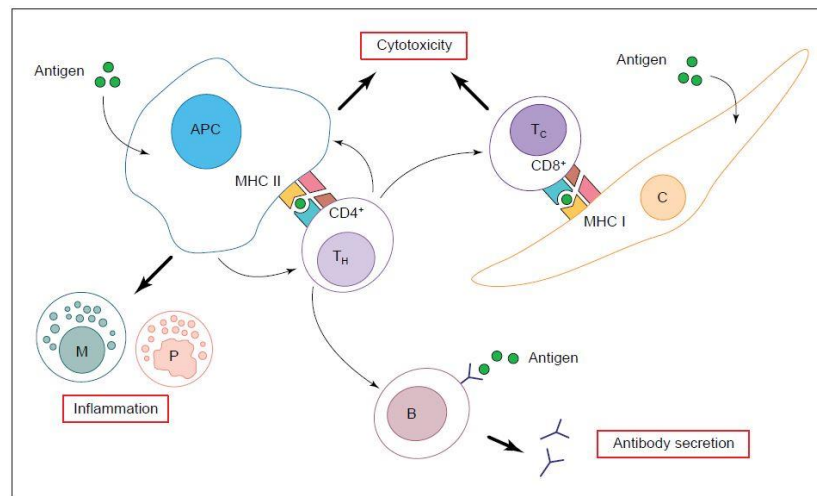
Figure 5: **Simplified schematic representation of the activation of leukocytes during the immune response.**
The immune response begins with presentation of an antigen, attached to a major histocompatibility complex (MHC) molecule, to an antigen-specific T lymphocyte (T cell). Most somatic cells (C) express MHC class I antigens on their surface, and can present antigens to CD8+ cytotoxic T cells (Tc cells). Antigen-presenting cells (APC), which express MHC class II molecules on their surface (for example, dendritic cells and activated macrophages) present antigens to CD4+ 'helper' T cells (T$_H$ cells). At the same time, antigen-specific B lymphocytes (B cells) will be primed by exposure to soluble antigen via their surface immunoglobulin receptors. Infiltrating mast cells (M) and polymorphonuclear cells (P) contribute to the inflammation. (From (Hedger, 1997).

Tolerance towards self-antigens prevents development of autoimmune diseases. It is achieved by both central and peripheral tolerance. On one hand, central tolerance is carried out when thymocytes that have a TCR with low affinity for self-peptide-MHC complexes are positively selected to further differentiate and function in adaptive immunity, while autoreactive T cell clones are deleted in the thymus. On the other hand, peripheral tolerance is accomplished by the suppressive influence of

CD4$^+$CD25$^+$FoxP3$^+$ regulatory T cells (Tregs) against specific antigens in the periphery (Burt, 2013, Xing and Hogquist, 2012).

Autoimmunity occurs when a specific adaptive immune response of the body is mounted against its own healthy cells and tissues. It is usually characterized by either production of autoantibodies against "self" antigens by self-reactive B cells or by inappropriate cytotoxic T cell responses. Diseases resulting from such an aberrant immune response are called autoimmune diseases. Well-known examples of such diseases are: rheumatoid arthritis, celiac disease, lupus, hemolytic anemia, multiple sclerosis and type 1 diabetes (Paradowska-Gorycka et al., 2016, Kalliokoski et al., 2016, Procaccini et al., 2016).

1.4.   The immune privilege of the testis

Immune privileged sites are places in the body where "non-self" or foreign antigens are tolerated without evoking inflammatory immune responses. Some of these immune privileged sites are: the brain, the eye, the placenta, and the testis (Fijak and Meinhardt, 2006, Fijak et al., 2011a, Amouzegar et al., 2016, Solomos and Rall, 2016, Ramhorst et al., 2012).

The testis was first identified as an immune-privileged organ when histo-incompatible allografts (transplantation of cells, tissue or organ to a recipient from a genetically different donor of the same species) and xenografts (transplantation of cells, tissue or organ from one species to another) transplanted into the testis were observed to survive for an indefinite period of time (Bobzien et al., 1983, Head et al., 1983).

In the testis, the germ cells are auto-antigenic as they express auto-reactive antigens (detailed in section 1.7.1). Therefore, they are protected by a special immune-privileged environment, which is supported by multiple mechanisms, including:

a) The Sertoli cells provide a physical structural support of the germ cells and a nourishing environment by secreting the necessary nutrients and growth factors for the correct development of the germ cells. Moreover, Sertoli cells form the BTB, which provides a "wall" between germ cells and molecules coming from the interstitial tissue, antibodies and immune cells.

b) The expression of immunoregulatory and immunosuppressive factors by Sertoli, peritubular, Leydig cells and testicular macrophages as described in section 1.4.2.

c) The presence of intra-testicular immune cells involved in the maintenance of the immune privilege as modulators of the immune response and maintaining the delicate equilibrium between immune privilege and inflammation by acting through local and systemic mechanisms. Cytokines produced by these immune cells play a dual role as immunosuppressors and pro-inflammatory mediators. The different testicular leukocytes and their function are described in detail in section 1.4.3.

1.4.1. The blood-testis-barrier (BTB)

The BTB, which is similar to the blood-brain-barrier or the blood-placenta-barrier, restricts or controls the entry of molecules or cells present in the circulation from the post-meiotic germ cell compartment. The BTB is formed by tight junctions located between adjacent Sertoli cells and is composed of claudin-11 and occludin, as well as gap junction proteins such as connexin 43 (McCabe et al., 2012). Inter-Sertoli cell junctions are the main contributors to separating the compartment containing the auto-reactive germ cells from circulating antibodies and immune cells, allowing the creation of a specific environment for the appropriate development of post-meiotic germ cells (Haverfield et al., 2014).

1.4.2. Immunoregulatory factors

Testicular somatic cells, namely Sertoli, peritubular and Leydig cells as well as testicular macrophages play an important role in maintaining the immune privilege by secreting immunoregulatory factors.

Sertoli cells are known to have immunosuppressive characteristics and their products can inhibit immune reactions (De Cesaris et al., 1992, Doyle et al., 2012, Dufour et al., 2005). They secrete immunomodulatory factors (e.g. indolamine-2,3-dioxygenase [IDO], galectin-1), anti-inflammatory cytokines (e.g. transforming growth factor-β1 [TGFβ1], activins) or chemokines (e.g. Chemokine (C-C motif) ligand 2 [CCL27]) (Doyle et al.,

2012, Guazzone et al., 2009, Fijak and Meinhardt, 2006, Meinhardt and Hedger, 2011, Franca et al., 2016). Immunoregulatory molecules secreted by Sertoli cells, work together to modify the immune response and induce tolerance to protect the germ cells. Recently, it has been shown that peritubular cells play also a role as a component of the BTB by preventing immune cell entry (Rebourcet et al., 2014, Smith et al., 2015). Moreover, peritubular cells have been implicated in the maintenance of the testicular immune environment (Schuppe and Meinhardt, 2005), as they produce a number of cytokines, and growth factors that maintain the immune privilege, e.g. activin A (Barakat et al., 2008). Nonetheless, the role of peritubular cells in testicular immunity and inflammatory responses remain to be elucidated.

1.4.3. Testicular leukocytes

Under normal conditions, in the adult testes of most species, leucocytes are another prominent population of cells present in the interstitial tissue aside from Leydig cells. This population consists mainly of macrophages, but also dendritic cells, lymphocytes as well as occasional subcapsular mast cells in mice and rats (Hedger, 1997).

1.4.3.1. Testicular macrophages and dendritic cells

Mononuclear phagocytes, namely macrophages, represent a substantial cellular population of the interstitial tissue compartment in the testis. In mice and rats, there is about one macrophage for every four Leydig cells in the interstitium (Niemi et al., 1986). These resident macrophages have been implicated in inducing and maintaining the immunosuppressive microenvironment of the testis, and they have been identified as predominantly anti-inflammatory M2 macrophages (Hedger, 1997, Jaiswal et al., 2014). They are specialized in providing protection for the newly formed germ cells in the testis (Schuppe and Meinhardt, 2005, Fijak and Meinhardt, 2006, Hedger, 2002). Immune cells are identified by their specific surface markers. Mouse macrophages can be identified using an antibody against F4/80, a general macrophage marker (Hume et al., 1983, Austyn and Gordon, 1981). The M1 population can be recognized by the CD86 or CD68 marker together with CD80 (as CD86 is also expressed on dendritic cells and activated T cells and CD68 is also expressed by monocytes) and M2 macrophages are

distinguished by expression of CD206 marker (Smith et al., 2016). Some macrophage surface markers provide co-stimulatory signals necessary for T cell activation. Moreover, dendritic cells, which are the most potent antigen presenting cells, have also been identified to be present in the rodent testis under normal conditions (Itoh et al., 1995, Hoek et al., 1997). Their maturation status, including expression of co-stimulatory molecules, chemokine receptors and cytokines, is a key point in the induction of peripheral immune tolerance or autoimmunity (Bhushan and Meinhardt, 2016, Bhushan et al., 2015, Rival et al., 2007, Rival et al., 2006a). In fact, it is known that, the number of macrophages is increased under inflammatory conditions in the testis and their function is altered as they produce high levels of inflammatory cytokines, such as tumor necrosis factor (TNF) and IL-6, promoting inflammation (Rival et al., 2008, Fijak et al., 2005, Fijak et al., 2011b, Rival et al., 2006b).

1.4.3.2.   T cells

In addition to testicular macrophages and dendritic cells, T cells, namely suppressor CD8+ cells, NK cells and regulatory T cells, are rarely found in the normal rat and mouse testis, (Tompkins et al., 1998, Mukasa et al., 1995). These cells are involved in regulation of the immune response by increasing cellular immune surveillance and appear to have a reduced capacity for initiating antigen-specific immune responses in the adult testis (Hedger, 1997, Dai et al., 2005, Nasr et al., 2005). The cell surface marker known as CD3 is a T cell antigen receptor complex that plays a critical role in T cell activation, signaling and antigen recognition (Miescher et al., 1989, Bluestone et al., 1987). T cells undergo maturation in the thymus and differentiate into specific mature T cell subtypes and contribute to the immune tolerance as briefly described in section 1.3. Immature T cells in the thymus are double positive CD4+CD8+ cells. They lose one of these clusters after maturation and become either CD4+ T cells, which are usually helper T Cells, or CD8+ T cells, which usually have cytotoxic activity (Parel and Chizzolini, 2004). CD4+ T cells are called regulatory T cells when they express CD25 (interleukin-2 (IL-2) receptor α-chain) and transcription factor Foxp3 (Sakaguchi et al., 2010). Helper T cells promote cellular immunity against specific antigens, while

regulatory T cells suppress cellular immunity against specific antigens. The presence of different T cells subtypes in the inflamed testis is investigated in this study.

1.5. Activin

Activins are members of the TGFβ superfamily of cytokines, which are involved in the control of inflammation, immunity and fibrosis (Hedger et al., 2011, Phillips et al., 2009). In the male, activins also play a role in spermatogenesis and steroidogenesis (Young et al., 2015).

1.5.1. Structure

Activin A is formed as a homodimer of two βA subunits of the Sertoli cell-derived heterodimeric hormone, inhibin, linked by a disulfide bond (Vale et al., 1986). A homodimer of two inhibin βB subunits forms activin B, which is believed to be less biologically active than activin A (Nakamura et al., 1992). The β subunits can also dimerize with an α subunit to form either inhibin A (αβA) or inhibin B (αβB). Inhibins are potent endogenous antagonists of activin A and B, as they block their activity by competing for the binding to the receptors or by reducing the availability of β subunits to form activin dimers (Hedger et al., 2011). **Figure 6** shows the formation of activins and inhibins from different subunits.
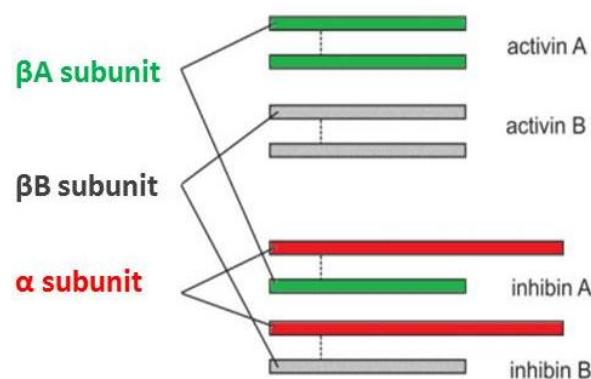
<u>Figure 6:</u> Activin and inhibin subunits.
Activin A and B are homodimers of two βA and βB subunits respectively, linked by a disulfide bond. Inhibin A and B are heterodimers formed by the βA and βB subunits respectively, and linked by a disulfide bond to an α subunit (modified from (Hedger, 2013).

1.5.2. Sites of production

Activins are widely produced by both reproductive and non-reproductive tissues, with the testis and epididymis being the main source of activin A in the male reproductive tract (Barakat et al., 2008, Winnall et al., 2013, Anderson et al., 1998). Somatic and germ cells, in both developing and adult testes, show inhibin βA and βB subunit and activin receptor subunit gene expression (de Winter et al., 1994, Anderson et al., 1998, Barakat et al., 2008, Okuma et al., 2006). The expression of activins and their receptors by different testicular cells during fetal and post-natal life is crucial for autocrine and paracrine modulation of germ cell development and Sertoli cell proliferation (Barakat et al., 2008). In mice, inhibin α, activin βA and βB subunit mRNAs were detected in Sertoli, germ and Leydig cells throughout testis development, with the βA subunit also detected in peritubular myoid cells. The α, βA and βB subunit proteins were detected in Sertoli and Leydig cells of developing and adult mouse testes (Barakat et al., 2008). Activins are also produced by immune cells, including activated monocytes and macrophages (Wang et al., 2008, Ebert et al., 2007).

1.5.3. Activin signaling

As activins are members of the TGFβ superfamily, they also act through a similar receptor-signaling pathway. The schematic signaling pathway of activins is shown in **Figure 7**. Activins bind to a type II receptor (*Acvr2a* or *Acvr2b*) on the target cell surface, which then recruits a type I receptor, activin-like kinase 4 (ALK4 or *Acvr1b*) specific for activin A, or ALK7 (*Acvr1c*) in the case of activin B. The type I receptor is a serine/threonine kinase which, upon recruitment, gets phosphorylated and leads to activation of Smad (Small body size Mothers Against Decapentaplegic) transcription factor signaling pathway (Logan et al., 2013, Wijayarathna and de Kretser, 2016). This, in turn, leads to activation or repression of Smad-regulated genes involved in proliferation, differentiation and survival of cells. Activins can also act via the mitogen-activated protein (MAP) kinase signaling pathway, which is induced during inflammatory conditions (Hedger and de Kretser, 2013).

Inhibins are endogenous antagonists of activin, as they lack receptor-activating activity, and can block activin action by competing for their receptors. More specifically, inhibins

bind to betaglycan, a type III TGFβ receptor, with high affinity, and this complex competes with activin for access to the type II receptor, but cannot recruit the type I receptors. This leads to prevention of the formation of the activin/type II receptor complex required for recruitment of type I receptor and initiation of the activin-signaling cascade (Hedger et al., 2011, Lebrun and Vale, 1997, Lewis et al., 2000).
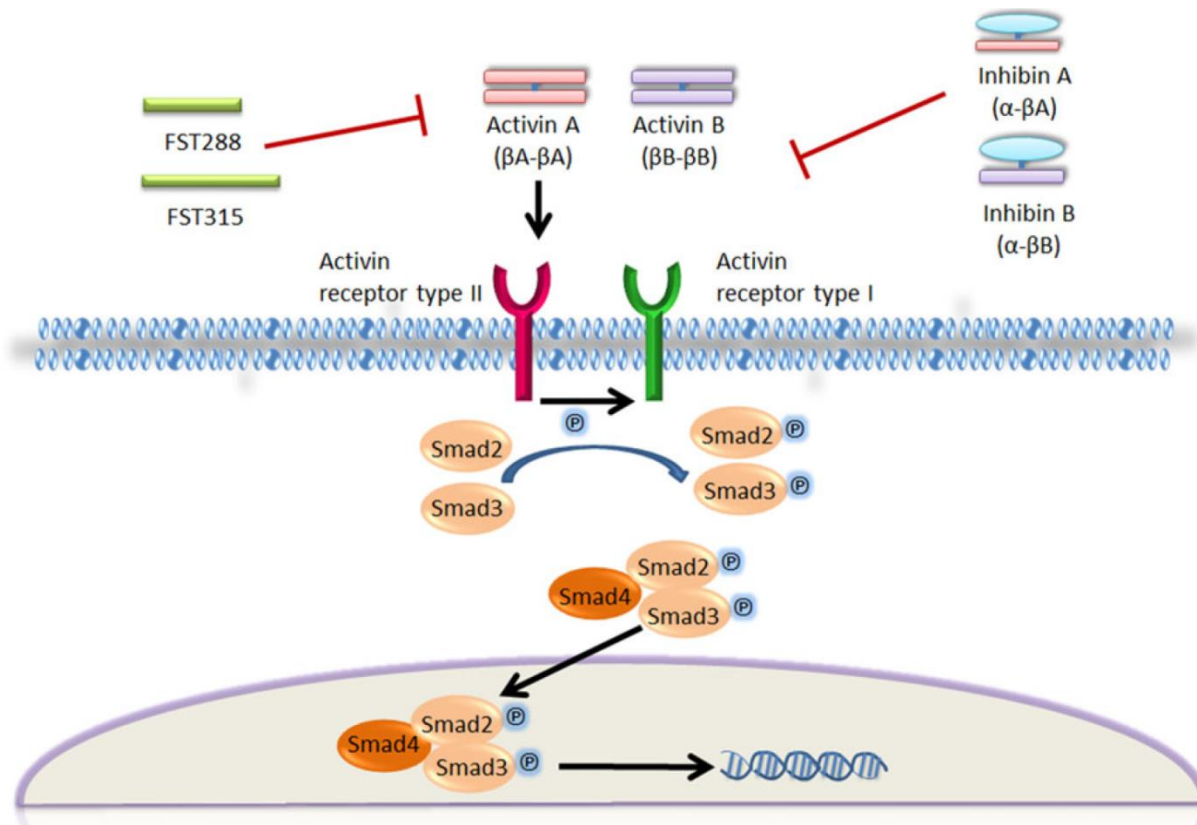
Figure 7: Activin signaling through the activin receptor signaling pathway.
Activins A and B bind to a type II receptor that recruits a type I receptor, which gets phosphorylated. Activated type I receptor leads to phosphorylation of Smad2/3, which then forms a complex with the co-activating Smad 4. The complex translocates to the nucleus, binds to the DNA at specific motifs and activates the expression of target genes. Follistatin (FST) binds to activin and limits its access to the receptor. Inhibins, together with betaglycan, bind to the type II receptor, but do not recruit the type I receptors (Wijayarathna and de Kretser, 2016).

1.5.4. Function

Activins are involved in the HPG axis by autocrine stimulation of the secretion of FSH in the pituitary (Vale et al., 1986, Ling et al., 1986). In the normal adult testis, activin A plays a crucial role in spermatogenesis and steroidogenesis (Winnall et al., 2013, Itman

et al., 2006, Young et al., 2015), as the expression of activin A in Sertoli cells is regulated in a cyclical manner during the cycle of the seminiferous epithelium. A peak of activin A secretion is observed at stage VIII of the cycle of seminiferous epithelium in the rat testis, coinciding with spermiation (Okuma et al., 2006). Activin A is a local regulator of Sertoli and germ cell development, proliferation, differentiation and function (Nicholls et al., 2012, Mithraprabhu et al., 2010, Mendis et al., 2011).

Furthermore, under normal conditions, activins play a role in immunoregulation, immune cell development and maintaining the immune privilege of the testis (Broxmeyer et al., 1988, Hedger and Winnall, 2012).

In a recent study, it has been shown that activin overexpression disrupts blood-testis-barrier function in adult mice and ablates tight junction formation in differentiated rat Sertoli cells. Moreover, activin reinitiates Sertoli cell proliferation, which start expressing juvenile markers (cytokeratin-18), while suppressing the expression of mature Sertoli cell markers (claudin-11) (Nicholls et al., 2012).

Moreover, dysregulation of activin A signaling can cause severe adverse effects. Overexpression of activin A, specifically in the testis, leads to disruption of spermatogenesis and infertility (Tanimoto et al., 1999), whereas chronic activin signaling causes reduction in testis weight and subsequent hypospermatogenesis (Nicholls et al., 2012).

Furthermore, activin A has been shown to play a role in immunity, inflammation, fibrosis and cachexia. Activin is involved in modulating progenitor immune cell development and proliferation (Broxmeyer et al., 1988). Under pathological conditions, excessive activin A is responsible for promoting fibrosis in several tissues, such as the liver, lung, and kidney (Patella et al., 2006, Hedger and de Kretser, 2013). It has been shown that, in many acute and chronic inflammatory conditions, activin A is systemically elevated (Michel et al., 2003, Leto et al., 2006, Zhang et al., 2009, Yang et al., 2015, Soler Palacios et al., 2015). Activin A is also involved in cancer development, cell proliferation and migration related to cancer cell invasiveness (Le Bras et al., 2014, Heinz et al., 2015). Activins are also the most potent negative regulators of muscle mass, as an increase of activin leads to a dramatic increase in muscle wasting leading to deleterious consequences, including increased transcription of atrophy-related ubiquitin ligases and

a severe profibrotic response (Chen et al., 2016, Chen et al., 2014). In contrast to activin A, the physiological and pathophysiological roles of activin B in the testis and in inflammation/fibrosis have received little attention.

Taken together, these data suggest that activin has important dual functions depending on its environment and activation status. Moreover, activin signaling needs to be strictly controlled in the adult testis in order to maintain Sertoli cell function, spermatogenesis, and integrity of the BTB, thus the immune privilege of the testis. Furthermore, the role of activins in regulating inflammation in the male genital tract remains to be defined.

1.6.   Follistatin

Follistatin is an endogenous antagonist of activin, which binds to it with high affinity and blocks its action by limiting its access to the receptors (Nakamura et al., 1990). Therefore, follistatin plays an important role in regulating the biological activity of activins.

1.6.1. Forms of follistatin

Two forms of follistatin, FST288 (288 amino acids) and FST315 (315 amino acids), are produced by alternative splicing of the follistatin gene, *FST* (Shimasaki et al., 1988). FST288 is predominantly the tissue bound form due to its ability to bind spontaneously to heparan sulfate containing proteoglycans on the cell surface, whereas FST315 is believed to be the main circulating form, as it only binds to heparan sulfate after it has formed a complex with activin (Lerch et al., 2007).

1.6.2. Sites of production

Both FST288 and FST315 mRNA and protein are present in the male reproductive tract, with an increasing expression gradient, being lowest in the testis and highest in the vas deferens (Winnall et al., 2013). In the rat testis, mRNA encoding follistatin is found in germ cells, Sertoli cells and endothelial cells, but not in Leydig cells, whereas the protein is localized in spermatogonia, primary spermatocytes at all stages except the zygotene stage, spermatids, endothelial cells and Leydig cells (Meinhardt et al., 1998, Wada et al., 1996, Anderson et al., 1998).

1.6.3. Function and therapeutic applications

Follistatin exerts its function indirectly by blocking activin. Follistatin is shown to induce muscle hypertrophy, because it also binds to myostatin, a TGFβ family cytokine involved in muscle development, and counters the effect of activin on muscle wasting and cachexia (Barbe et al., 2015). Currently, follistatin is being considered as a potential therapeutic target for numerous inflammatory diseases, and related fibrosis (Myllarniemi et al., 2014, Hardy et al., 2013, Datta-Mannan et al., 2013, Yaden et al., 2014, Rodino-Klapac et al., 2009).

1.7. Male infertility

Infertility is one of the major health issues worldwide. As defined by the World Health Organization (WHO): "Infertility is the inability of a sexually active, non-contracepting couple to achieve pregnancy in one year" (Rowe et al., 2000). Male factors are involved in 45 to 50% of infertile couples (Rowe et al., 2000). Many causes of male infertility remain idiopathic, but several different candidates affecting the testis have been identified (Jungwirth et al., 2012, de Kretser, 1997). The main known etiological factors can be separated into the following categories:

- untreated cryptorchidism, a common birth defect represented by the absence of one or both of the testes in the scrotum due to failure to descend from the abdominal cavity via the inguinal canal,

- testicular cancer and, more specifically, testicular germ cell neoplasia in situ (GCNIS),

- genetic disorders, such as chromosome abnormalities, with Klinefelter syndrome being the most frequent one,

- varicocele, which is an enlargement of the veins of the scrotum that drain the testis,

- immunological disorders, like infection and/or inflammation of the male genital tract, including the testis, which can be caused by trauma, viral (mumps) or bacterial (*E. coli*) infections, or sterile autoimmune inflammation. These disorders constitute 15% of men undergoing andrological examination in infertility clinics (Dohle et al., 2005, Schuppe et al., 2008, Schuppe and Bergmann, 2013).

Chronic testicular inflammation, known as epididymo-orchitis, is defined as an inflammatory lesion of one or both testes, caused by infectious or noninfectious factors (like trauma or chemical compounds), associated with a predominantly leukocytic exudate, inside and outside the seminiferous tubules, resulting in tubular damage (Dohle et al., 2005). The reasons for infertility are not always easy to diagnose and, commonly testicular inflammation might be hidden by an asymptomatic course of the disease (Schuppe et al., 2008). Therefore, it is crucial to explore and understand the mechanisms of epididymo-orchitis by using an experimental animal model. Furthermore, rodent models of the disease offer a tool to develop new therapeutic strategies.

1.7.1. Experimental autoimmune epididymo-orchitis (EAEO)

Although exceedingly rare in humans, autoimmune orchitis is a chronic inflammation of the testis and/or activation of the immune system against the male gametes and their precursor cells in the testis by production of auto-antibodies (i.e. testicular autoimmunity) (Dohle et al., 2005, Schuppe and Bergmann, 2013, Schuppe and Meinhardt, 2005, Schuppe et al., 2008).

EAEO is a model of autoimmune based testicular inflammation that has been established in several experimental rodent models in order to understand the pathomechanisms of immunological male infertility. The disease can be induced by active immunization of rats and mice with homogenized testicular tissue suspended in a suitable adjuvant. It is an established model of testicular and epididymal inflammation (Tung and Teuscher, 1995, Doncel et al., 1989), leading to histopathological changes in the testis and a humoral and cellular immune response. The model mimics several of the pathological changes seen in some forms of human infertility. From studies in a rat model of EAEO, it is known that the disease is characterized by elevated levels of FSH, LH and decreased levels of testosterone in serum (Suescun et al., 1994, Fijak et al., 2011b). It also features an increase in production of antibodies against testicular antigens, like heat shock proteins 60 (Hsp60) and 70 (Hsp70), disulfide isomerase ER-60, alpha-1-anti-trypsin, heterogeneous nuclear ribonucleoprotein H1 (hnRNP H1), sperm outer dense fiber major protein 2 (ODF-2), and phosphoglycerate kinase 1 (Fijak

et al., 2005). The disease involves increased production of inflammatory mediators, e.g. TNF, IL-6 and monocyte chemoattractant protein-1 (MCP-1) (Guazzone et al., 2003, Suescun et al., 2003, Rival et al., 2006b). Moreover, increased numbers of infiltrating immune cells in the testis and epididymis are observed (e.g. macrophages, dendritic cells, CD4+ and CD8+ T cells), leading to formation of granulomas (Jacobo et al., 2011, Rival et al., 2008, Aslani et al., 2015, Fijak et al., 2011b). These inflammatory events cause significant damage to testicular cells, leading to apoptosis of germ cells and varying degrees of cell sloughing, frequently resulting in subsequent aspermatogenesis and testicular atrophy (Aslani et al., 2015, Doncel et al., 1989). Consequently, EAEO is a useful model to study the pathogenesis of male testicular inflammation, and the physiological and immunological mechanisms that regulate its severity.

Different models of EAEO induction have been documented in the literature. In general, experimental autoimmune orchitis has been induced using three standard protocols, as described in the literature: (a) induction by immunization using testicular homogenate (TH) and adjuvants, (b) induction by adoptive transfer of activated immune cells into naïve animals, or (c) by injection with viable syngeneic testicular germ cells (TGC) in susceptible mouse strains. The first studies describing spermatogenic impairment after active immunization with TH and adjuvants in guinea pig and rats date from the 1950s (Freund et al., 1954, Freund et al., 1953). These experiments were followed by studies in BALB/c, BALB/cBy and (C57BL/6 X A/J) F1 mice, where the injection of *Bordetella pertussis* extract was first introduced together with the immunization with TH and adjuvant (Kohno et al., 1983, Tung et al., 1987, Yule et al., 1988). This "classical" method of EAEO induction leads to severe histopathological changes in the testis of immunized animals and a strong inflammatory reaction causing infertility.

The induction of EAEO by adoptive transfer of immune cells was reported in 1987 using (C57BL/6J X A/J)F1 (B6AF1) mice (Mahi-Brown et al., 1987).

Finally the induction of orchitis by injection of TGC was performed in C3H/He, A/J mice (Itoh et al., 1991). This model showed altered testicular histology and significantly elevated mRNA levels of testicular TNF and interferon-γ (IFNγ) (Terayama et al., 2011, Naito et al., 2012, Li et al., 2015).

1.8.   Hypothesis and aim of the study

Basic research about the diseases affecting male fertility in general and the testis in particular, has contributed to significant knowledge in this field, although still little is known about the mechanisms underlying many infertility disorders and, more specifically, chronic testicular inflammation and autoimmune orchitis.

Given the collected findings from the literature that activins play an important role in regulating the male reproductive tract, and is increased in a number of inflammatory and fibrotic diseases, it was **hypothesized that the activins play an important regulatory role during the course of testicular inflammation and have a stimulatory effect upon the severity of EAEO by stimulating the immunological response and associated damage.** Blocking activin activity with exogenous follistatin could inhibit the disease progression, reduce the inflammation and protect spermatogenesis.

The primary *aim of the study was to use two mouse models: (a) adult C57BL/6N mice with normal levels of activin and follistatin, and (b) adult C57BL/6J mice with elevated systemic follistatin levels, in order to investigate the susceptibilities of these mouse models to EAEO development.* The following parameters were investigated: the rate of onset, severity and duration of testicular inflammation, spermatogenic impairment, immune cell composition, fibrosis and testicular dysfunction, with a particular focus on the expression levels of activins and activin receptors, as well as inhibin and follistatin. Since activin A is a potent regulator of immune cell recruitment and activity, infiltration of these cells into the testis and their functional status was also investigated.

These studies will lead to an improved understanding of the development of EAEO and the potential involvement of activins in the process, in order to define the functional importance of activin as a target protein in autoimmune inflammation, genital tract damage and infertility, which in turn can help develop therapeutic strategies against this disease.

2. MATERIALS AND METHODS

All materials, buffers, antibodies and primers used are listed in the appendix.

2.1. Animals

In vivo study I: Adult 10-12 week old C57BL/6N male mice were purchased from Charles River Laboratories. Animal experiments were approved by the responsible committee on animal care (Regierungspraesidium Giessen GI 58/2014 — Nr. 735-GP).

In vivo study II: Adult 6 week and 10 week old C57BL/6J mice were purchased from the Monash Animal Research Platform (MARP) of Monash University, Clayton campus. Animal experiments were approved by the responsible Monash University Animal Ethics committee (MMCB/2015/16).

The use of the different mouse strains in the two studies was based on the logistics of the different laboratories where the studies were performed.

In vitro experiments: for the isolation of Sertoli and peritubular cells, immature 21 day old C57BL/6J mice were purchased from the Monash Animal Research Platform (MARP) of Monash University, Clayton campus.

All experiments involving animals were carried out in strict accordance with the recommendations of the Guide for the Care and Use of Laboratory Animals of the German law of animal welfare and with the requirements from the Australian Code for the Care and Use of Animals for Scientific Purposes, 8th Edition 2013 (the Code) and relevant Victorian legislation.

The animals were housed under specific-pathogen-free (SPF) conditions (12 hours light/dark cycle, 20~22°C), with access to water and food *ad libitum*.

Mice received analgesia in a form of Tramadol (STADApharm GmbH, Bad Vilbel, Germany) in drinking water (2.5 mg/ml) starting 24 hours before each immunization and kept for the following 3 days. During immunization, animals were anesthetized by inhalation of 3-5% isoflurane and all efforts were made to minimize suffering. For euthanasia, animals were deeply anesthetized by inhalation of 5% isoflurane and sacrificed by cervical dislocation.

2.2. Human testicular biopsies

Bouin's fixed and paraffin-embedded human testicular biopsies were provided by the Giessen Testicular Biopsy Repository, (Profs. Hans-Christian Schuppe, Martin Bergmann). The specimens were obtained from infertile men with non-obstructive azoospermia and a histological diagnosis of focal inflammatory lesions associated with disturbed spermatogenesis (Schuppe and Bergmann, 2013). Biopsies from patients with obstructive azoospermia, i.e. intact spermatogenesis without any signs of inflammation, served as control. From all men undergoing testicular biopsy, written informed consent was obtained. The study was approved by the local institutional review board (Ref.No. 100/07).

2.3. Induction of EAEO

In order to induce EAEO, adult male C57BL6/N or C57BL/6J mice aged 10-12 weeks were actively immunized with syngeneic testicular homogenate as described in a rat model (Doncel et al., 1989, Aslani et al., 2015, Fijak et al., 2011b), with some modifications. The testicular homogenate (TH) was prepared from testes collected from C57BL/6N or C57BL/6J mice. After removal of the tunica albuginea, the testes were homogenized by Potter S homogenizer in sterile 0.9% NaCl at a ratio of 1:1. Animals were immunized 2 or 3 times, every 14 days by using testicular homogenate mixed with either Freund's adjuvant or TiterMax® Gold adjuvant at a ratio 1:1, followed by *i.p.* injection of 100 ng *Bordetella pertussis* toxin (Calbiochem, Germany) in 100 μl Munõz Buffer (Kohno et al., 1983). Each animal was immunized by four *s.c.* injections with a total volume of 200 μl (50 μl per side of injection). The animals were injected on the back in the area of the shoulders and the hind limbs in the proximity of the lymph nodes. Adjuvant control animals received respective adjuvant mixed with 0.9 % NaCl instead of testicular homogenate followed by *i.p.* injection of 100 ng *B. pertussis* toxin, as above. In the current studies, the following adjuvants were used: complete Freund's adjuvant (CFA) containing killed Mycobacterium tuberculosis, incomplete Freund's adjuvant (IFA) or TiterMax® Gold adjuvant (all from Sigma-Aldrich, St Louis, USA). Age-matched untreated mice were also included.

Animals were divided into 5 groups in two separate studies (Study I and Study II) and a schematic of the treatment groups and time-line of the injections is shown below in **Figures 8** - **12**. The immunization protocol in Study II was modified according to the Monash University Animal Ethics committee requirements regarding the use of the adjuvants.

Study I:

Group I: CFA+TH+Bp toxin or CFA+NaCl+Bp toxin

0d   14d   28d 30d   50d   80d

3 immunizations   **Collection of organs**

Figure 8: **Schematic diagram illustrating the time course of immunizations for the induction of EAEO in C57BL/6N mice from study I, group I.**
Mice received three subcutaneous injections of either testicular homogenate (TH; EAEO group) or saline (adjuvant control group) mixed with CFA (complete Freund's adjuvant) at ratio 1:1, every 14 days. Each immunization was followed by an i.p. injection of Bp (*Bordetella pertussis*) toxin. Mice were killed at 30, 50 and 80 days after the first immunization and testes and blood were collected.

Group II: TiterMax Gold+TH+Bp toxin or TiterMax Gold+NaCl+Bp toxin

0d   14d   28d   50d   80d

3 immunizations   **Collection of organs**

Figure 9: **Schematic diagram illustrating the time course of immunizations for the induction of EAEO in C57BL/6N mice from study I, group II.**
Mice received three subcutaneous injections of either testicular homogenate (TH; EAEO group) or saline (adjuvant control group) mixed with TiterMax Gold adjuvant at ratio 1:1, every 14 days. Each immunization was followed by an i.p. injection of Bp (*Bordetella pertussis*) toxin. Mice were killed at 50 and 80 days after the first immunization and testes and blood were collected.

Group III: TiterMax Gold+TH+Bp toxin or TiterMax Gold+NaCl+Bp toxin

Figure 10: Schematic diagram illustrating the time course of immunizations for the induction of EAEO in C57BL/6N mice from study I, group III.
Mice received two subcutaneous injections of either testicular homogenate (TH, EAEO group) or saline (adjuvant control group) mixed with TiterMax Gold adjuvant at ratio 1:1, every 14 days. Each immunization was followed by an i.p. injection of Bp (*Bordetella pertussis*) toxin. Mice were killed at 50 and 80 days after the first immunization and testes and blood were collected.

Study II:

Group IV:
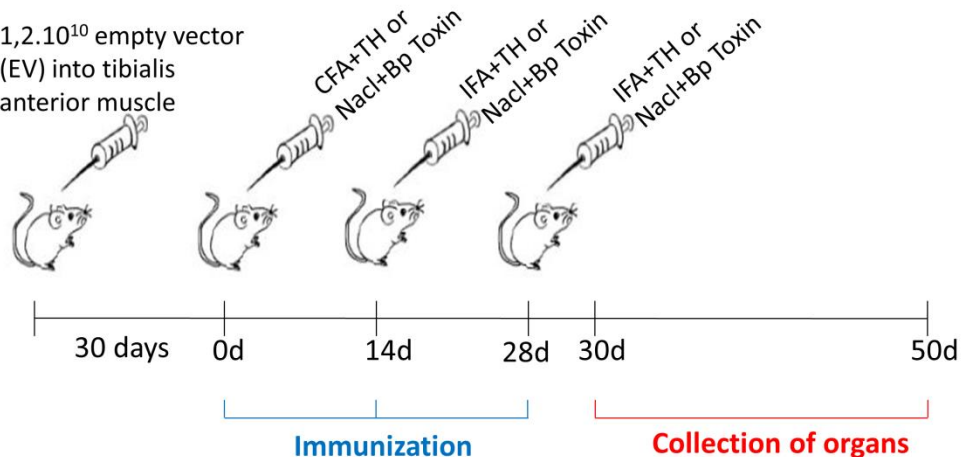
Figure 11: Schematic diagram illustrating the time course of treatments and immunizations for the induction of EAEO in C57BL/6J mice from study II, group IV.
Mice received an intramuscular injection of 1.2×10^{10} empty rAAV (recombinant adenovirus-associated viral vector) (EV group) in the tibialis anterior 30 days prior to the first immunization, then three subcutaneous injections of either testicular homogenate (TH; EAEO group) or saline (adjuvant control group) mixed with an adjuvant at ratio 1:1, every 14 days. CFA was used for the first immunization and IFA was used for the two following immunizations. Each immunization was followed by an i.p. injection of Bp (*Bordetella pertussis*) toxin. Mice were killed at 30 and 50 days after the first immunization. Testes and blood were collected.

Group V:

1,2.10^{10} FST315 vector into tibialis anterior muscle

CFA+TH or Nacl+Bp Toxin

IFA+TH or Nacl+Bp Toxin

IFA+TH or Nacl+Bp Toxin

30 days 0d 14d 28d 30d 50d

Immunization **Collection of organs**
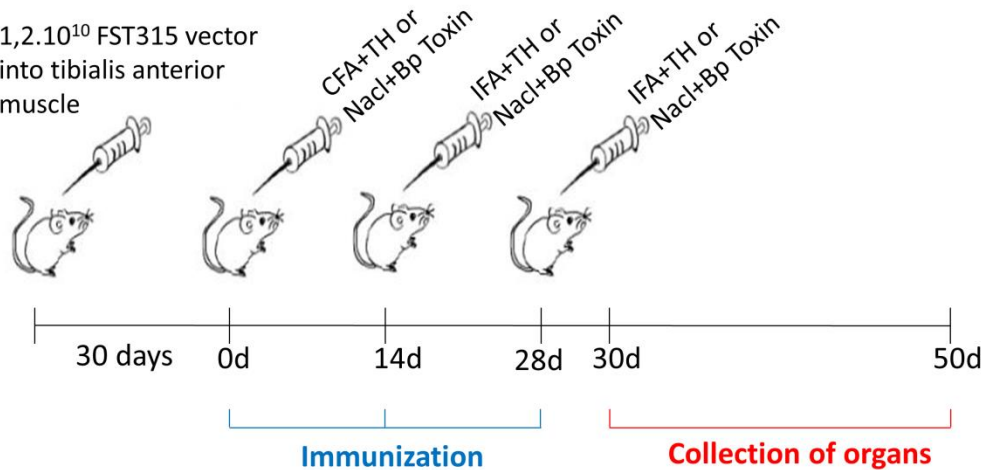
<u>**Figure 12:**</u> **Schematic diagram illustrating the time course of treatments and immunizations for the induction of EAEO in C57BL/6J mice from study II, group V.** Mice received an intramuscular injection of 1.2 x 10^{10} rAAV (recombinant adenovirus-associated viral vector) carrying a gene cassette of the circulating FST315 form of follistatin (FST group), in the tibialis anterior, 30 days prior to the first immunization, then three subcutaneous injections of either testicular homogenate (TH; EAEO group) or saline (adjuvant control group) mixed with an adjuvant at ratio 1:1, every 14 days. CFA was used for the first immunization and IFA was used for the two following immunizations. Each immunization was followed by an i.p. injection of Bp (*Bordetella pertussis*) toxin. Mice were killed at 30 and 50 days after the first immunization. Testes and blood were collected.

Experimental endpoints were selected based on previous EAEO studies described in the literature. Thirty, fifty and/or eighty days after the first immunization, animals were sacrificed and blood was collected by cardiac puncture and the testes were removed. After clotting, the blood was centrifuged at 1000 x g for 15 minutes at 4°C and sera were stored at -80°C for further analysis. The testes were weighed, and either snap-frozen in liquid nitrogen or fixed in Bouin's solution and embedded in paraffin. For flow cytometric analysis, fresh testes were used.

2.4. Therapeutical elevation of circulating follistatin levels in mice

In order to investigate the effects of increased follistatin levels during the course of testicular inflammation, follistatin was over-expressed in adult wild-type C57BL/6J mice at 6 weeks of age, by transfection of leg muscle cells with a non-replicative recombinant

adenovirus-associated viral vector (rAAV) carrying a gene cassette of the circulating FST315 form of follistatin (rAAV-FST315) (in collaboration with Dr. Justin Chen and Dr. Paul Gregorevic, Baker IDI, Melbourne, Australia). The rAAV vector consists of a sequence of DNA, therefore it is not a virus, is not replicative and is not infectious. Typically, mice transfected with these vectors express the target protein at a level proportional to the transfection dose (Hagg et al., 2016, Chen et al., 2014, Winbanks et al., 2012, Nicholls et al., 2012).

The vector carrying the follistatin gene (rAAV-FST315) and an empty control vector (rAAV) were administered to adult 6 week old male mice in study II, in the form of a single i.m. injection into the right tibialis anterior muscle at a dose of 1.2 x 10^{10} vector genomes in a volume of 5 µl saline. The vector becomes integrated into the muscle cells and acts as a production reservoir, leading to elevated levels of the protein encoded by the vector. Control mice received the viral vector with an empty expression cassette. The injections were performed under specific-pathogen-free (SPF) conditions in the Monash Medical Centre animal house by Dr. Chen. To monitor the levels of follistatin in serum from treated animals, a radioimmunoassay was performed (detailed explained in paragraph 2.11.4).

2.5. Biotin tracer study for analysis of the integrity of the blood-testis-barrier

In order to assess the integrity of the blood-testis-barrier (BTB) in mouse testes, an NHS-linked biotin tracer was perfused into the testes by immersion as follows: after collection of the testis, a hole in the tunica albuginea was performed by a needle puncture. Afterwards the testes were immersed in NHS-linked biotin (10 mg/ml in PBS with 10 mM $CaCl_2$; EZ-Link® Sulfo-NHS-LC-Biotin; Thermoscientific, Rockford, USA) and incubated for 30 min at room temperature (RT) (Meng et al., 2005, McCabe et al., 2012). As the tracer is incorporated in the testis, it binds covalently to every amine ($-NH_2$) group on every protein that it encounters. Each protein bound to the tracer is now biotinylated and can be detected by immunohistochemistry. After incubation in the tracer, the testes were removed from the solution and fixed in Bouin's solution for 5 hours and further processed for paraffin-embedding.

2.6. Paraffin-embedding

Collected testes were weighed, and then fixed in Bouin's solution for 5 hours. Bouin's solution was freshly prepared from 75 ml picric acid, 25 ml formaldehyde solution (37%) and 5 ml acetic acid. After fixation, samples were dehydrated in increasing ethanol series starting from 70% and followed by 96% and 100%. The solutions were changed several times and the organs were kept for minimum 2 hours in each concentration of ethanol. Testes were then transferred into pure benzoic acid methyl ester (>99%) (Carl Roth, Karlsruhe, Germany) for 2 hours and finally in xylol for 2 hours before transferring them into a mixture of xylol and paraffin (1:1) for one hour at 60°C. Finally, the organ samples were transferred to pre-warmed liquid paraffin at 60°C overnight. On the following day, the testes were embedded in paraffin.

2.7. Histochemistry

2.7.1. Periodic acid Schiff (PAS) staining

PAS staining is a widely used histological stain as it allows the identification of different tissue constituents such as polysaccharides (i.e. glycogen) and mycosubstances (i.e. glycoproteins and glycolipids) (Niakani et al., 2013, Ahmed and de Rooij, 2009). Bouin's fixed, paraffin-embedded testis samples were cut on the microtome (Leica, Mount Waverly, Australia) at a thickness of 5 µm and mounted on SuperFrost® Plus microscope slides (R. Langenbrinck, Emmendingen, Germany). The sections were de-paraffinized in xylene, rehydrated through a series of decreasing ethanol concentrations ranging from 100% to 50%, and rinsed in distilled water. Tissue sections were oxidized in 1% periodic acid solution (Amber Scientific, Midvale, Australia) for 5 min, rinsed and placed in Schiff's reagent (37% formalin and a few drops of Schiff's reagent [Amber Scientific, Midvale, Australia]) for 10 min. Afterwards, they were washed in tap water for 10 min and counterstained in Harris's hematoxylin solution (Sigma, St Louis, USA) for 5 min, washed again, dehydrated in a series of increasing ethanol concentrations ranging from 50% to 100% and cleared in xylene. Finally, sections were

mounted with coverslips using DPX mounting medium and glass coverslips (Merck, Darmstadt, Germany).

2.7.2. Azo-carmine and aniline blue (azan) staining

Azan staining is used for evaluation of the fibrotic response as it stains the collagen fibers blue and connective tissue red (Carvajal Monroy et al., 2015, Kikui and Miki, 1995).

5 µm thin paraffin sections were de-paraffinized in xylene, rehydrated through a series of decreasing ethanol concentrations as described previously, rinsed in distilled water and then stained in aniline alcohol (0.1% aniline oil [VWR, Fontenay-sous-Bois, France] in 90% ethanol). Afterwards, sections were dyed with preheated 0.1% azo-carmine G solution (Chroma-Gesellschaft, Stuttgart, Germany), 1% glacial acetic acid (Merck, Darmstadt, Germany), rinsed in distilled water and nuclei were differentiated in aniline alcohol. Afterwards, connective tissue was stained for 2 hours in 5% phosphotungstic acid. Sections were rinsed with distilled water and then stained for 2 hours in aniline blue-orange mixture (0.5% aniline blue [Merck], 2% Orange G [Merck], 8% glacial citric acid). Differentiation was performed in 96% ethanol until tissue constituents emerged. Subsequently the sections were dehydrated in isopropanol, treated with xylene and mounted in Eukitt Quick hardening mounting medium (Sigma-Aldrich, Saint Louis, USA) using glass coverslips.

2.7.3. Masson's trichrome staining

Masson's trichrome staining, like azan staining, is one of the most widely used trichrome stains for examining collagen deposition within tissue (Hong et al., 2016, Michel et al., 2016). 5 µm thin paraffin sections were de-paraffinized in xylene, rehydrated through a series of decreasing ethanol concentrations as described previously, rinsed and stained for 5 min in celestin blue (5% ferric ammonium sulfate [Ajax Finechem, Seven Hills, Australia], 0.5% celestin blue [Merck, Poole, UK], 14% glycerin [Ajax Finechem] in distilled water). Sections were then washed in tap water and placed in Weigert's iron hematoxylin (1% hematoxylin [Sigma] in ethanol, 1.15% ferric chloride [Ajax Finechem], 1% concentrated hydrochloric acid [Merck, Munich, Germany]

in distilled water) for 30 min, then washed again in running tap water. Tissue components were differentiated briefly in acid alcohol (0.5% concentrated hydrochloric acid [Merck] in 70% ethanol). Sections were washed in running tap water for 10 min and stained with Biebrich scarlet-acid fuchsin (0.9% Biebrich scarlet [Merck], 0.1% acid fuchsin [Merck], 1% glacial acetic acid [Merck] in distilled water) for 5 min. 5% aqueous phosphotungstic acid (Ajax Finechem) was applied for 5 min after washing briefly with distilled water and then washed again before the sections were stained in aniline blue staining solution (2.5% aniline blue [Merck], 2.5% glacial acetic acid [Merck] in distiller water) for 5 min. Finally, sections were washed in 1% aqueous acetic acid (Merck) for 3 min, dehydrated in a series of increasing ethanol concentrations ranging from 50% to 100%, cleared in xylene and cover slipped using DPX mounting medium.

2.7.4. Toluidine blue staining of mast cells

Mast cells are found in the connective tissue and their cytoplasm contains granules composed of heparin and histamine (Wernersson and Pejler, 2014). Toluidine blue stains mast cell granules red-purple (metachromatic staining) and the cytoplasm blue (orthochromatic staining). Metachromasia is the property of certain tissue elements to be stained in a different color from the dye solution, due to the pH, dye concentration and temperature of the basic dye. Blue and violet dyes will show a red color shift, and red dyes will show a yellow color shift with metachromatic tissue elements. Toluidine blue staining was performed as described previously (Iosub et al., 2006). Briefly, 5 µm thin paraffin sections were de-paraffinized in xylene, rehydrated through a series of decreasing ethanol concentrations as described above, rinsed and stained in toluidine blue working solution (10% of the 1% toluidine stock solution in 0.5% sodium chloride). Sections were then washed in distilled water, dehydrated in 95% and 100% ethanol, cleared in xylene and cover slipped using Entellan® new mounting medium (Merck, Darmstadt, Germany).

2.7.5. Proliferating cell nuclear antigen (PCNA) staining

PCNA staining is commonly used to detect cell's proliferative ability (Wu et al., 2016, Hall et al., 1990). After de-paraffinization in xylol and rehydration in 100% ethanol, 5 µm

thin paraffin testicular sections were incubated for 30 min in 4% H_2O_2 in methanol solution in order to block endogenous peroxidase activity. Sections were then placed in 96% followed by 70% ethanol and washed with distilled water and PBS. Subsequently, sections were incubated for 1 hour at RT with the mouse monoclonal anti-PCNA, IgG2aκ, Clone PC10 (M0879, Dako, Glostrup, Denmark) diluted 1:500 in PBS, washed and incubated again in undiluted HRP-labeled polymer conjugated to goat anti-rabbit immunoglobulins (K4003, Dako, Glostrup, Denmark) for 30 min at RT. Sections were then washed in PBS and the colorimetric reaction was developed by using diaminobenzidine (DAB) (DAKO, Carpinteria, CA, USA) under the microscope. Finally, slides were washed in distilled water, dehydrated in a series of increasing ethanol concentrations ranging from 70% to 100%, cleared in xylene and cover slipped using Entellan® new mounting medium.

2.7.6. TUNEL staining of apoptotic cells

Terminal deoxynucleotidyl transferase (TdT) dUTP Nick-End Labeling (TUNEL) staining is performed in order to detect apoptotic cells that undergo extensive DNA degradation during the late stages of apoptosis (Arguello et al., 1998, Carmeliet et al., 1998). The staining was performed using the ApopTag® Peroxidase *In Situ* Apoptosis Detection Kit (S7100, Merck, Darmstadt, Germany). The method is based on the ability of TdT to label blunt ends of DNA strand breaks that are detected by enzymatic labeling of free 3'-OH termini with modified nucleotides (Gavrieli et al., 1992, Schmitz et al., 1991). These new DNA ends generated upon DNA fragmentation are typically localized in morphologically identifiable nuclei and apoptotic bodies. In contrast, normal or proliferative nuclei, which have relatively low numbers of DNA 3'-OH ends, usually do not stain. The TUNEL staining detects single-stranded and double-stranded breaks associated with apoptosis (McGahon et al., 1994). The procedure was performed as follows: 5 μm thin paraffin testis sections were de-paraffinized in xylene, rehydrated in 100% and 70% ethanol and washed in PBS. Sections were covered and incubated with the provided equilibration buffer for 10 min at RT. 30 μl of the TdT enzyme was diluted in 70 μl of the reaction buffer. Sections were incubated with the TdT enzyme, while specimens for a negative control were covered with PBS only and incubated for 1 hour

at 37°C. In the meantime, the supplied stop buffer was prepared at 1:34 ratio in distilled water and pre-heated at 37°C. Sections were then immersed in the stop/wash buffer for 30 min at 37°C, washed with PBS and then quenched in 3% H_2O_2 in PBS for 15 min in the dark in order to block endogenous peroxidases. After washing twice with PBS, sections were covered with 100 µl of CAS block reagent (Life Technologies, Frederick, MD, USA) and incubated for 30 min at RT, then with 30 µl of the provided anti-dig peroxidase for 30 min at RT. Finally, sections were washed in PBS and the colorimetric reaction was developed by using DAB. Sections were counterstained with hematoxylin, washed in water and dehydrated in 70% and 100% ethanol, cleared in xylene and coverslips were mounted on slides using DPX mounting medium.

2.8.   Immunofluorescence microscopy

2.8.1. Immunofluorescence staining of testicular macrophages

A double staining of F4/80 (general macrophage marker) and CD206 (a mannose receptor, marker of M2 macrophages) was performed on 8 µm thin testis cryosections fixed in 4% paraformaldehyde (Merck, Darmstadt, Germany) for 10 min, washed in TBST (Tris buffered saline with 0.1% Tween 20) and blocked for one hour in 10% normal goat serum (Dako, Glostrup, Denmark) diluted in TBST at RT. Sections were then stained using MaxFluor^{TM} Rat on Mouse Fluorescence Detection Kit (MaxFluor 488) (MaxVision Biosciences Inc., Washington, USA) according to the manufacturer's protocol. Briefly, sections were incubated in serum-free blocker for 10 min followed by overnight incubation with rat anti-mouse F4/80 (MCA497G, AbD Serotec, Kidlington, UK) and rabbit anti-mouse CD206 (mannose receptor) (ab64693, Abcam, Cambridge, UK) antibodies diluted 1:100 and 1:200, respectively, in 1% normal goat serum diluted in TBST at 4°C. Subsequently, slides were washed and incubated in rat signal amplifier (MaxVision) for 30 min, followed by incubation with MaxFluor488 labeled linker (MaxVision) for 1 hour, and finally washed and incubated for one hour with F(ab')2-goat anti-rabbit IgG (H+L) AlexaFluor546 (A11071, Life Technologies, Carlsbad, USA) diluted 1:1000 in 1% normal goat serum diluted in TBST. Glass coverslips were

mounted on slides with ProLong Gold Antifade mountant with 4',6-diamidino-2-phenylindole (DAPI) (Life Technologies, USA).

2.8.2. Activin A immunofluorescence staining

In order to detect the localization of activin A protein in the testis, immunofluorescence staining was performed (Barakat et al., 2008). After de-paraffinization and rehydration, 5 µm thin paraffin sections were rinsed in distilled water and placed in TBST. Sections were then boiled in the microwave for antigen retrieval in citrate buffer (10 mM, pH 6.0) for 6 min at full power, left to cool down and washed in TBST.

Afterwards sections were stained following the manufacturer's instructions included in the MaxFluor^{TM} Mouse on Mouse Fluorescence Detection Kit (MaxFluor 488) (MaxVision Biosciences Inc. Washington, USA). Briefly, sections were blocked with a drop of the ready to use protein blocking solution for 10 min, then with the MaxMOMTM blocking reagent for 1 hour. Sections were washed and incubated with the E4 antibody (mouse anti-activin βA, 1.3 mg/ml, supplied by Oxford-Brooks University, Oxford, UK) diluted 1:200 in TBST and incubated overnight at 4°C. Sections were then washed and incubated with the Fluorescence Signal Enhancer for 30 min, washed again and incubated for 1 hour with the MaxFluor 488 labeled linker concentrate diluted 1:400 in the fluorescent diluent. Finally, slides were washed and mounted with coverslips and ProLong Gold Antifade mountant with DAPI.

2.8.3. Alpha smooth muscle actin (α-SMA) immunofluorescence staining

In order to detect the localization and distribution of the α-smooth muscle actin layer within the testicular peritubular cells, immunofluorescence staining was performed on testis sections. 5 µm thin paraffin sections were de-paraffinized, rehydrated, rinsed in distilled water and TBST then boiled for antigen retrieval in citrate buffer (pH 6.0) for 6 min in the microwave at full power, left to cool down and washed in TBST. Sections were then incubated overnight with the mouse monoclonal FITC conjugated anti - α smooth muscle actin antibody (F3777, Sigma, St Louis, USA) diluted 1:1000 in TBST. Subsequently, slides were washed and mounted in ProLong Gold Antifade mountant with DAPI.

2.8.4. Immunofluorescence staining for detection of the integrity of the BTB

In order to detect the integrity of the BTB and assess its disruption during the development of EAEO, immunofluorescence staining of the NHS-linked biotin tracer was performed (McCabe et al., 2012, Meng et al., 2005, Perez et al., 2012).

5 µm thin paraffin sections were de-paraffinized, rehydrated, rinsed in distilled water then incubated for 1 hour with streptavidin - AlexaFluor488 conjugate (S32354, Life Technologies, Carlsbad, USA) diluted 1:500 in PBS. Slides were then mounted in VECTASHIELD® Antifade mounting medium with DAPI (Vector, Burlingame, USA).

2.8.5. Evaluation of Sertoli and peritubular cells purity by α-SMA and Sox9 double staining

In order to estimate the purity of isolated Sertoli and peritubular cells, an immunofluorescence staining was performed using a Sertoli cell marker, Sox9 (SRY-box9) and a peritubular cell marker, αSMA. At 24 hours after the hypotonic shock treatment, cultured Sertoli and peritubular cells in 8 well slides, were washed with PBS and fixed for 10 min in 4% PFA. Afterwards, cells were permeabilized in 0.1% Triton X and blocked for one hour with 10% normal goat serum in TBST. Cells were then washed in TBST and incubated overnight with the mouse monoclonal FITC conjugated anti - α smooth muscle actin antibody (F3777, Sigma, Saint Louis, USA) diluted 1:1000 in 1% normal goat serum in TBST followed by incubation with rabbit polyclonal anti-Sox9 antibody (sc-20095, Santa Cruz Biotechnology, Dallas, USA) diluted 1:100 in 1% normal goat serum in TBST. Cells were then washed and incubated with secondary goat anti-rabbit IgG (H+L) Alexa Fluor® 594 conjugate for 1 hour in the dark. Finally, cells were washed twice with TBST, and slides were mounted with a drop of VECTASHIELD® Antifade mounting medium with DAPI.

2.9.　　Flow cytometric analysis of T cells

All incubation steps were conducted at 4°C for 30 min. Briefly, a maximum of 1 x 10^6 interstitial cells were incubated with mouse FcR blocking reagent (Miltenyi Biotech, Bergisch-Gladbach, Germany) for 10 min at 4°C. After blocking, the following monoclonal antibodies (all from Miltenyi Biotec) were used: rat anti-mouse CD45-VioBlue (clone 30F11.1), hamster anti-mouse CD3ε-APC (clone 145-2C11), rat anti-mouse CD4-APC-Vio770 (clone GK1.5), rat anti-mouse CD8a-PE-Vio770 (clone 53-6.7) and rat anti-mouse CD25-PE (clone 7D4). Background staining was evaluated using appropriate isotype controls: rat IgG2b-VioBlue, rat IgG2b-APC-Vio770, rat IgG2a-PE-Vio770, rat IgM-PE (all from Miltenyi Biotec) and hamster IgG1-APC (eBioscience, San Diego, USA). Afterwards cells were rinsed with washing buffer (PBS, 0.5% BSA, 2mM EDTA). Data were collected for 300,000 events using a MACS Quant Analyzer 10 flow cytometer (Miltenyi Biotech, Bergisch-Gladbach, Germany) and analyzed with FlowJo software version 10.0.8 (Ashland, Oregon, USA). The gating strategy is presented in **Figure 13**: After gating out debris, doublets, and nonviable cells (**Fig. 13a, b and c**), immuno-labeled CD45+ cells were gated (**Fig. 13d**). For further analysis, CD3+ cells (**Fig. 13e**) were selected within the CD45+ gate and then several T cell subtypes, namely CD4+, CD8+ as well as CD4+CD25+ and CD4+CD8+ cells were gated within CD3+ cells (**Fig. 13 f and g**). All flow cytometry measurements and analysis were performed by Dr. Monika Fijak.
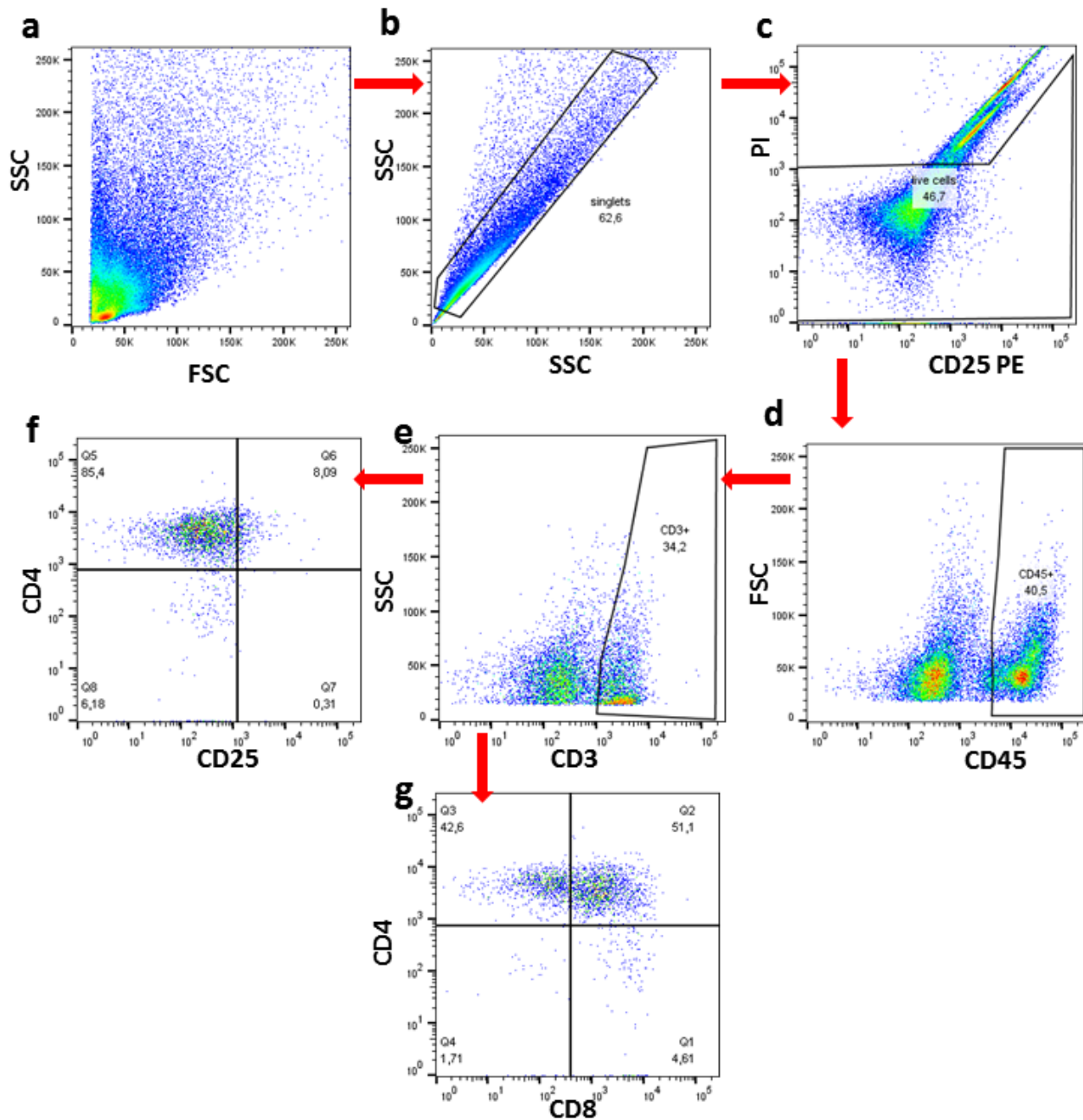
Figure 13: Representative dot plots showing the gating strategy for flow cytometric analysis of testicular immune cells.
Detected cells were plotted using a forward (FSC) and a side scatter (SSC) (**a**). Doublets (**b**), cell debris and non-viable cells (**c**) were gated out. CD45+ cells were selected from singlets and viable cells (**d**). CD3+ cells (**e**) were gated out from CD45+ cells, and then CD4+CD8-, CD4-CD8+ as well as CD4+CD25+ (**f**) and CD4+CD8+ (**g**) T cells were selected from CD3+ T cell population (courtesy of Dr. Monika Fijak).

2.10.   Analysis of gene expression by quantitative RT-PCR

2.10.1.   RNA isolation

Total RNA was isolated from frozen mouse testes using RNeasy Mini kit (Qiagen, Hilden, Germany) according to the manufacturer's instructions. Briefly, about 20 mg of each testis was cut and homogenized with 350 µl RLT Lysis buffer containing 1% β-mercaptoethanol either with a Potter S or using stainless steel beads and a tissue lyser (Qiagen, Hilden, Germany) at 40 oscillations/second for a minimum of 1 min. Lysates were collected after centrifugation for 3 min at 14,000 x g, and equal volume of 70% ethanol was added, mixed well, and then transferred to and RNeasy mini spin column. Columns were centrifuged at 10,000 x g for 1 min and washed once with RW1 wash buffer. On column DNase I treatment (Qiagen, Hilden, Germany) was performed to digest genomic DNA (gDNA) as follows: 10 µl DNase I stock solution was added to 70 µl provided RDD buffer. Afterwards, 80 µl of the DNase solution was administered to the column and incubated for 30 min at RT. Columns were washed once more with RW1 buffer followed by washing with RPE buffer containing 90% ethanol to precipitate RNA and dried by centrifugation for 2 min at 14,000 x g. RNA was eluted in 50 µl RNase free water, pre-warmed at 65°C.

RNA concentrations were quantified using the NanoDrop ND2000 (Promega, Mannheim, Germany). The yield of RNA concentration obtained was approximately 1 µg/µl with highly pure RNA based on the 260/280 and 260/230 wavelength ratios, which were around 2, indicating no contamination with proteins, phenols, carbohydrates or other compounds that might interfere.

2.10.2.   Test for presence of genomic DNA contamination

2.10.2.1. B-actin amplification

The absence of gDNA was confirmed by amplification of β-actin (*actb*) transcript using an isolated RNA sample as a template. 1 µl of RNA was added to a master mix (Promega) containing 5 µl of 5x green Go Taq Flexi buffer, 2 µl MgCl$_2$ (25 mM), 0.5 µl dNTPs (10 mM), 0.25 µl Go Taq Flexi polymerase and 0.5 µl of each β-actin forward

and reverse primer (10 pM each) in 15.25 µl distilled water. RT-PCR was run on a PCR thermocycler (PeqLab, Erlangen, Germany) for 25 cycles as shown in **Table 1**.

Table 1: RT-PCR program for β-actin amplification.

RT-PCR for β-actin check			
Cycles	**Temperature**	**PCR step**	**Time**
1	94	Denaturation	4 min
25	94	Denaturation	40 sec
	55	Annealing	40 sec
	72	Elongation	40 sec
1	72	Enzyme deactivation	10 min

2.10.2.2. DNA agarose gel electrophoresis

1.5% agarose gels were prepared by dissolving 1.5 g of agarose in 1x TAE buffer. After cooling, ethidium bromide (0.5 µg/ml) was added to the agarose solution and gels were casted. Samples were loaded next to a 100 bp DNA ladder (Promega, Mannheim, Germany). Gels were run at 110 V (2-10 V/cm gel). Finally, agarose gels were examined on a UV transilluminator and photographed using a gel jet imager 2000 documentation system (Intas, Göttingen, Germany). cDNA used as positive control showed a band with a β-actin transcript at the expected size of 156 bp. Negative control with RNase free water as template and RNA samples showed no bands.

2.10.3.   Reverse transcription (RT) by PCR

For study I (group I), reverse transcription was performed using 1 µg RNA sample mixed with 2 µl Oligo (dT) 15 Primer (Promega, Mannheim, Germany) in a total volume of 18 µl and denatured at 70°C for 10 min. RT master mix (Promega) containing 8 µl of 5x RT buffer, 2 µl of 10mM PCR nucleotide mix, 1 µl of recombinant RNasin ribonuclease inhibitor, and 18 µl of RNase free water was pre-warmed at 42°C. Finally, denatured RNA was mixed with the RT master mix before adding 1 µl of M-MLV reverse transcriptase, RNase (H-), point mutant (Promega) to each sample and reverse transcribed at 42°C for 75 min. Afterwards, the enzyme was inactivated at 72°C for 15 min and cDNA samples were store at -20°C for further use.

In study II, RNA from testes of animals from groups IV and V was reverse transcribed by using 800 ng RNA mixed with 1 µl of random hexamers (50 ng/µl) (Invitrogen, Carlsbad, USA) and 1 µl of dNTPs (10 mM) (Invitrogen), then denatured at 65°C for 5 min. RT master mix (Invitrogen) containing 2 µl of 10x RT buffer, 4 µl of $MgCl_2$ (25 mM), 2 µl of DTT (0.1 M), 1 µl of RNaseOUT (40 U/µl) and 1 µl of superscript III reverse transcriptase (200 U/µl) was prepared and added to each sample. The mixture was kept at 25°C for 10 min then heated to 50°C for 50 min, and finally for 5 min at 85°C. Afterwards, 1 µl of *E. Coli* RNase H (2 U/µl) was added to each sample and incubated at 37°C for 20 min. Finally, cDNA samples were stored at -20°C for further use.

Genomic DNA contamination of RNA samples was checked following the same procedure as for the reverse transcription, but with omitting the superscript III RT (200 U/µl) from the RT master mix and by verifying that there was no amplified PCR product for the specific gene after RT-PCR.

2.10.4.　　Quantitative RT-PCR

Quantitative RT-PCR is a technique used in order to monitor and quantify the amplification of a target gene under real time conditions by polymerase chain reaction (PCR). The quantity of the specific gene can be either an absolute number of copies or a relative amount when normalized to housekeeping genes. Fluorescent dyes (SYBR green) that intercalate with the double stranded DNA are used for the detection of the PCR products in real-time (Bustin et al., 2009).

For study I, quantitative RT-PCR was performed using CFX Touch[TM] Real-Time PCR detection system (Bio-Rad, Munich, Germany).

For the evaluation of *Inhba, Inhbb, Inha, Acvr1b, Acvr2b, Fst, Fst288 and Fst315* mRNA expression, iTaq Universal SYBR Green Supermix (Bio-Rad) was used as described in **Table 2**. QuantiTect SYBR green PCR Master Mix and QuantiTect primer assay (Qiagen) were used to evaluate *IL-6*, *IL-10*, *Ccl2* and *Tnf* mRNA expression. The reaction mix is described in **Table 2**.

For study II, the evaluation of all the above mentioned genes was performed using Power SYBR green PCR master mix (Applied Biosystems, Warrington, UK) on Fast

Real-Time PCR system (Applied Biosystems, Forest City, USA). The reaction mix is described in **Table 2**.

Table 2: Quantitative RT-PCR reaction mixes.

Real Time PCR master mixes	
Bio-Rad	
Volume	Material
10 µl	2x iTaq Universal SYBR Green Supermix
0.5 µl	Forward primer 10 pM
0.5 µl	Reverse primer 10 pM
1 µl	Template cDNA
8 µl	Rnase free water
20 µl	Final volume
Qiagen QuantiTect	
Volume	Material
10 µl	2x QuantiTect SYBR Green PCR Master Mix
2 µl	10x QuantiTect primer assay
1 µl	Fluorescein 20 nM
1 µl	Template cDNA
6 µl	Rnase free water
20 µl	Final volume
Applied Biosystems	
Volume	Material
5 µl	2x Power SYBR Green PCR master mix
0.25 µl	Forward primer 100 µM
0.25 µl	Reverse primer 100 µM
1 µl	Template cDNA
3.5 µl	Rnase free water
20 µl	Final volume

All primers used are listed in **Table 7** in the appendix. Relative gene expression was calculated using the $2^{-\Delta\Delta Ct}$ method (Livak and Schmittgen, 2001) and normalized to three housekeeping genes *(B2M* [β2-microglobulin], *HPRT* [hypoxanthine guanine phosphoribosyl transferase] and *18S rRNA*) used as internal controls for samples from study I, or normalized to two housekeeping genes (*HPRT* and *18S rRNA*) used as internal controls for samples from study II. Briefly, the $2^{-\Delta\Delta Ct}$ method is based on

calculation of ∆Ct by subtracting the Ct value of the housekeeping gene from the Ct value of the amplified gene in a sample. ∆∆Ct is then calculated by subtracting the ∆Ct value of each sample to the mean of the control samples. Finally, $2^{-\Delta\Delta Ct}$ represents the relative expression of the gene. Quantitative RT-PCR programs are described in **Table 3**.

Table 3: Quantitative RT-PCR programs.

Real Time PCR programs			
Bio-Rad			
Cycles	Temperature	PCR step	Time
1	95	Denaturation	30 sec
45	95	Denaturation	15 sec
	55	Annealing	30 sec
	72	Elongation	30 sec
Melt curve	50 to 95	Dissociation	5 sec
Qiagen QuantiTect			
Cycles	Temperature	PCR step	Time
1	95	Polymerase activation	13 min 30 sec
45	95	Denaturation	15 sec
	55	Annealing	30 sec
	72	Elongation	30 sec
Melt curve	50 to 95	Dissociation	5 sec
Applied Biosystems			
Cycles	Temperature	PCR step	Time
1	95	Polymerase activation	10 min
40	95	Denaturation	15 sec
	55 or 60	Annealing	1 min
Melt curve	95	Dissociation	15 sec
	60		15 sec
	95		15 sec

A melt curve analysis was also performed in parallel with the relative gene expression, allowing the assessment of the dissociation characteristics of double-stranded DNA during heating. As the temperature is raised, the double DNA strand starts to dissociate leading to the release of the intercalating SYBR green fluorescent

dye and therefore a decrease of the emitted fluorescent signal. The change in slope of the fluorescence curve is then plotted as a function of temperature to obtain the melt curve. Analysis of the melt curve allows assessing whether the quantitative RT-PCR assay has produced one single specific product during the amplification of the target gene. A single peak shown by the melt curve represents one single amplicon. **Figure 14** shows a representative melt curve for all the studied transcripts.
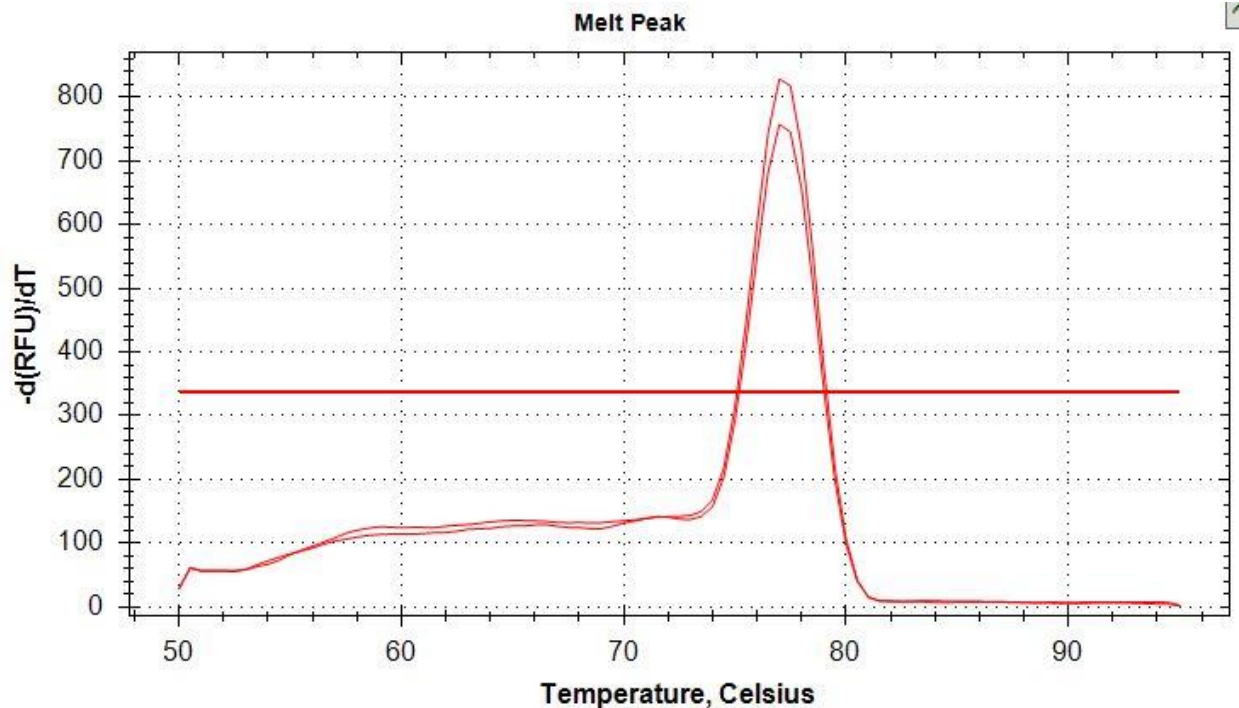
Figure 14: Representative melt curves from quantitative RT-PCR of a single transcript for HPRT performed in duplicate.
The single peak represents one single specific amplicon.

2.11. ELISA (enzyme-linked immunosorbent assay) and RIA (radioimmunoassay)

2.11.1. Preparation of protein lysates

Testis tissue samples were homogenized with PBS and protease inhibitor cocktail (Sigma, Steinheim, Germany or Calbiochem, MA, USA) using a Potter S tissue homogenizer or by using 5 mm stainless steel beads (Qiagen) and tissue lyser (Qiagen)

at 40 oscillations/second for at least 1 min. Insoluble components were removed by centrifugation of homogenized tissues at 14,000 x g for 10 min at 4°C.

2.11.2. Measurement of protein concentration

Total protein measurement was performed using the Pierce BCA Protein Assay (Thermo Scientific, Rockford, USA) following the manufacturer's instructions. Briefly, samples were diluted 1:10 in distilled water. Different concentration of the provided BSA standard were prepared ranging between 0 and 2000 µg/ml. 25 µl of each standard and each unknown sample duplicate were pipetted into a 96 well microplate. 200 µl of the BCA working reagent (1 part of reagent B into 50 parts of reagent A) were added to each well. The plate was incubated at 37°C for 30 min. Finally, concentrations were assessed after measuring the optical density by the microplate ELISA reader (Berthold, Bad Wildbad, Germany and Labsystems, Vantaa, Finland) at either 570 nm (Giessen) or 492 nm (Monash).

2.11.3. Activin A and B ELISA

Activin A was measured using a specific two-site enzyme immunoassay as described previously (Knight et al., 1996, O'Connor et al., 1999, Okuma et al., 2006). The optical density was measured in a microplate ELISA reader (Labsystems) using dual wavelengths (450 nm and 630 nm). The concentration was calculated by Genesis software based on the measurement of optical density of the recombinant activin A standard and each sample. Sensitivity of the activin A ELISA ranged between 6.1 pg/ml and 1.98 ng/ml with an intra-assay coefficient of variability (CV) of 5.6% for the study I (samples from groups I, II and III). For the study II (samples from groups IV and V) sensitivity ranged between 12 pg/ml and 3.97 ng/ml with an intra and inter-assay CV of 7%.

Activin B protein levels were also evaluated using the enzyme linked immunosorbent assay (ELISA) as described previously (Ludlow et al., 2009). Briefly, plates were coated overnight with the 46A/F activin B antibody (3.9 mg/ml), then washed and blocked with 1% BSA in PBS with 6% sucrose. Samples were denatured in 6% SDS by boiling for 3

min, and then added to the wells with human recombinant activin B used as a standard. Biotinylated 46A/F was used as detection antibody, followed by streptavidin-poly-HRP (horseradish peroxidase) and incubated for 1 hour, then the TMB (tetramethylbenzidine) substrate solution (Life Technologies, Frederick, USA) was added for 20 min. Finally, 300 mM H_2SO_4 was added to stop the enzymatic reaction and absorbance at 450 nm was measured. Sensitivity of the activin B ELISA ranged between 8.1 pg/ml and 2.46 ng/ml and intra-assay CV was 7.8%.

2.11.4. Measurement of follistatin, inhibin and hormones (FSH, LH and testosterone) by RIA

Concentrations of follistatin in mouse tissue homogenates and serum samples were measured using a heterologous, discontinuous radioimmunoassay (RIA), as described previously (O'Connor et al., 1999, Winnall et al., 2013). Assay sensitivity ranged between 1.33 ng/ml and 87.1 ng/ml and an intra assay CV of 9.8% for the study I samples from groups I, II and III. For study II samples from groups IV, V and VI, sensitivity ranged between 0.95 ng/ml and 199 ng/ml and the intra-assay CV was 12.3%.

Inhibin levels in mouse testicular homogenates were also measured by a heterologous RIA, as described previously (Robertson et al., 1988, Winnall et al., 2013). This assay detects total inhibin, e.g. all proteins containing the inhibin α-subunit (inhibin A and B, as well as some free α-subunit peptides). The intra-assay CV was 6.4%, inter-assay CV was 5.9% and the sensitivity ranged between 58.76 ng/ml and 1.24 ng/ml for the samples from groups I, II and III (study I). For samples from groups IV, V and VI (study II), sensitivity ranged between 0.94 ng/ml and 315.42 ng/ml.

FSH, LH and testosterone serum levels were also measured by RIA. FSH and LH assays were provided by the National Hormone and Peptide Program (Harbor-UCLA Medical Center, Dr. A.F. Parlow) and testosterone assay was done using a testosterone kit (Immunotech IM1119, Beckman Coulter, Prague, Czech Republic) provided by Beckman. The intra-assay CV of the FSH assay was 3.9% and sensitivity ranged

between 0.94 ng/ml and 28.70 ng/ml. The intra-assay CV of the LH assay was 7.7% and sensitivity ranged between 0.10 ng/ml and 14.7 ng/ml. The intra-assay CV of the testosterone assay was 9.5% and sensitivity ranged between 47.6 pg/ml and 46.6 ng/ml.

2.12.   Isolation of mouse testicular cells

Mouse testicular somatic cells (peritubular and Sertoli cells) were isolated to study the effects of cytokines on the inflammatory and fibrotic response by these cells. The isolation protocols were based on well-established protocols for isolating testicular cells from rodents (Bhushan et al., 2016, Okuma et al., 2005, Zeyse et al., 2000, O'Brien et al., 1989, Fillion et al., 1994), which were modified and optimized as described in the following sections.

2.12.1.   Isolation of peritubular cells

Ten 21 day old C57BL/6J mice were killed by cervical dislocation. Testes were collected and kept in sterile DMEM/F12 medium. Under a laminar flow, testes were decapsulated and dissociated using 2 forceps. In order to isolate the seminiferous tubules, tissue was placed in a 50 ml falcon tube and digested with 5 ml collagenase solution (1 mg/ml) in a 34°C shaking water bath (60 cycles/min) for 20 min, (**Fig. 15a**). Afterwards, 40 ml of DMEM/F12 medium was added in order to dilute the collagenase and tubules were left to settle at the bottom of the tube for 5 min. The supernatant was discarded carefully using a 5 ml serological pipette in order to eliminate the interstitial cells. Then tubules were washed twice with DMEM/F12 medium. In order to further dissociate the tubules and release the peritubular cells (PTC), a second digestion of the tubules in 5 ml trypsin (1 mg/ml) was performed for 20 min in a 34°C shaking water bath (60 cycles/min) (**Fig. 15b**). 5 ml of soybean trypsin inhibitor solution (SBTI; 0.1 mg/ml) was added to the tubules to neutralize trypsin and the tubules were left to settle at the bottom of the tube for 5 min. The supernatant containing the PTC was carefully collected and transferred into a new Falcon tube (**Fig. 15c**). The remaining tubules were washed twice with DMEM/F12 medium, left to settle each time and the supernatant was collected and added to the tube containing the PTC. PTC were centrifuged at 400 x g for 10 min,

supernatant was discarded and pellet containing PTC was resuspended in 20 ml DMEM with 10% FCS and plated in one 75 cm^2 flask. Cells were cultured for 48 hours at 37°C and 5% CO_2. After 48 hours, attached PTC were washed twice with sterile PBS in order to remove contaminating interstitial and germ cells, and then left for approximately 48 hours to become confluent. Afterwards, cells were transferred into two new 75 cm^2 flasks. PTC were grown until confluence of 90% was reached and then seeded into 48-well plate for treatments and evaluation of purity by αSMA and Sox9 staining (**Fig. 15d**).
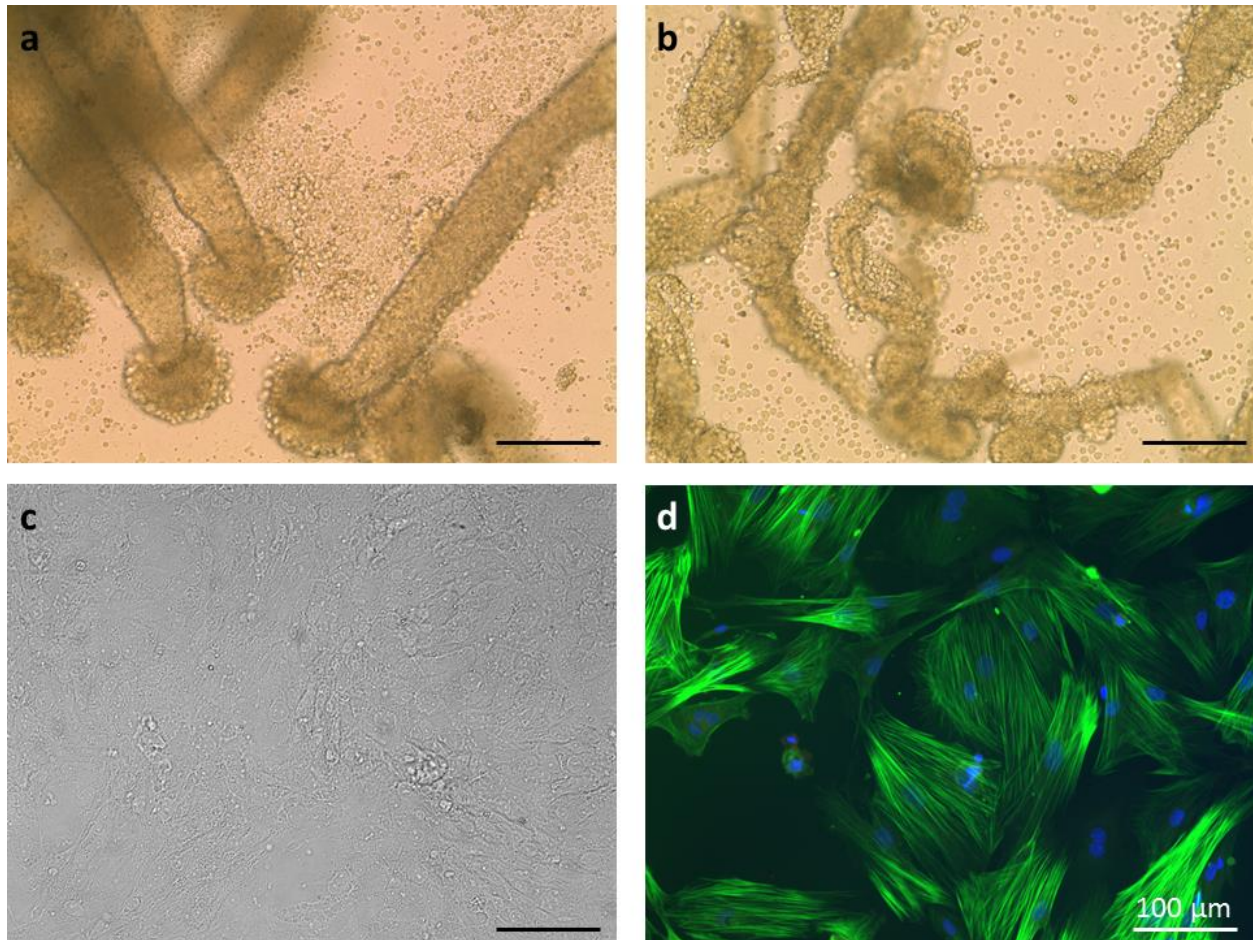
Figure 15: Isolation of peritubular cells from immature mouse testes.
Decapsulated testes from 21 day old C57BL/6J mice were digested using collagenase for 20 min causing seminiferous tubule dissociation (**a**). PTC were released in the supernatant following trypsin-DNase digestion for 20 min at 34°C (**b**). Trypsin activity was inhibited using SBTI. PTC culture after splitting and removal of contaminating cells (**c**). Sox9 (SC marker) and αSMA double staining of PTC (green) after passaging showing very high purity, and no contamination with SC, (**d**). Scale bars represent 100 μm.

2.12.2.   Isolation of Sertoli cells

In order to purify the Sertoli cells, the remaining seminiferous tubules were digested further with 5 ml hyaluronidase solution (1 mg/ml) for 15 min in a shaking water bath (60 cycles/min) at 34°C, then the cells were dissociated by aspirating and releasing them for 4-5 times using a 5 ml serological pipet. DMEM/F12 was added to inhibit hyaluronidase activity and tubules were centrifuged at 400 x g for 3 min. Finally the supernatant was discarded and the pellet was resuspended in DMEM/F12 and filtered into a new tube through a 100 µm cell strainer to remove existing cell clumps. The solution containing cells was centrifuged at 400 x g for 3 min, the supernatant was discarded and SC were resuspended in 2 ml DMEM + 0.1% BSA. Cells were stained with trypan blue (Sigma, St Louis, USA) and counted using a Neubauer counting chamber, resuspended to a concentration of 1 x 10^6 cells/ml and 500 µl of cell suspension was seeded (500,000 cells/well) in a 48-well plate. The steps of the Sertoli cell isolation are shown in **Figure 16**. Cells were cultured for 48 hours at 37°C and 5% CO_2. Subsequently, contaminating germ cells were treated by hypotonic shock and removed. Briefly, SC medium was removed, and 20 mM Tris-HCl solution was added to each well for 1.5 min. Afterwards SC were washed with PBS and cultured for 24 hours in DMEM + 0.1% BSA before following treatments.
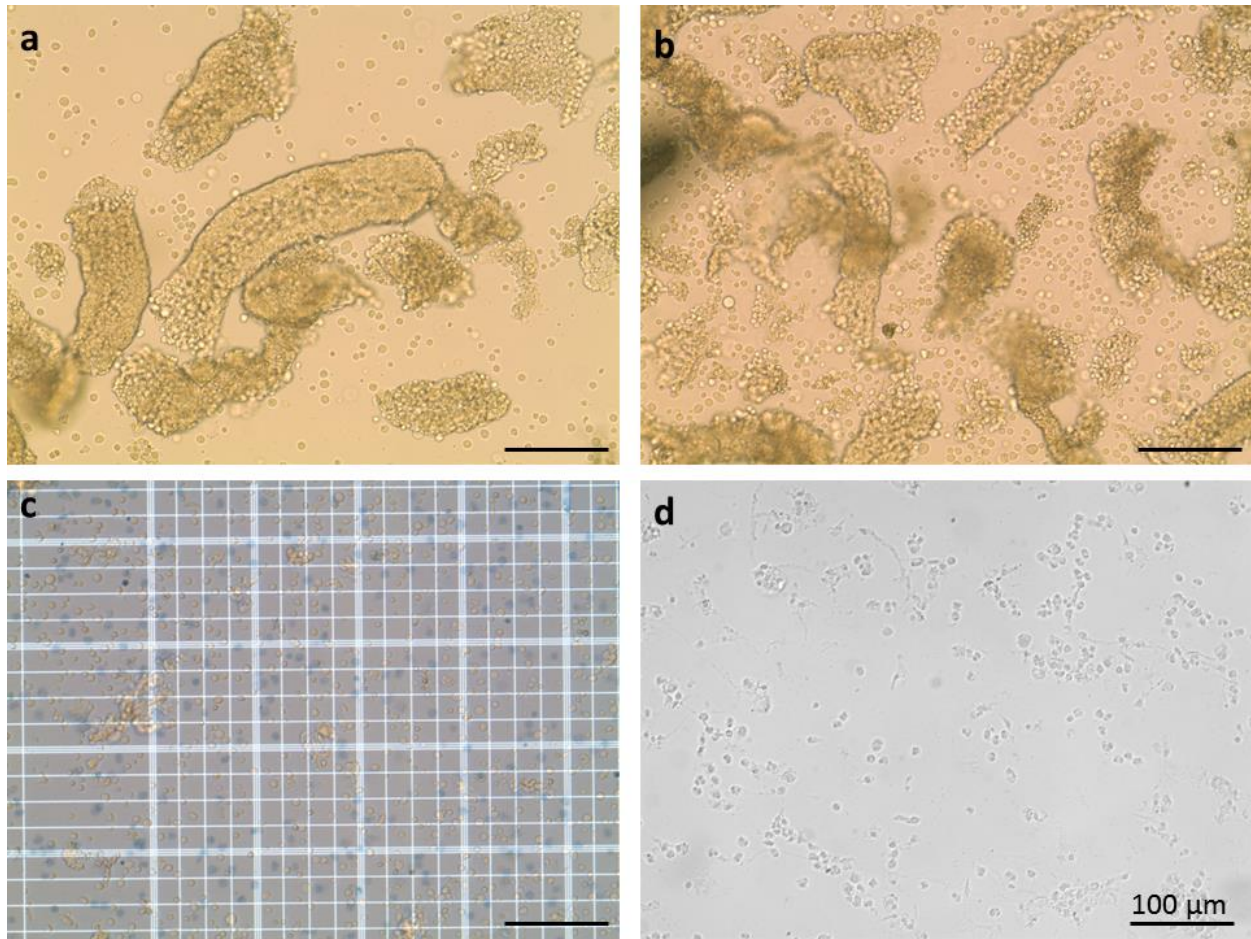
<u>Figure 16:</u> Isolation of Sertoli cells from immature mouse testes.
Seminiferous tubules after removal of peritubular cell formed very small tubular fragments (**a**). Fragments of seminiferous tubules were further digested for 15 min by hyaloronidase solution (**b**). A small aliquot of Sertoli cell suspension was stained by trypan blue and counted in a Neubauer counting chamber (**c**). Two days after seeding, contaminating germ cells were removed from the Sertoli cell culture by hypotonic shock treatment (**d**). Scale bars represent 100 µm.

2.13. Effect of TNF and activin A on Sertoli and peritubular cells *in vitro*

In order to directly investigate changes in the function and the regulation of fibrotic genes in Sertoli and peritubular cells during EAEO, an *in vitro* model mimicking aspects of the *in vivo* inflammatory milieu of the EAEO testis was established. Isolated Sertoli cells or peritubular cells were seeded in a 48-well plate at a concentration of 200,000 cells per well. Cells were treated with recombinant mouse TNF (aa 80-235, R&D Systems, Minneapolis, USA) or recombinant human/mouse/rat activin A (338-AC/CF,

R&D Systems). Eight doses of TNF and activin A, ranging from 0 to 200 ng/ml were tested. Treatments were performed for 24 and 48 hours. Experiments were carried out on four independent cell isolations. Each treatment was performed in triplicate. After 24 or 48 hours, media were collected and frozen at -20°C for activin A ELISA.

2.14.   Statistical analysis

Data were expressed as means ± SEM from at least 3 independent experiments. Statistical analyses were performed using the unpaired t-test followed by Welch's correction when 2 experimental groups were compared; one-way ANOVA followed by Tukey's multiple comparisons or two-way ANOVA followed by Sidak's multiple comparisons when more than 2 experimental groups were compared. Pearson's correlation was used in order to show the linear relationship between two sets of data and how well they relate. Pearson's correlation coefficient "r" is a measure of the strength of the association between the two variables. r=-1 represents a negative correlation, r=0 represents no correlation and r=+1 represents a positive correlation. P-values <0.05 were considered as a statistically significant difference. All tests were performed using GraphPad Prism 6 software (GraphPad Software, San Diego, USA).

3. RESULTS

Study I

Study I involved comparison of the induction of EAEO in C57BL/6N mice using TH with two different adjuvants, CFA and TiterMax Gold, and *B. pertussis* toxin injection. In this study, the efficiency of each adjuvant was evaluated in relation to the induction rate of EAEO. Moreover, the testes from mice that developed the disease were analyzed in terms of (a) inflammation as assessed by presence of immune cell infiltrates and expression of cytokines, (b) fibrosis, and (c) the expression profile of activins, follistatin, inhibin and activin receptors.

3.1. Induction rate of EAEO in C57BL/6N mice

A reduction in the weight of one or both testes was an indicator of EAEO development. The paired testis weights from mice in the different immunization groups and their respective controls are shown in **Figure 17**. The average testis weight 30 days after the first immunization was similar in all investigated mice from group I (**Fig. 17**). Animals from group I, immunized three times with TH in CFA, showed an approximately 2-fold reduction in testis weight at 50 (n = 7) and 80 (n = 5) days after the first immunization compared with untreated (n = 5) and adjuvant control (n = 5 for 50 days and n= 4 for 80 days) groups (**Fig. 17**). Mice from group II, immunized three times with TH in TiterMax Gold adjuvant, showed a decrease in mean testis weight at 50 days (n = 8) after the first immunization compared with untreated (n = 5) controls, but no change was observed in the testis weight 80 days (n = 8) after the first immunization compared with both controls (n =5) (**Fig. 17b**). In contrast, mice from group III, immunized only twice with TH in Titermax Gold adjuvant (**Fig. 17c**), did not show any change in the testicular weight at all time points investigated. The macroscopic difference in testicular size of control and mice with severe EAEO, 50 days after the first immunization is shown in **Fig. 17d**.
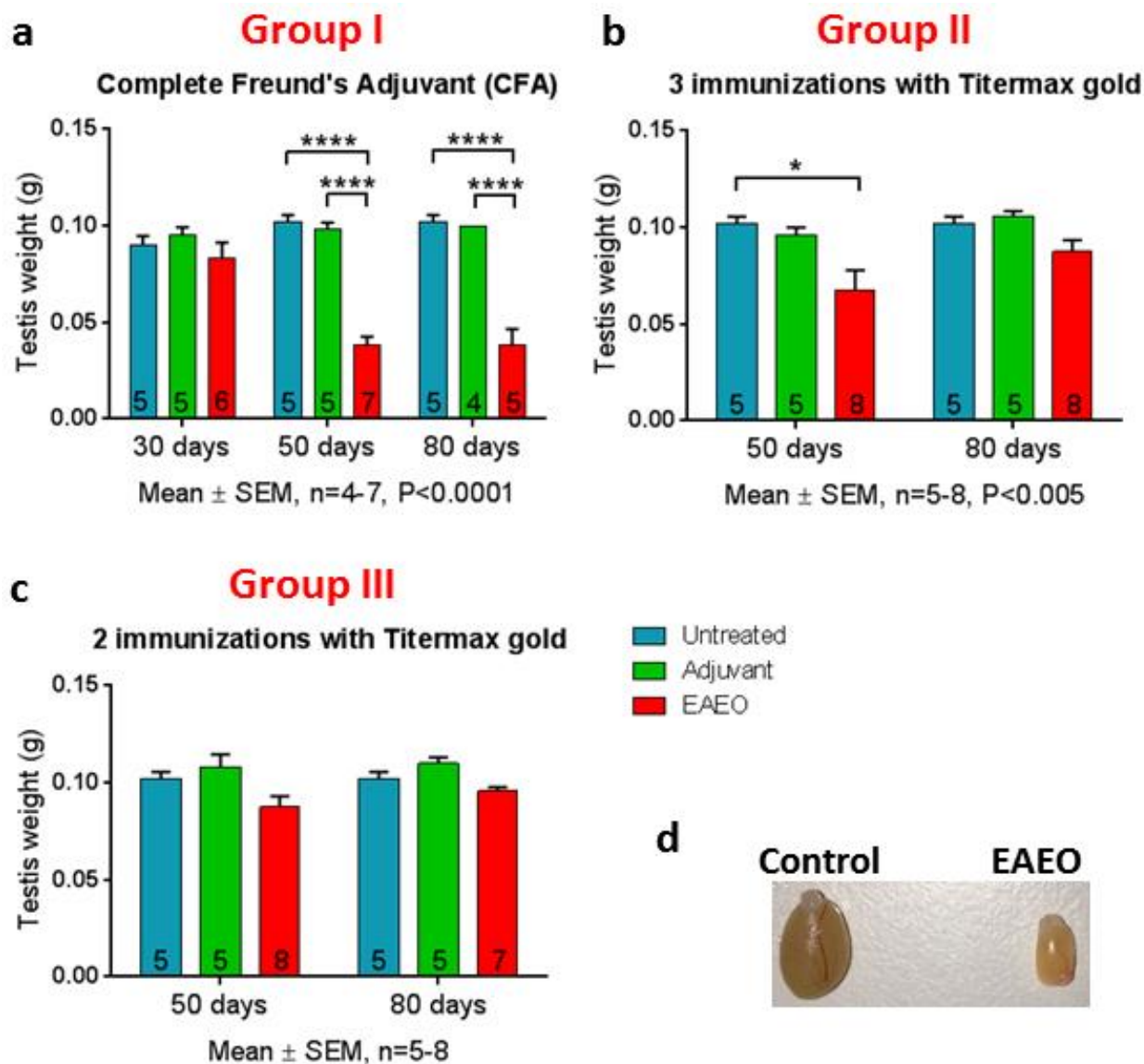
Figure 17: Testicular weights and size of mice in study I.
Paired testicular weights of untreated, adjuvant control and immunized (EAEO) mice 30, 50 and 80 days after the first immunization from study I (**a-c**). Representative image showing macroscopic difference in testicular size from control mice and EAEO mice 50 days after the first immunization (**d**). Data are expressed as mean ± SEM (n = 4 - 8 animals per group; numbers of animals per group are shown in the respective columns). Statistical analysis was performed using one-way ANOVA followed by Tukey's multiple comparison test; *P<0.05 and ****P<0.0001, all other comparisons were not statistically significant.

The induction rate of EAEO was calculated based on testicular weight and histopathological changes in the testicular architecture (**Table 4**) (described in detail in section 3.2). All immunized mice from group I developed EAEO at 50 and 80 days after the first immunization (7/7 and 5/5 mice, respectively), whereas 30 days after the first immunization, only 33% (2/6) mice showed histological signs of the disease.

Animals from groups II and III showed a significantly lower induction rate of EAEO. 50% of the mice from group II developed the disease (4/8 mice) and only 12.5% from group III (1/8 mice) at 50 days and from group II at 80 days, respectively as shown in **Table 4b and c**. Therefore the mice from groups II and III were not considered for further investigations and all subsequent data shown from study I is only from mice of group I.

Table 4: Induction rate of EAEO in treatment groups from study I.

a

Treatment group I	Induction rate at 30 days (number of animals)	Induction rate at 50 days (number of animals)	Induction rate at 80 days (number of animals)
Untreated	0% (0/5)	0% (0/5)	0% (0/5)
Adjuvant	0% (0/5)	0% (0/5)	0% (0/4)
EAEO	33% (2/6)	100% (7/7)	100% (5/5)

b

Treatment group II		Induction rate at 50 days (number of animals)	Induction rate at 80 days (number of animals)
Untreated		0% (0/5)	0% (0/5)
Adjuvant		0% (0/5)	0% (0/5)
EAEO		50% (4/8)	12.5% (1/8)

c

Treatment group III		Induction rate at 50 days (number of animals)	Induction rate at 80 days (number of animals)
Untreated		0% (0/5)	0% (0/5)
Adjuvant		0% (0/5)	0% (0/5)
EAEO		12.5% (1/8)	0% (0/7)

Group I: three immunizations with CFA, group II: three immunizations with TiterMax Gold, group II: two immunizations with TiterMax Gold.

3.2. Morphological changes in EAEO testes

The grade of EAEO development was variable between individual mice from group I, therefore TH-immunized mice that developed EAEO were subdivided into mice with severe disease symptoms (severe EAEO) and mice showing only mild symptoms of EAEO (low grade EAEO). Histopathological changes and the fibrotic response were assessed by azo-carmine and aniline blue staining (azan), as shown in **Figure 18**.

3.2.1. Altered histology in EAEO testes

The changes in inflamed testes included reduced diameter of the seminiferous tubules, germ cell sloughing leading to Sertoli cell only tubules and leukocytic infiltrates in the interstitium (**Fig. 18**).

Testes from the severe EAEO group at 50 (**Fig. 18h**) and 80 (**Fig. 18l**) days after the first immunization, displayed a complete destruction of testicular morphology with a reduction of the diameter of the seminiferous epithelium, tubular atrophy and thickening of the seminiferous lamina propria. An increase of the immune cell infiltrates in EAEO testes was also observed (as described in section 3.3.2). In contrast, in the mild form of the disease, some of the seminiferous tubules were still intact. Moreover, testes from untreated (**Fig. 18a, e, i**) and adjuvant control mice (**Fig. 18b, f, j**) showed a normal morphology with seminiferous tubules containing Sertoli cells as well as germ cells at all stages of spermatogenesis. In accord, morphological changes were also observed in human testicular biopsies with impaired spermatogenesis and inflammatory infiltrates (**Fig. 19b**).
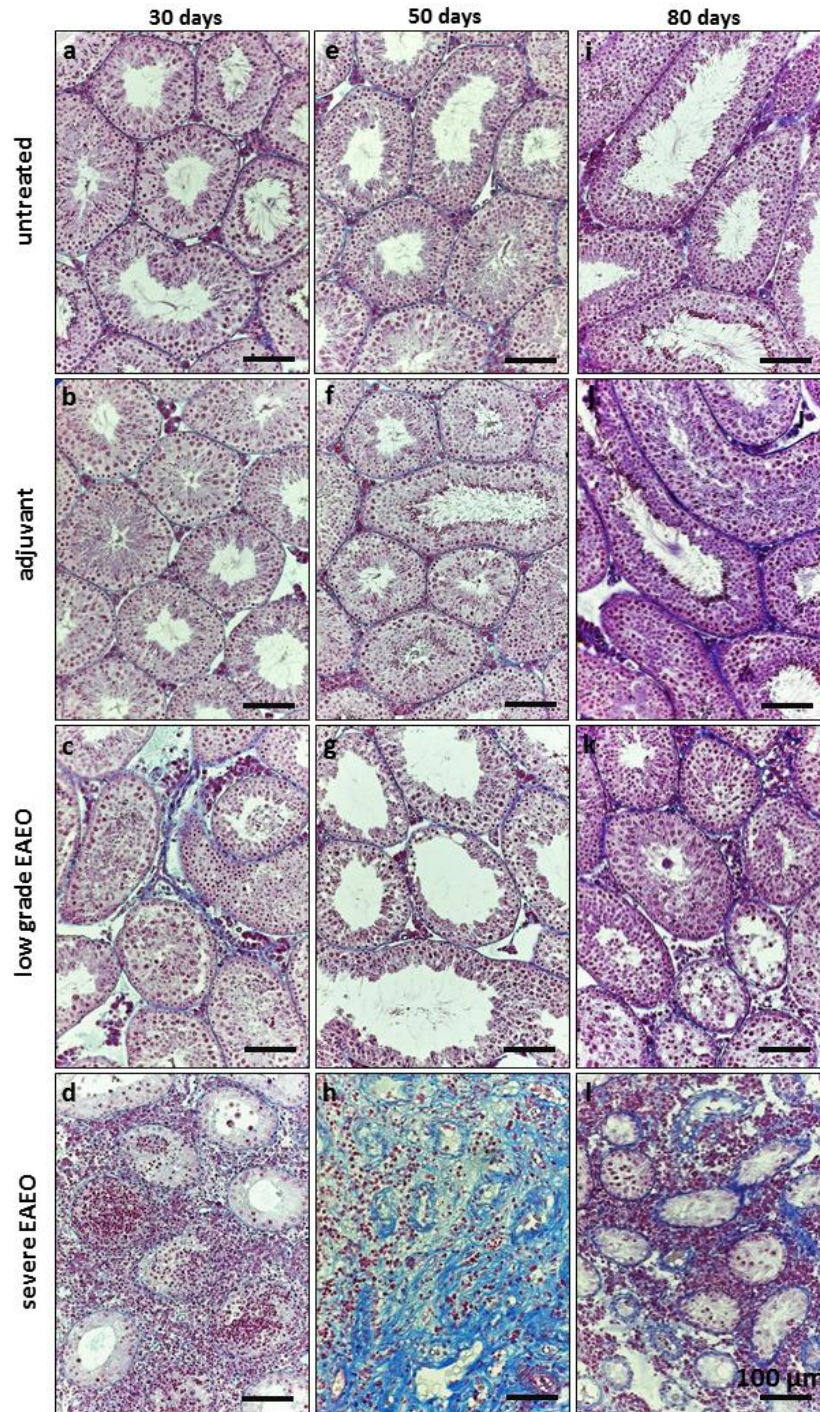
Figure 18: Morphological changes and fibrotic response in EAEO testes.
Azo-carmin and aniline blue staining of collagen fibers in paraffin sections from untreated (**a, e, i**), adjuvant control (**b, f, j**), low grade (**c, g, k**) and severe EAEO (**d, h, l**) mouse testes at 30 (**a - d**), 50 (**e - h**) and 80 (**i - l**) days after the first immunization. An increase in collagen fibers was visible in low grade EAEO in the areas with lymphocytic infiltrates. A strong peritubular fibrotic response was detectable in EAEO mouse testes at 50 (**h**) and 80 (**l**) days after the first immunization. Scale bars represent 100 µm.
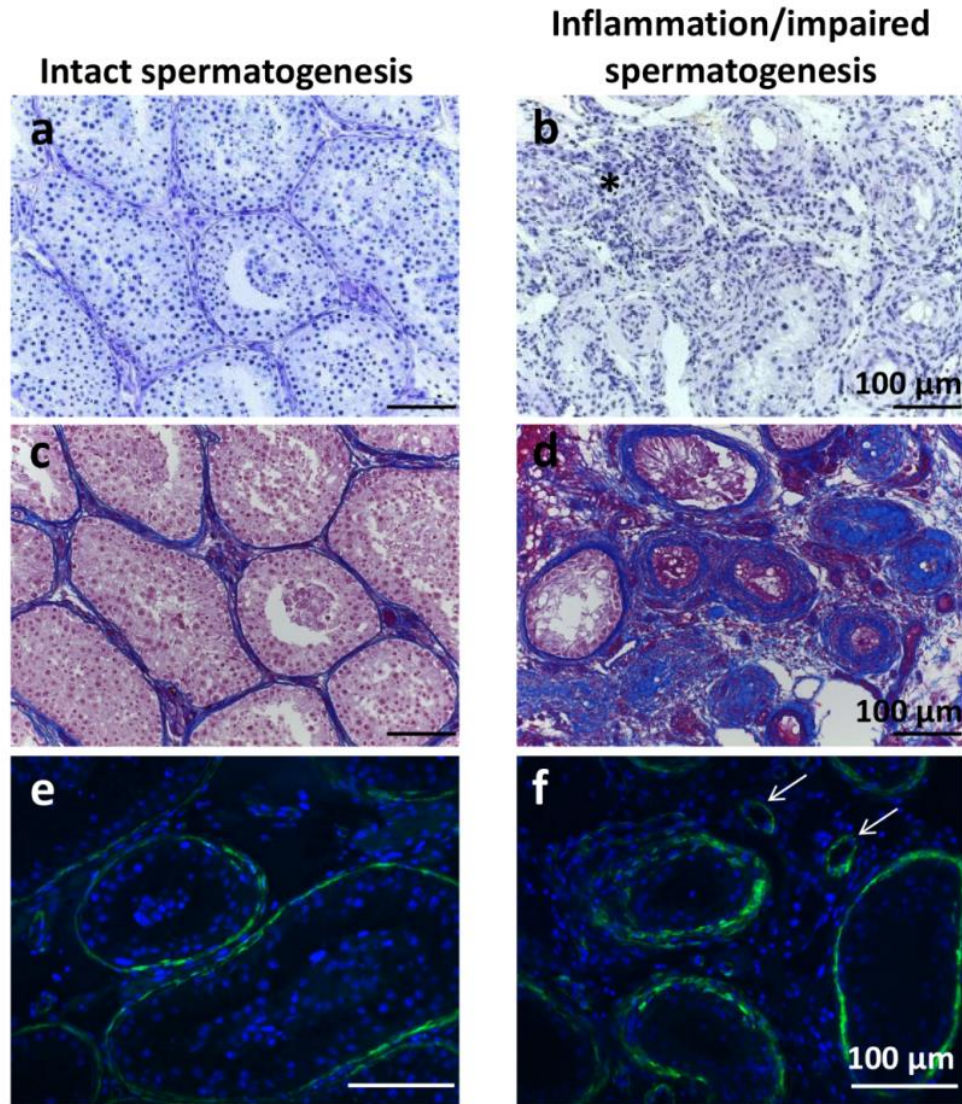
Figure 19: Morphological differences between human testes with intact spermatogenesis and inflamed testes with impaired spermatogenesis.
Hematoxylin and eosin staining (**a, b**), azo-carmine and aniline blue staining of collagen fibers (**c, d**) and immunofluorescence distribution of αSMA (**e**, **f**) in testicular biopsies from infertile men showing seminiferous tubules with intact spermatogenesis and absence of any signs of inflammation in the interstitial compartment (**a, c**, **d**) and human testis specimens with impaired spermatogenesis and infiltration by non-resident immune cells (**b, d**, **f**). An increase in collagen fibers reflecting severe alteration of the lamina propria (thickening, "meshwork" pattern), tubular atrophy and expanded vascularization was visible in the testes with impaired spermatogenesis (**d**) close to the areas with lymphocytic infiltrates (asterisks) (**b**), accompanied by a thicker distribution of the αSMA layer which was spread within the cells (**f**). αSMA was also seen in the blood vessels (arrows) within the interstitium. In testes with normal spermatogenesis, there was no detectable fibrotic response (**c**) and αSMA is localized in the peritubular cells as a thin layer (**e**). Scale bars represent 100 μm.

3.2.2. Strong fibrotic responses in EAEO testes

The morphological changes in EAEO were accompanied by a strong fibrotic response in the testes represented by an increase of the collagen fibers around the remaining empty tubules, and thickening of the lamina propria, especially at 50 (**Fig. 18h**) and 80 (**Fig. 18l**) days after the first immunization. Similar changes were also observed in human testicular biopsies with impaired spermatogenesis and inflammatory infiltrates (**Fig. 19d**).

3.2.2.1. *Altered distribution of α-smooth muscle actin (αSMA) in EAEO testes*

In order to investigate further the peritubular fibrotic response observed in EAEO testes, an analysis of α-smooth muscle actin (αSMA) localization and distribution by immunofluorescence staining was performed (**Fig. 20**). The staining revealed a change in the distribution of the αSMA layer in low grade EAEO at 30, 50 and 80 days (**Fig. 20c, g, k, o**) in areas where the seminiferous tubules were smaller and spermatogenesis was disrupted. The altered distribution and thickening of the αSMA layer was more pronounced in severe EAEO at 30, 50 and 80 days (**Fig. 20d, h, l, p**). The layer of αSMA was diffusely distributed within the peritubular cells in EAEO testes compared to a thin and compact layer in untreated and adjuvant control testes. The same altered distribution of the layer of αSMA was also observed in human testis samples with focal inflammatory lesions and impaired spermatogenesis (**Fig. 19f**).
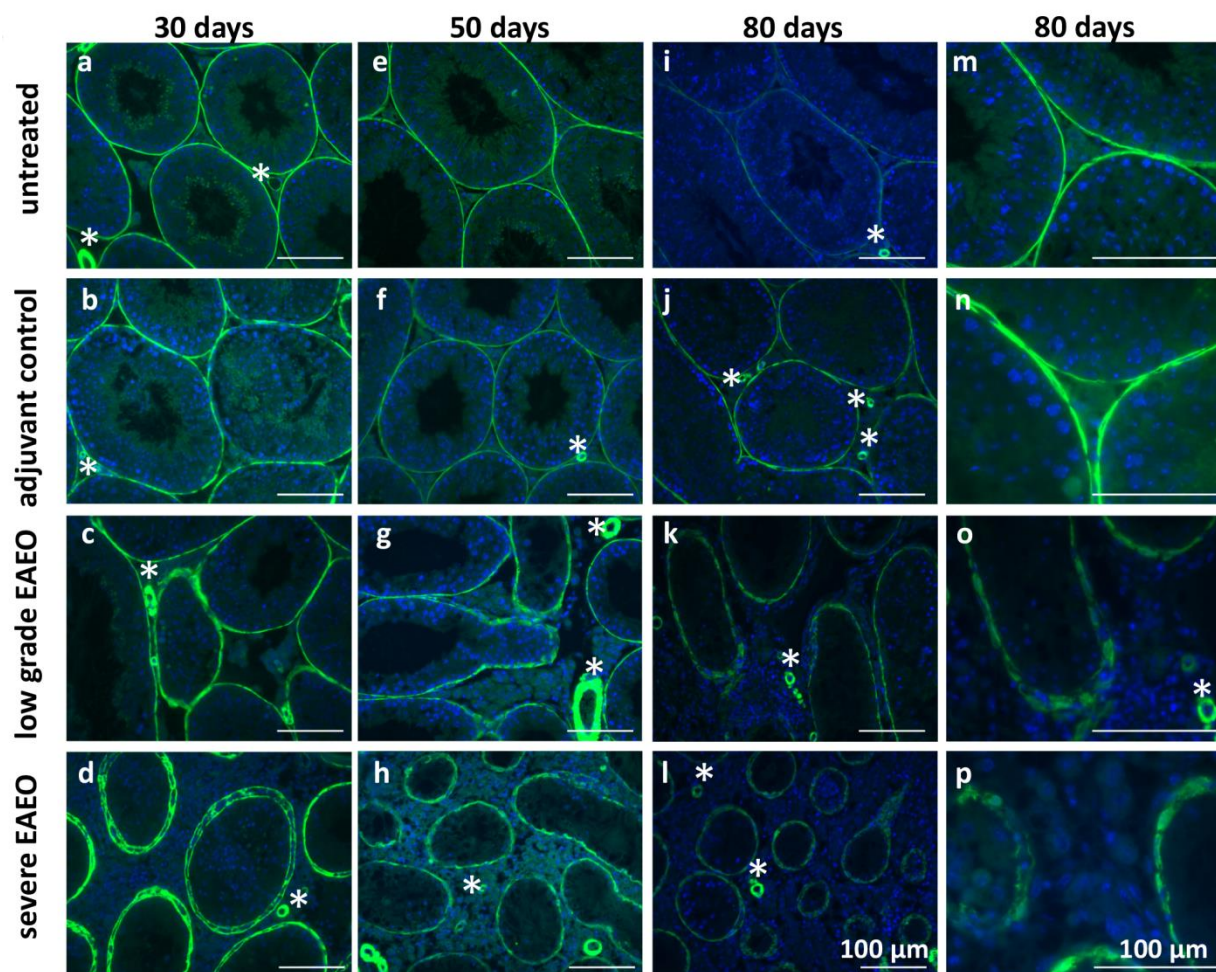
Figure 20: Distribution of α-smooth muscle actin (αSMA) was altered in EAEO testes.

Distribution of α-smooth muscle actin (αSMA) in paraffin sections from untreated (**a, e, i, m**), adjuvant control (**b, f, j, n**), low grade (**c, g, k, o**) and severe EAEO (**d, h, l, p**) testes at 30 (**a - d**), 50 (**e - h**) and 80 (**i - l**) days after the first immunization. Panels **m - p** represent a higher magnification of images **i - l**. In the testes from untreated and adjuvant controls, αSMA was localized in the peritubular cells as a thin layer, but in low grade and severe EAEO testes, the αSMA was diffusely distributed within the cell. αSMA was also seen in the blood vessels (asterisks) within the testes. Scale bars represent 100 µm.

3.2.2.2. *Increased numbers of mast cells in EAEO testes*

Since mast cells are involved in promoting fibrotic response in several diseases by releasing tryptase from their granules (Wilgus and Wulff, 2014), staining of testicular mast cells was performed as shown in **Figure 21**. The staining revealed that, although scarce, mast cells were present in testes under normal conditions (**Fig. 21a-b**). The

mast cells were found either within the blood vessels of the testis or in close proximity to the tunica albuginea. In low grade EAEO (**Fig. 21c**), mast cells seemed more prevalent in the areas of leukocytic accumulation and around smaller tubules showing a thickening of the lamina propria as shown in **Figure 18c**, whereas in severe EAEO, mast cells seemed more evenly distributed within the testes and the increase in their number was visibly evident, although not counted.
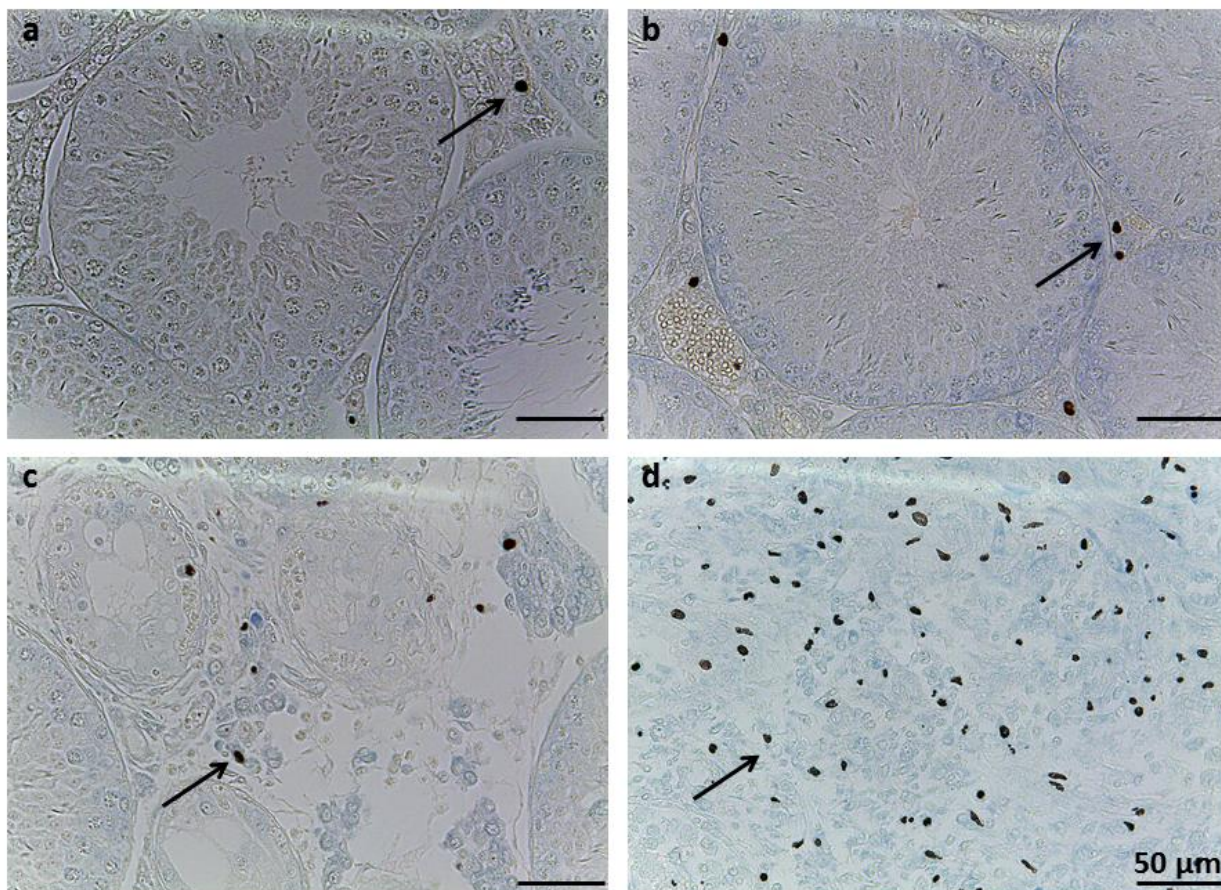
Figure 21: Mast cell numbers were increased in EAEO testes.
Toluidine blue staining of mast cells in testicular paraffin sections from untreated (**a**), adjuvant control (**b**), low grade (**c**) and severe EAEO (**d**) testes. Arrows point to mast cells. Under normal conditions, mast cells were present in very low numbers in the interstitial space (**a-b**). An accumulation of mast cells was observed in low grade EAEO testes (**c**) around areas with immune cell infiltrates and smaller seminiferous tubules. An evident increase in the number of mast cells was seen in severe EAEO testes (**d**). Scale bars represent 50 μm.

3.3.   Inflammatory responses in EAEO testes

In order to investigate the inflammatory response in the EAEO and control testes, an analysis of the mRNA expression of inflammatory mediators and presence of different immune cell populations was performed.

3.3.1. Expression of inflammatory mediators was increased in EAEO testes

Relative mRNA expression of inflammatory mediators (TNF, IL-6, IL-10 and MCP-1) was quantified using quantitative RT-PCR in order to evaluate if immunized mice developed testicular inflammation.

At 30 days after the first immunization, the mRNA expression levels of TNF, MCP-1 (encoded by the *Ccl2* gene), IL-10 and IL-6 in EAEO testes were unchanged in EAEO testes and controls (**Fig. 22**). Further analysis showed a 20-fold increase of TNF (**Fig. 22a**) and MCP-1 (**Fig. 22b**), as well as an approximately 10-fold upregulation of IL-10 (**Fig. 22c**) mRNA expression in EAEO testes 50 days after the first immunization compared to untreated and adjuvant control testes. At 80 days after the first immunization, an increase of TNF (**Fig. 22a**), MCP-1 (**Fig. 22b**) and IL-10 (**Fig. 22c**) mRNA levels was also observed in EAEO testes, by comparison with untreated control groups and both untreated and adjuvant controls for MCP-1 (**Fig. 22b**). Notably, the IL-10 mRNA level was slightly increased in adjuvant control testes, by comparison with untreated control group 50 days after the first immunization (**Fig. 22c**). IL-6 mRNA levels in EAEO were comparable to both controls at all time points investigated (**Fig. 22d**).
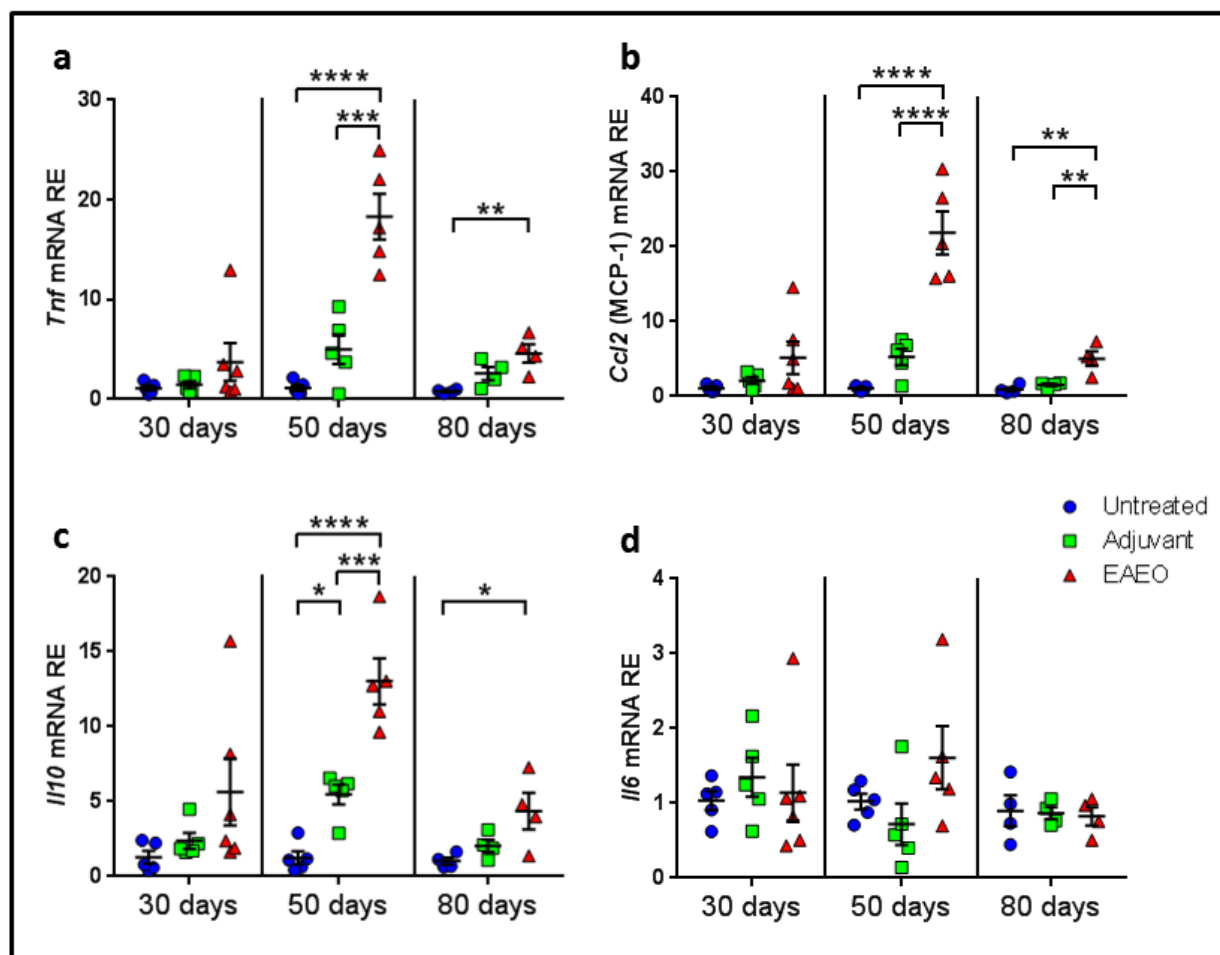
Figure 22: Expression of inflammatory mediators was elevated in EAEO testes.
Tnf (**a**), *Ccl2* (MCP-1) (**b**), *Il10* (**c**) and *Il6* (**d**) mRNA expression was measured in untreated, adjuvant control and EAEO mouse testes at 30, 50 and 80 days after the first immunization. Relative mRNA levels were analyzed using quantitative RT-PCR. Data are represented as mean ± SEM (n = 4 - 5 animals per group). Statistical analysis was done using one-way ANOVA followed by Tukey's multiple comparisons; *P<0.05, **P<0.01, ***P<0.001, ****P<0.0001, all other comparisons were not statistically significant.

3.3.2. Immune cell populations were increased in EAEO testes

In addition to the increased numbers of mast cells (as presented in section 3.2.2.2), the presence of different immune cell populations in testes under normal or inflammatory conditions was evaluated either by immunofluorescence staining or flow cytometry.

3.3.2.1. Testicular macrophages were increased in EAEO testes

Although not quantified, immunofluorescence analysis data suggested that the number of F4/80 and CD206 positive macrophages were considerably more prominent in EAEO testes (**Fig. 23**). In untreated mouse testes, few macrophages were found in the interstitial space (**Fig. 23c**). Notably, the majority of these cells were F4/80 and CD206-positive indicating an M2 anti-inflammatory phenotype (**Fig. 23a**). A similar distribution of the testicular macrophages was also observed in adjuvant control testes (**Fig. 23f**). However, adjuvant treatment alone led to a slight increase in the number of macrophages by comparison with untreated controls. In contrast, in low grade EAEO testes, an accumulation of co-localized F4/80 and CD206-positive cells with increased numbers of F4/80-positive/CD206-negative cells (**Fig. 23i**) was observed, mainly in the areas where the diameter of the seminiferous tubules was reduced. This accumulation was evident in severe EAEO (**Fig. 23l**) at 50 days after the first immunization, suggesting that the infiltrating macrophages possess a pro-inflammatory M1 phenotype.
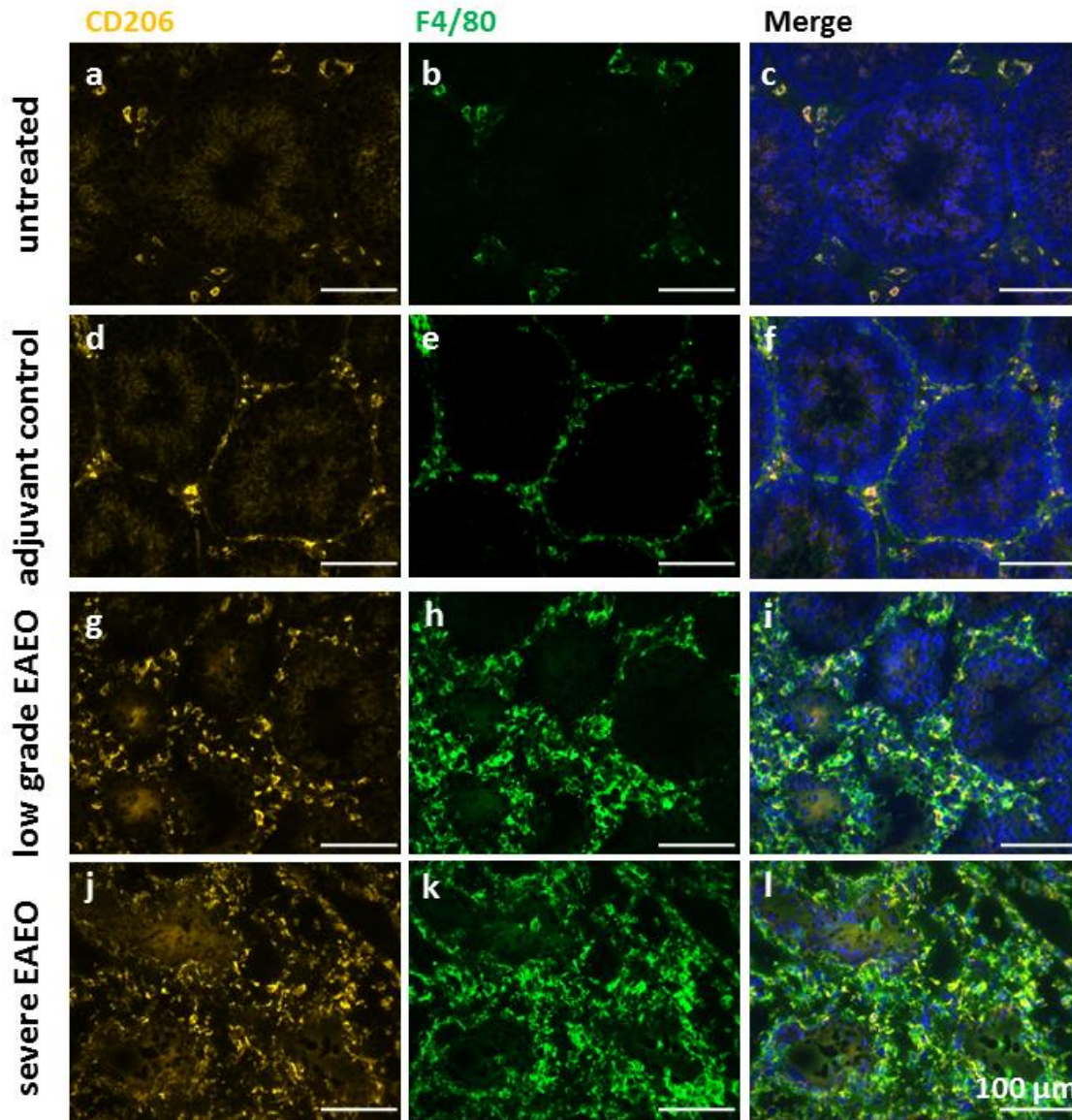
Figure 23: Increased numbers of pro-inflammatory M1 macrophages in EAEO testes.

Double staining for CD206 (AlexaFluor546, orange) (**a, d, g, j**) and the macrophage marker F4/80 (AlexaFluor488, green) (**b, e, h, k**) in testicular cryosections from untreated (**a - c**), adjuvant control (**d - f**), low grade EAEO (**g - i**) and severe EAEO (**j - l**) mice. Nuclei were counterstained with DAPI (blue). Under non-inflammatory conditions, co-localized CD206 and F4/80-positive macrophages were present in low numbers in the interstitial space (**c, f**). An accumulation of double positive F4/80 and CD206 macrophages was observed in adjuvant controls (**f**), inflamed low grade (**i**) and severe 50 day EAEO testes (**l**), with a higher number of F4/80 positive only (CD206-negative) cells. In low grade 50 day EAEO testes (**i**), the accumulation of macrophages was present in areas with reduced tubule diameter, whereas in severe 50 day EAEO testes (**l**) macrophages were more evenly distributed in the interstitial space. Scale bars represent 100 μm.

3.3.2.2. CD45+ leukocytes and CD3+ T cells numbers were increased in EAEO testes

After gating out debris, doublets, and nonviable cells, flow cytometric analysis revealed an increased percentage of leukocytes (CD45+) in EAEO testes (**Fig. 24a and b**). Depending on the stage of the disease, the highest increase in the number of CD45+ cells was observed in severe EAEO testes, showing in some animals that nearly 50% of testicular cells were CD45+ leukocytes. Within the population of leukocytes, an increase of CD3+ T cell numbers was observed (**Fig. 24c**). Further analysis of different T cell subtypes within the gated CD3+ T cell population revealed an increase in the population of CD4+CD8- and activated CD4+CD25+ T cells in inflamed testes, while the percentage of CD4-CD8+ T cells was decreased, by comparison with untreated and adjuvant control testes. Interestingly, a new subpopulation of double positive CD4+CD8+ T cells within testicular CD3+ T cell population was identified in EAEO testes (**Fig. 24d**). Moreover, the CD4+/CD8+ T cell ratio showed an approximately 5-fold increase in EAEO testes, by comparison with untreated and adjuvant control testes (**Fig. 24e**).
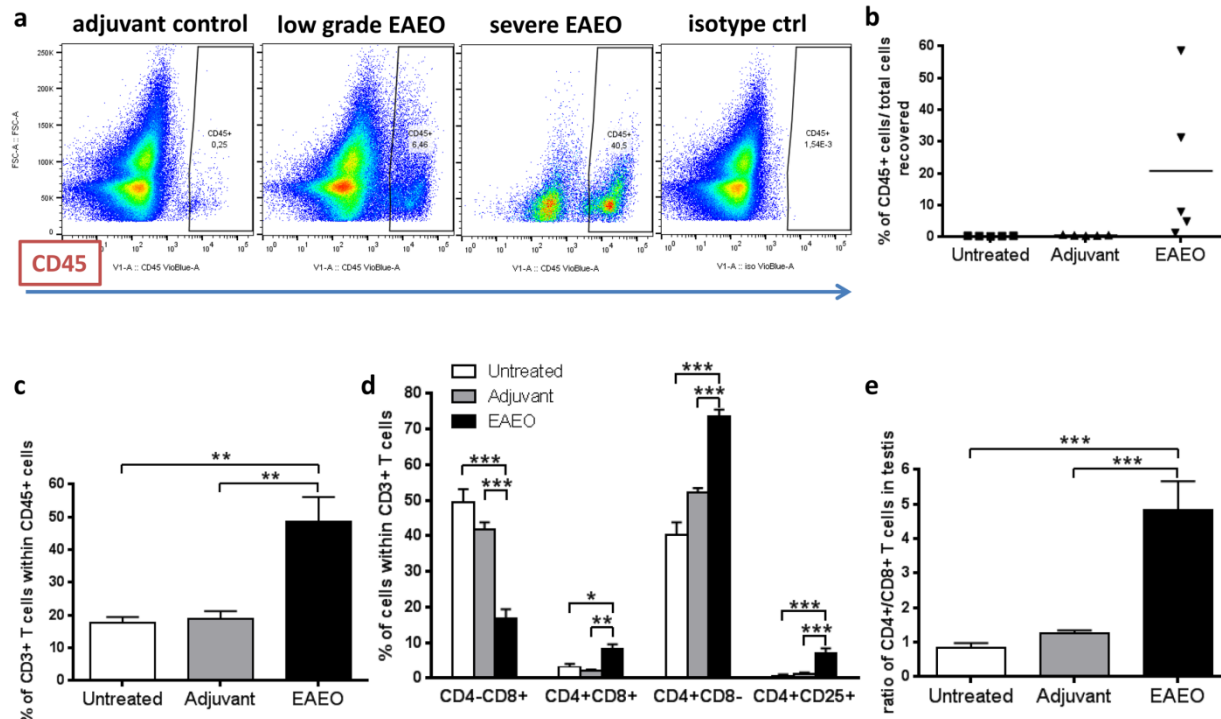
Figure 24: T cells (CD3+) and their different subtypes (CD4-CD8+, CD4+CD8+, CD4+CD8- and CD4+CD25+) were increased in EAEO testes.
Representative flow cytometry plots for testicular CD45+ leukocytes (**a**) evaluated in the testicular single cell suspension. Percentage of CD45+ leukocytes (**a, b**), CD3+ T cells within CD45+ leukocytes (**c**) and different subtypes of CD3+ T cells such as CD4-CD8+, CD4+CD8+, CD4+CD8- and CD4+CD25+ T cells (**d**) was analyzed in untreated, adjuvant control and EAEO testicular single cell suspension 50 days after the first immunization, by flow cytometry. The ratio between CD4+ / CD8+ T cells in testes from untreated, adjuvant control and EAEO mouse was calculated using flow cytometric analysis (e). After gating out cell debris, doublets and nonviable cells, the population of CD45+ leukocytes and CD3+ T cells was selected for further analysis. Data are expressed as mean ± SEM (n = 5 animals per group); *P<0.05, **P<0.01, ***P<0.001, all other comparisons were not statistically significant. (Courtesy of Dr. Monika Fijak).

3.4. Peritubular cells did not proliferate in EAEO testes

PCNA staining for detecting cell proliferative ability in testes was performed in order to evaluate if the morphological change in the distribution of the αSMA layer was due to a potential for proliferation of peritubular cells. PCNA staining showed that in untreated (**Fig. 25a**) and adjuvant control (**Fig. 25b**) testes, spermatogonia and spermatocytes in the seminiferous tubules were proliferating. This proliferation was gradually lost in low grade EAEO in the areas where the seminiferous epithelium was affected (**Fig. 25c**). In

severe EAEO, only a small number of cells within the seminiferous epithelium showed evidence of proliferation but not peritubular cells. Interestingly, some cells in the interstitial space in EAEO testes showed proliferative activity.
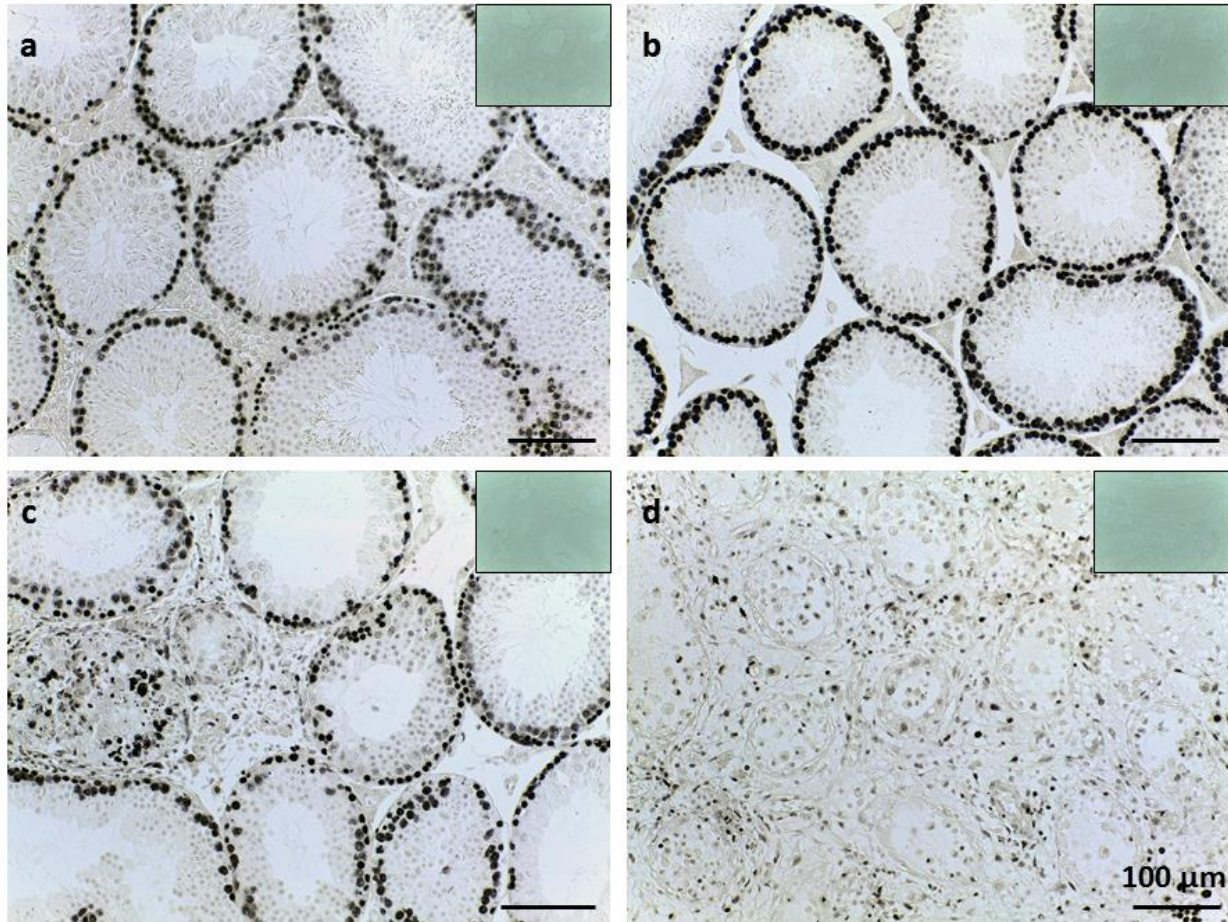
Figure 25: Proliferation of testicular cells was altered in EAEO testes.
PCNA staining of paraffin-embedded testicular sections from untreated (**a**), adjuvant control (**b**), low grade EAEO (**c**) and severe EAEO (**d**) mice 50 days after the first immunization. Under normal conditions, spermatogonia and spermatocytes were PCNA positive (**a, b**). During inflammation, a very small number of germ cells was PCNA positive particularly in seminiferous tubules with smaller diameter in closer proximity to leukocytic infiltrates and also some cells in the interstitial space were PCNA positive (**c, d**). Insets are negative controls lacking primary antibody. Scale bars represent 100 µm.

3.5. Expression of activin, inhibin and follistatin was altered in EAEO testes

3.5.1. Localization of activin βA in normal and inflamed mouse testes

Activin βA immunofluorescence staining (**Fig. 26**) revealed that the βA subunit was localized mainly in the cytoplasm of Sertoli cells, as well as in some interstitial cells in untreated and adjuvant control testes at 30 (**Fig. 26a, b**), 50 (**Fig. 26e, f**) and 80 (**Fig. 26i, j**) days. A similar pattern of activin βA expression was also observed in low grade EAEO at 30 (**Fig. 26c**), 50 (**Fig. 26g**) and 80 (**Fig. 26k**) days. In contrast, in severe EAEO testes at 30 (**Fig. 26d**), 50 (**Fig. 26h**) and 80 (**Fig. 26l**) days after the first immunization, strong activin βA staining was detectable in cells within the inflammatory infiltrates and in Sertoli cells.
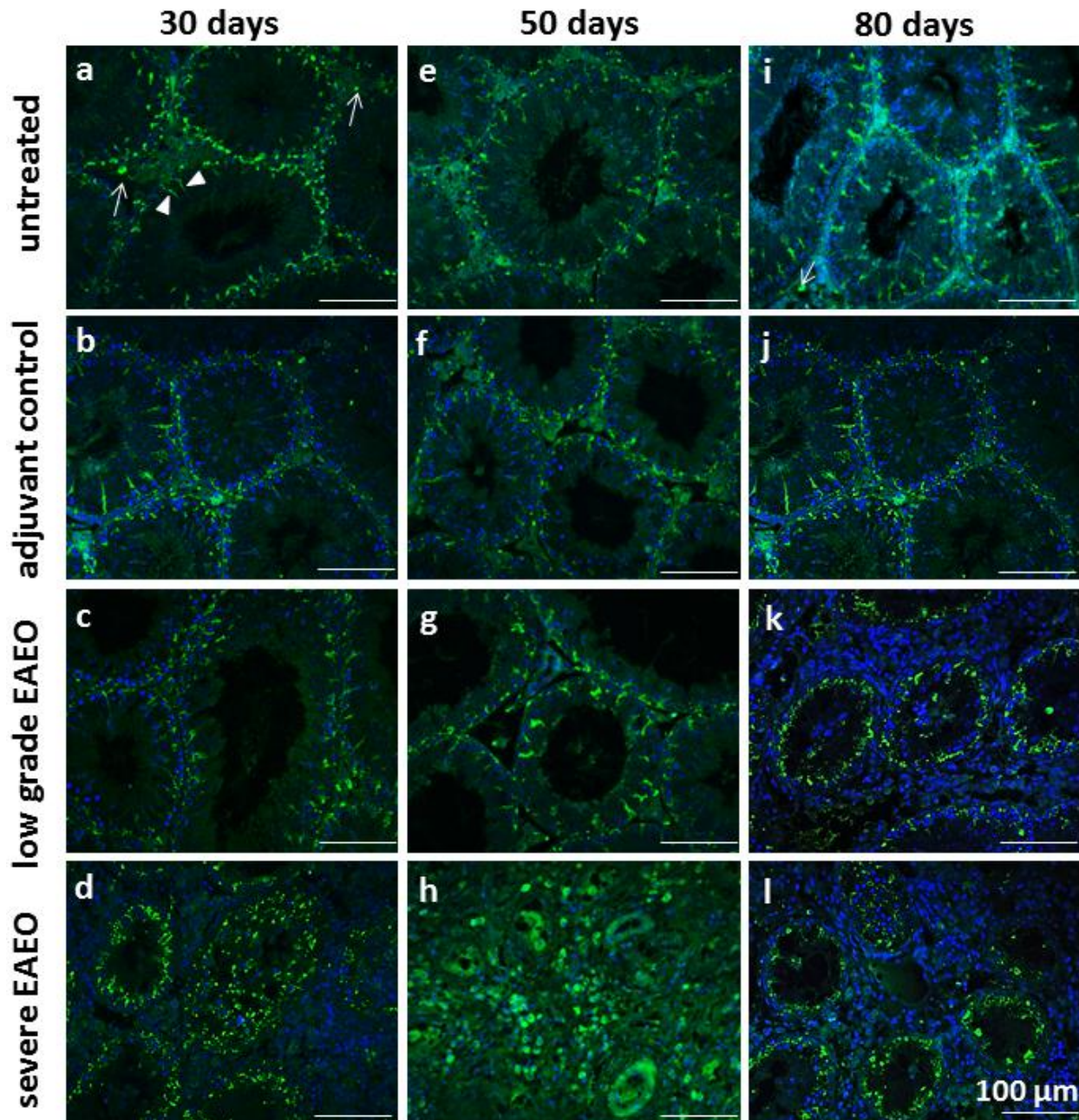
Figure 26: **Localization of activin βA subunit in EAEO testes was different from normal testes.**

Immunofluorescence staining of activin βA subunit using the E4 antibody on paraffin sections from untreated **(a, e, i)**, adjuvant control (**b, f, j**), low grade (**c, g, k**) and severe EAEO (**d, h, l**) testes at 30 (**a - d**), 50 (**e - h**) and 80 (**i - l**) days after the first immunization. The activin βA subunit was localized in the cytoplasm of Sertoli cells (arrowheads), peritubular cells and some interstitial cells (arrows) in untreated, adjuvant controls and low grade EAEO. In severe EAEO testes, the staining was present in Sertoli cells and individual immune cells (**d**, **h, l**). Scale bars represent 100 μm.

3.5.2. Activin A and B but not inhibin expression was changed in EAEO testes

Activin A (**Fig. 27a**), activin B (**Fig. 27b**) and inhibin (**Fig. 27c**) protein levels in EAEO testes were similar to untreated and adjuvant control testes at 30 days after the first immunization. In contrast, in 50 days EAEO testes, protein levels of activin A and B showed an approximately 4-fold and 2-fold increase, respectively, by comparison with untreated and adjuvant control mice, whereas inhibin levels in EAEO testes did not show significant change compared to both controls. In the chronic phase of the disease at 80 days, no significant change in the testicular concentrations of activin A and B or inhibin was detected, although a slight increase in protein levels of activin A and B was observed by comparison with controls (**Fig. 27**).
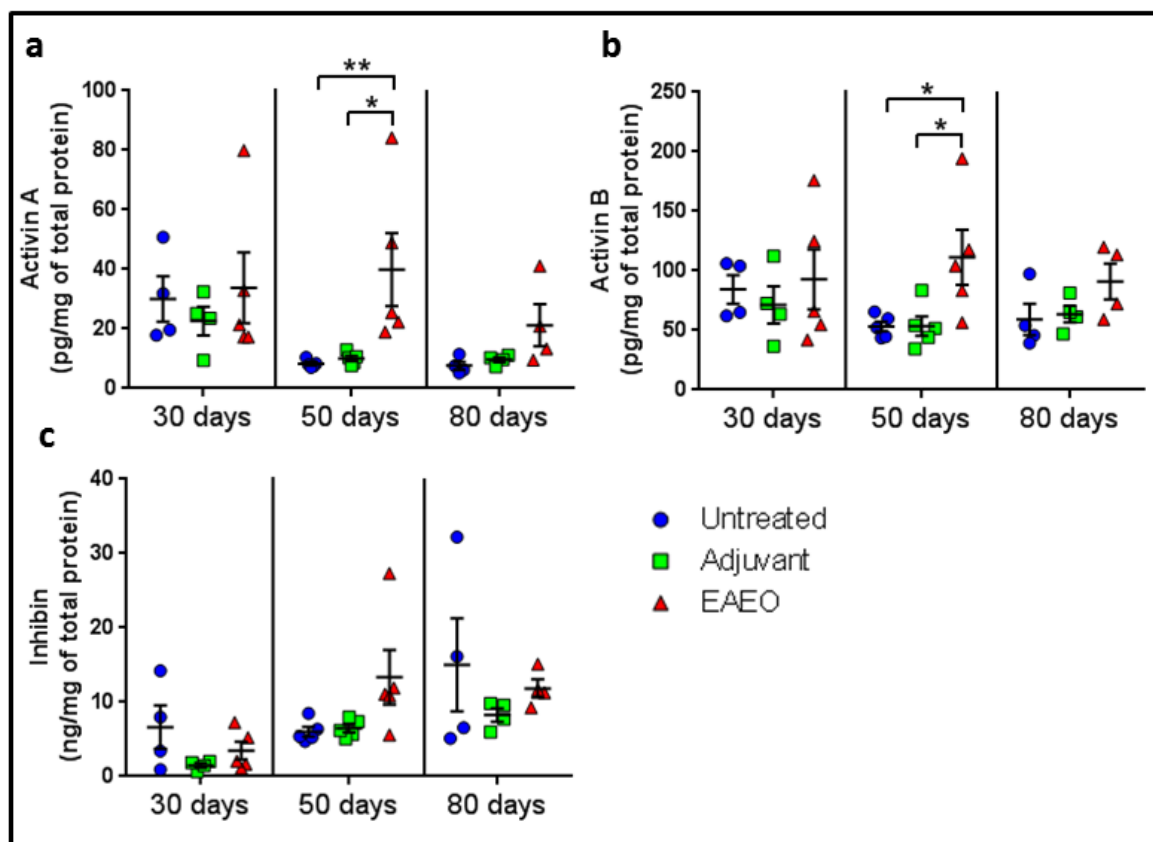
Figure 27: Elevated protein levels of activins A and B and inhibin in EAEO testes. Protein levels of activin A (**a**), activin B (**b**) and inhibin (**c**) were measured in testicular homogenates from untreated, adjuvant control and EAEO animals 30, 50 and 80 days after the first immunization. Data are represented as mean ± SEM of 4 - 5 animals per group. Statistical analysis was done using one-way ANOVA followed by Tukey's multiple comparisons; *P<0.05, **P<0.01, all other comparisons were not statistically significant.

Interestingly, gene expression analysis showed no significant change in activin βA (*Inhba*) mRNA levels in testes of all mice at any time point (**Fig. 28a**). The mRNA levels of activin βB (*Inhbb*) (**Fig. 28b**) and inhibin α (*Inha*) (**Fig. 28c**) subunits were unchanged in EAEO testes, untreated and adjuvant controls at 30 and 50 days after the first immunization, however, their expression decreased in 80 days EAEO testes compared to adjuvant control testes (**Fig.28b and c**).
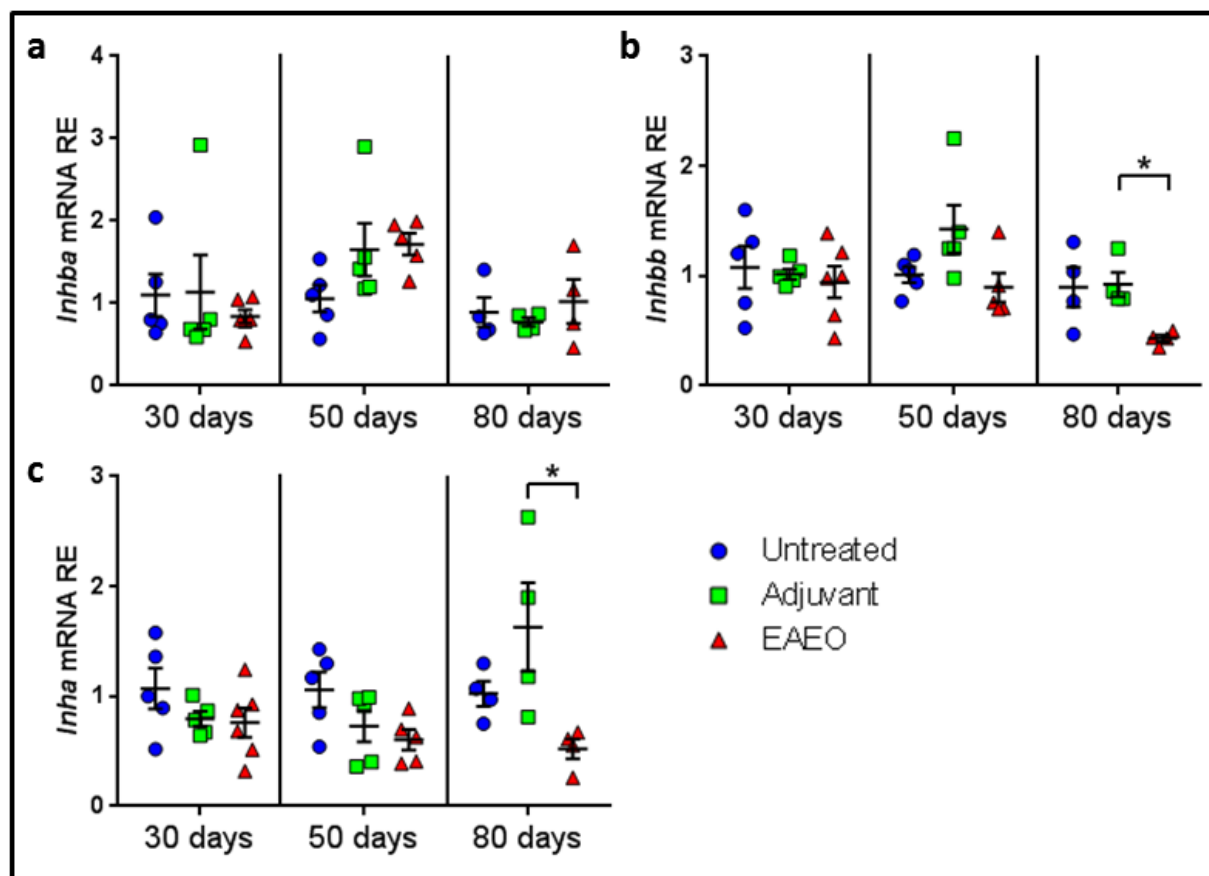
Figure 28: Decreased mRNA expression of inhibin subunits *Inhbb* (inhibin βB) and *Inha* (inhibin α) in 80 day EAEO testes.
Relative mRNA expression of *Inhba* (inhibin βA) (**a**), *Inhbb* (inhibin βB) (**b**), *Inha* (inhibin α) (**c**) in testes from untreated, adjuvant control and EAEO mice 30, 50 and 80 days after the first immunization, analyzed by quantitative RT-PCR. Data are represented as mean ± SEM of 4 - 5 animals per group. Statistical analysis was done using one-way ANOVA followed by Tukey's multiple comparisons; *P<0.05, **P<0.01, ***P<0.001, all other comparisons were not statistically significant.

3.5.3. Activin A receptor expression was decreased in EAEO testes

In order to elucidate the influence of testicular inflammatory processes on activin A signaling, mRNA expression of activin receptors was analyzed. Interestingly, activin A receptor type IB (*Acvr1b*) mRNA expression was decreased in 50 and 80 days, but not in 30 day EAEO testes, by comparison with untreated and adjuvant control testes (**Fig. 29a**). Similarly, activin receptor type IIB (*Acvr2b*) mRNA levels were decreased in 50 days EAEO testes, by comparison with untreated control testes (**Fig. 29b**). No significant difference in the *Acvr2b* mRNA expression levels was detected in testes from 30 and 80 days EAEO animals, by comparison with control testes (**Fig. 29b**).
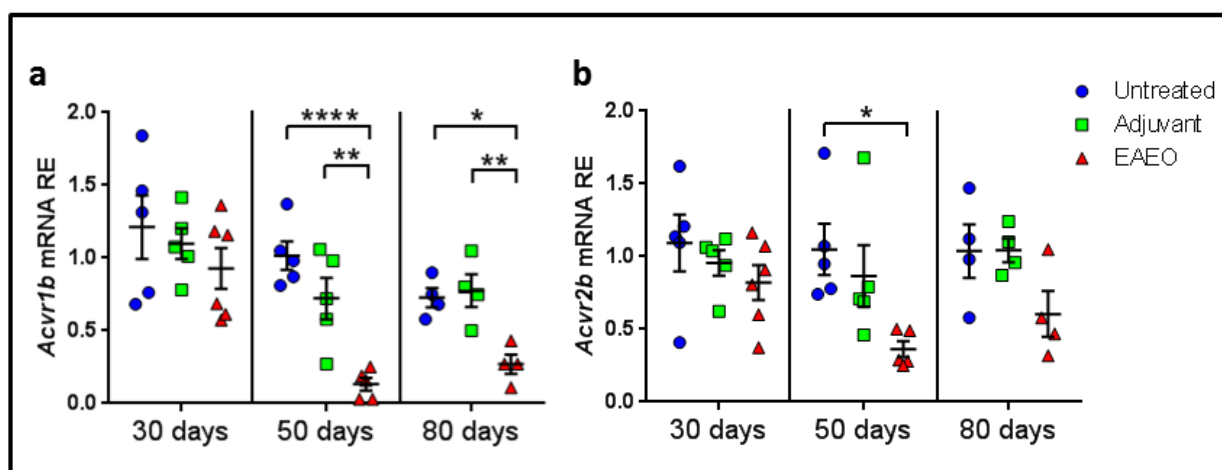
Figure 29: Decreased mRNA expression of activin A receptors in EAEO testes.
Relative mRNA expression of *Acvr1b* (activin receptor, type IB) (**a**) and *Acvr2b* (activin receptor, type IIB) (**b**) in testes from untreated, adjuvant control and EAEO mice 30, 50 and 80 days after the first immunization, analyzed by quantitative RT-PCR. Data are represented as mean ± SEM of 4 - 5 animals per group. Statistical analysis was done using one-way ANOVA followed by Tukey's multiple comparisons; *P<0.05, **P<0.01, ***P<0.001, all other comparisons were not statistically significant.

3.5.4. Follistatin expression was upregulated in EAEO mouse testes

Protein levels of follistatin (**Fig. 30a**) were unchanged in testes of all mice investigated at 30 days after the first immunization. In contrast, elevated testicular concentration of follistatin was measured in EAEO at 50 and 80 days after the first immunization by comparison with both controls (**Fig. 30a**).

The mRNA levels of total follistatin *Fst* (**Fig. 30b**), tissue bound *Fst288* (**Fig. 30c**) and circulating *Fst315* form of follistatin (**Fig. 30d**) were not significantly changed at any time

points. However, mRNA levels of *Fst* showed a slight increase in expression in EAEO testis at 50 days and 80 days after the first immunization by comparison with both controls (**Fig. 30b**).
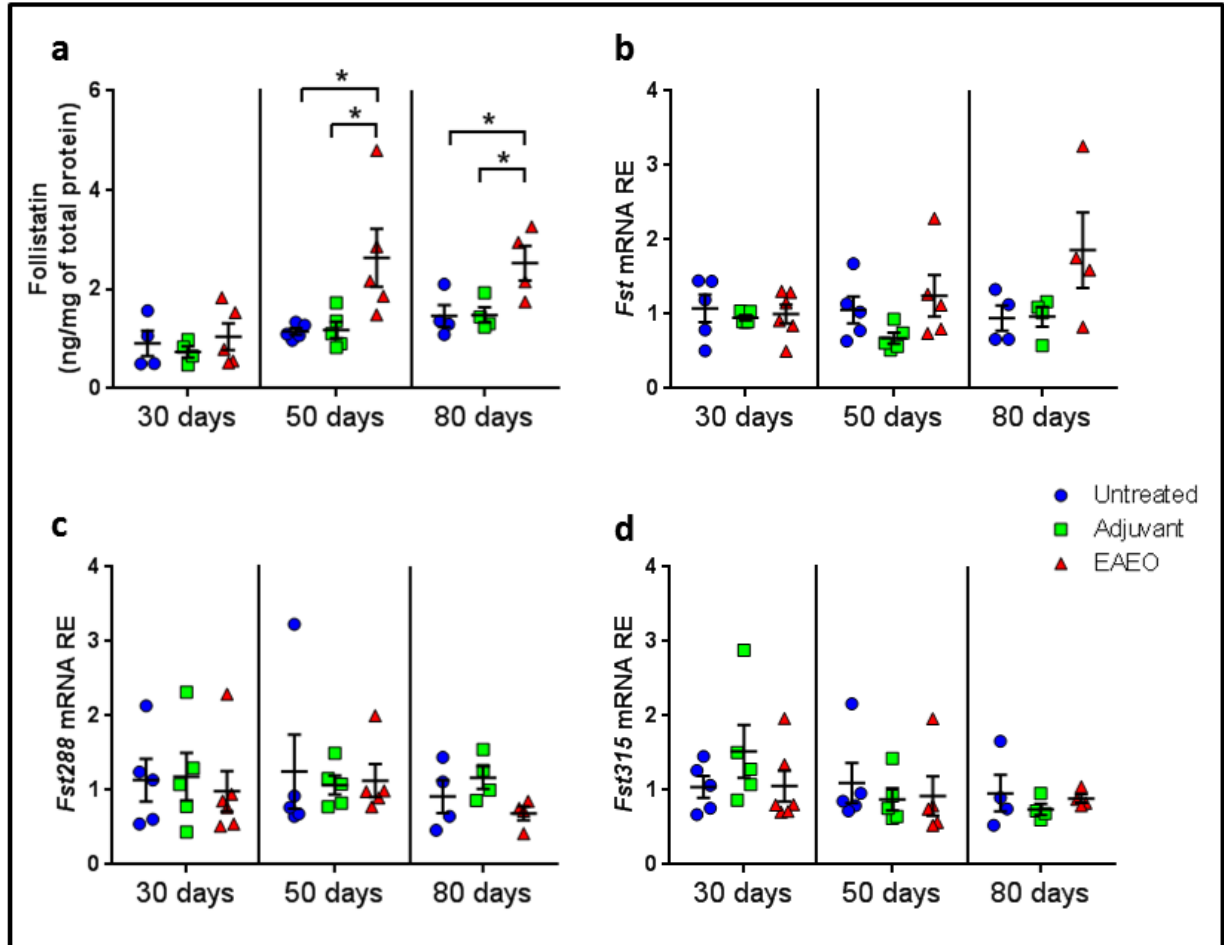
Figure 30: **Elevated levels of follistatin in EAEO testes.**
Protein levels of follistatin (**a**) and relative mRNA expression of *Fst* (**b**), *Fst288* (**c**), and *Fst315* (**d**) were measured in testicular homogenates from untreated, adjuvant control and EAEO mice testes 30, 50 and 80 days after the first immunization and relative mRNA expression was analyzed by quantitative RT-PCR. Data are represented as mean ± SEM of 4 - 5 animals per group. Statistical analysis was done using one-way ANOVA followed by Tukey's multiple comparisons; *P<0.05, all other comparisons were not statistically significant.

Study II

The aim of this study was to evaluate the potential therapeutic role of exogenous follistatin for treatment of testicular inflammation. Circulating follistatin levels were elevated in C57BL/6J mice by an injection of recombinant adenovirus-associated viral vector containing the gene cassette of the circulating FST315 form of follistatin, 30 days before induction of EAEO. EAEO was induced using a modified immunization protocol with CFA + TH or CFA + NaCl for the first immunization and IFA + TH or IFA + NaCl for the following two booster immunizations. <u>The immunization protocol in Study II was modified according to the Monash University Animal Ethics committee requirements regarding the use of the adjuvants.</u> All immunizations were followed by an i.p. injection of *Bordetella pertussis* toxin. The induction rate of EAEO, histopathological changes, inflammatory and fibrotic responses as well as follistatin, activin and hormonal systemic and testicular levels were analyzed at 30 and 50 days after the first immunization.

3.6. Serum levels of follistatin were elevated after FST315 vector injection

Follistatin and activin A serum levels were measured 30 days after the injection of the FST315 vector and the empty vector as a control (one day before the first immunization). Follistatin serum levels were 5-fold elevated in mice that received the FST315 vector (FST) compared to control mice injected with an empty vector (EV) (**Fig. 31a**) alone. Activin A serum levels were not different between FST and EV mice (**Fig. 31b**).
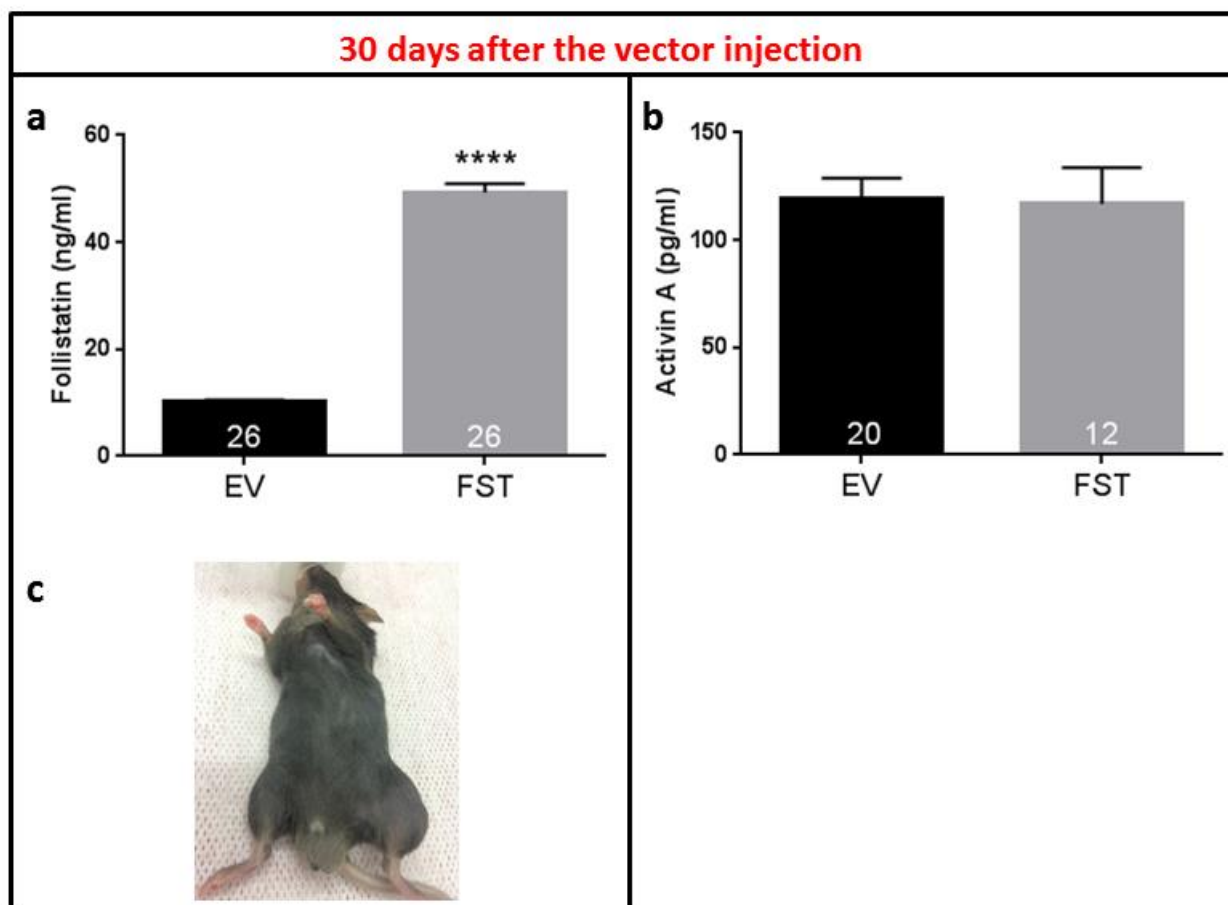
Figure 31: Elevated follistatin serum levels in mice 30 days after injection of the FST315 vector (one day before induction of EAEO).
Protein levels of follistatin (**a**) and activin A (**b**) were measured in serum from mice 30 days after the i.m. injection with empty (EV) or FST315 (FST) vector and exactly one day before the start of the induction of EAEO. Data are represented as mean ± SEM of 12- 26 animals per group; numbers of animals per group are shown in the respective columns. Statistical analysis was done using unpaired T-test with Welch's correction; ****$P<0.0001$, all other comparisons were not statistically significant. Representative image of a male mouse injected with a follistatin vector in its tibialis anterior muscle developing a muscle hypertrophy 30 days after the vector injection (**c**).

In order to verify whether follistatin levels were elevated at the final time points of the experiment, i.e. at 30 days and 50 days after the first immunization, follistatin levels were measured in serum of all mice. At 30 days after the first immunization (**Fig. 32a**), follistatin levels were 5-fold elevated in mice that received the FST315 vector and 3-fold elevated at 50 days after the first immunization compared to control mice injected with an empty vector (EV) alone (**Fig. 32b**).
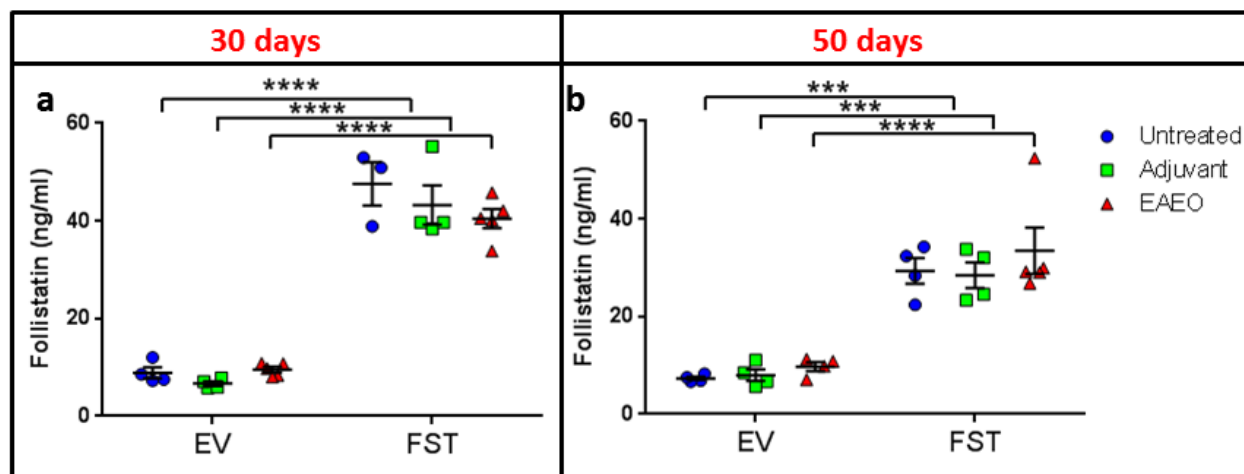
Figure 32: Elevated follistatin serum levels in mice 30 and 50 days after the first immunization.
Follistatin protein levels were measured in serum from untreated, adjuvant control and TH-immunized mice (EAEO) injected with empty (EV) or FST315 (FST) vector 60 and 80 days after the vector injections (30 [**a**] and 50 [**b**] days after the first immunization, respectively). Data are represented as mean ± SEM of 3 - 6 animals per group. Statistical analysis was done using one-way ANOVA followed by Tukey's multiple comparisons for all treatment groups and two-way ANOVA comparing EV and FST groups followed by Sidak's multiple comparisons; ***P<0.001, ****P<0.0001; all other comparisons were not statistically significant.

3.7.   Induction rate of EAEO

Similar to mice from group I (study I) that received three immunizations with TH in CFA, mice from group IV in study II injected with an empty vector showed a 2-fold reduction in the mean testis weight at 50 days (n = 4) after the first immunization, by comparison with untreated (n = 4) and adjuvant (n = 4) controls (**Fig. 33a**). Mice from group IV and V were immunized by using a modified immunization procedure, namely TH in CFA for the first immunization and TH with IFA for the following booster immunizations. Mice from group V treated with the FST315 vector (**Fig. 33b**) didn't show any change in the mean testis weight in all investigated experimental groups.
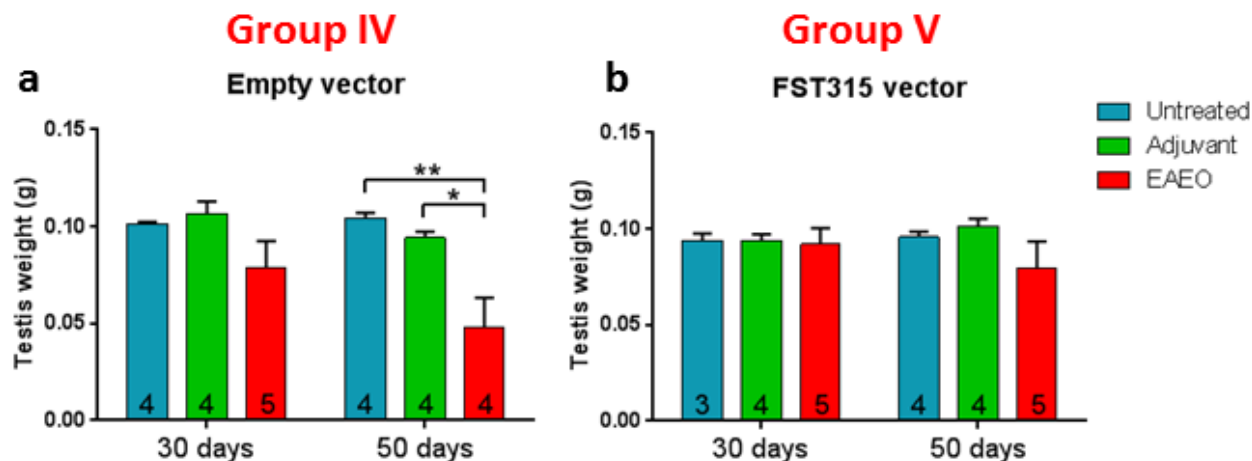
Figure 33: Testicular weights of mice in study II.
Paired testicular weight of untreated, adjuvant control and TH-immunized (EAEO) mice with normal (empty vector injection) (**a**) and elevated levels (FST315 vector injection) (**b**) of follistatin, 30 and 50 days after the first immunization (**a - b**). Data are expressed as mean ± SEM (exact numbers of animals per group are shown in the respective columns). Statistical analysis was done using one-way ANOVA followed by Tukey's multiple comparisons; *P<0.05, **P<0.01, all other comparisons were not statistically significant.

Successful induction of EAEO (**Table 5**) was determined based on parameters including reduced testis weight, histopathological changes in the testicular architecture (this aspect will be described in paragraph 3.8) and expression of pro-inflammatory mediators.

40% (2/5) of mice from group IV injected with an empty vector before the induction of EAEO developed the disease 30 days after the first immunization compared to 75% (3/4) of mice that developed the disease at 50 days. In group V (FST315 vector injected), 40% (2/5) of mice developed the disease at 30 days and 50 days after the first immunization.

Table 5: Induction rate of EAEO in mice from study II.

a	Treatment group IV	Induction rate at 30 days (number of animals)	Induction rate at 50 days (number of animals)
	Untreated	0% (0/4)	0% (0/4)
	Adjuvant	0% (0/4)	0% (0/4)
	EAEO	40% (2/5)	75% (3/4)

b	Treatment group V	Induction rate at 30 days (number of animals)	Induction rate at 50 days (number of animals)
	Untreated	0% (0/3)	0% (0/4)
	Adjuvant	0% (0/4)	0% (0/4)
	EAEO	40% (2/5)	40% (2/5)

Group IV: mice injected with a recombinant adenovirus-associated viral vector carrying an empty gene cassette and immunized with CFA for the first immunization and IFA for the two following immunizations, group V: mice injected with a recombinant adenovirus-associated viral vector carrying a gene cassette of the circulating FST315 form of follistatin and immunized with CFA for the first immunization and IFA for the two following immunizations.

3.8.　Morphological changes in EAEO testes of mice with normal and elevated levels of follistatin

Histopathological changes in the testes of immunized mice from study II were assessed by PAS staining as represented in **Figure 34**. Moreover, the fibrotic response in the testes of investigated animals was assessed by Masson's trichrome staining as shown in **Figure 35** and by quantitative RT-PCR of fibrotic marker mRNA expression as shown in **Figure 36**.

3.8.1. Scoring of testicular damage in mice injected with an empty vector or the FST315 vector

PAS staining was performed in order to assess the histopathological changes observed in testes of mice from study II (**Figure 34**). Testes from immunized mice showed a variable grade of EAEO development between individual mice. Overall, a milder form of the disease was observed by comparison with the mice developing EAEO from study I, where CFA was used for all three immunizations. Therefore, a scoring system of the disease progression was established as follows:

- score 0 - normal testicular histology (**Fig. 34a**),
- score 1 - normal testicular histology, but elevated levels of inflammatory mediators (TNF, IL-6, IL-10 and MCP-1) in the testis evaluated by quantitative RT-PCR as described in section 3.9 (**Fig. 34b**),
- score 2 - focal leukocytic infiltrates accompanied by reduced diameter of the seminiferous tubules representing altered spermatogenesis (some seminiferous tubules has normal spermatogenesis) (**Fig. 34c**),
- score 3 - sloughing of germ cells, numerous leukocytic infiltrates within the interstitial space, but also within some seminiferous tubules (**Fig. 34d**),
- score 4 - significantly smaller testis weight showing a very damaged testicular histology, numerous leukocytic infiltrates, disrupted spermatogenesis and the majority of seminiferous tubules with reduced diameter (**Fig. 34e**),
- score 5 - significantly smaller testis weight representing a complete destruction of the testicular morphology, loss of germ cells and overall infiltration of the testis by immune cells (**Fig. 34f**).

All untreated and adjuvant control animals showed completely normal testicular morphology and spermatogenesis.
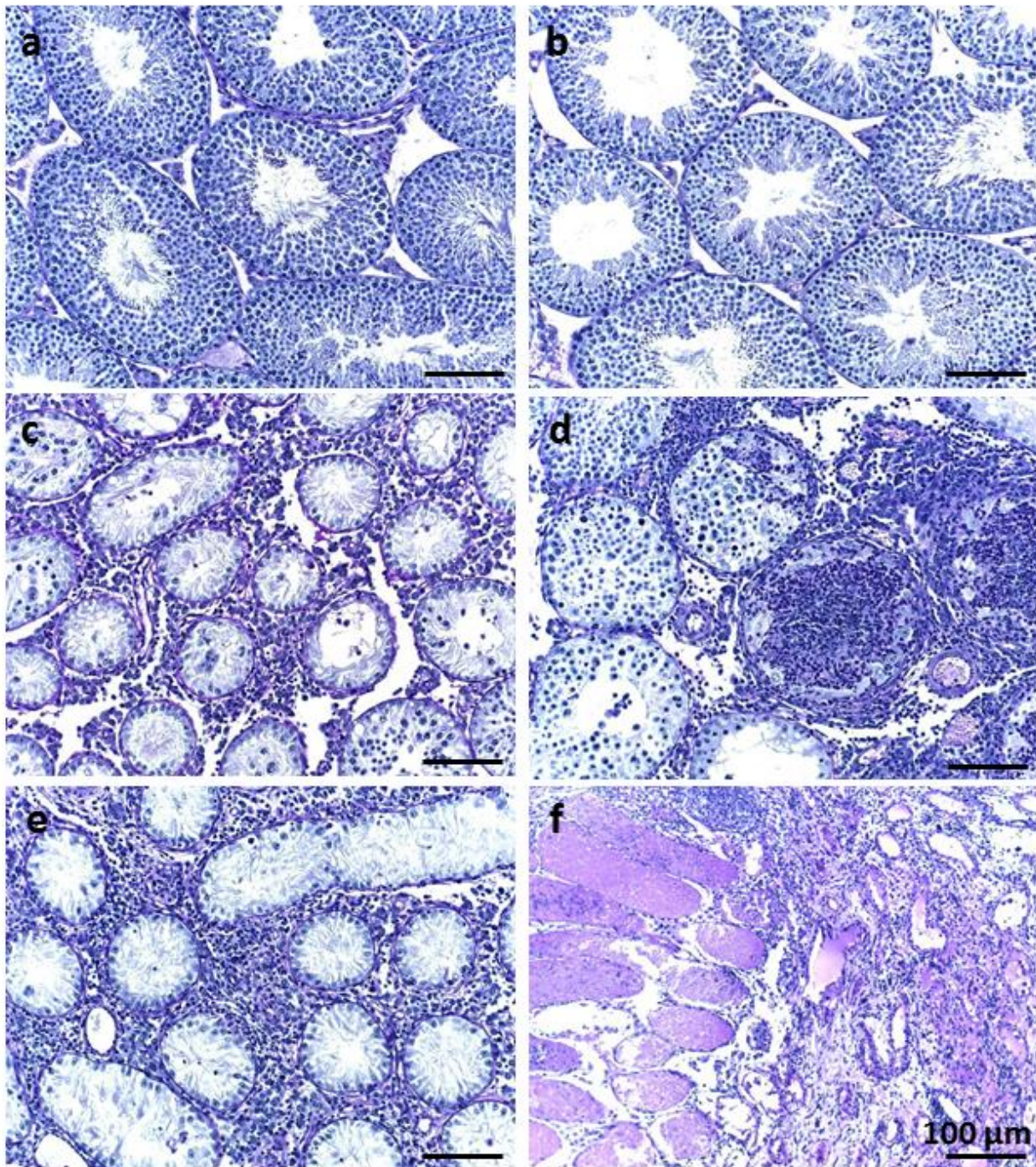
Figure 34: **Score of EAEO development in mice from study II.**
PAS staining of testicular paraffin sections from immunized mice. Score 0 (**a**), score 1 (**b**), score 2 (**c**), score 3 (**d**), score 4 (**e**), score 5 (**f**). Scale bars represent 100 μm.

3.8.2. Fibrotic responses in EAEO testes of mice with normal and elevated levels of follistatin

Masson's trichrome staining on testicular sections, from both TH-immunized mice with normal levels of follistatin and of those with elevated levels of follistatin, revealed an increase in collagen fibers in the areas with leukocytic accumulation and smaller seminiferous tubules with impaired spermatogenesis (score 2; **Fig. 35c**). The fibrotic response was stronger in testes of TH-immunized mice during the progression of the disease as classified by score 3 and 4 (**Fig. 35d and e**, respectively) by comparison with untreated and adjuvant controls and testes of TH-immunized mice with scores of 0 to 2. An evident increase in the collagen deposits was observed at score 5 in EAEO testes, where the morphology was destroyed (**Fig 35f**), by comparison with untreated and adjuvant controls and testes of TH-immunized mice with scores of 0 to 2.
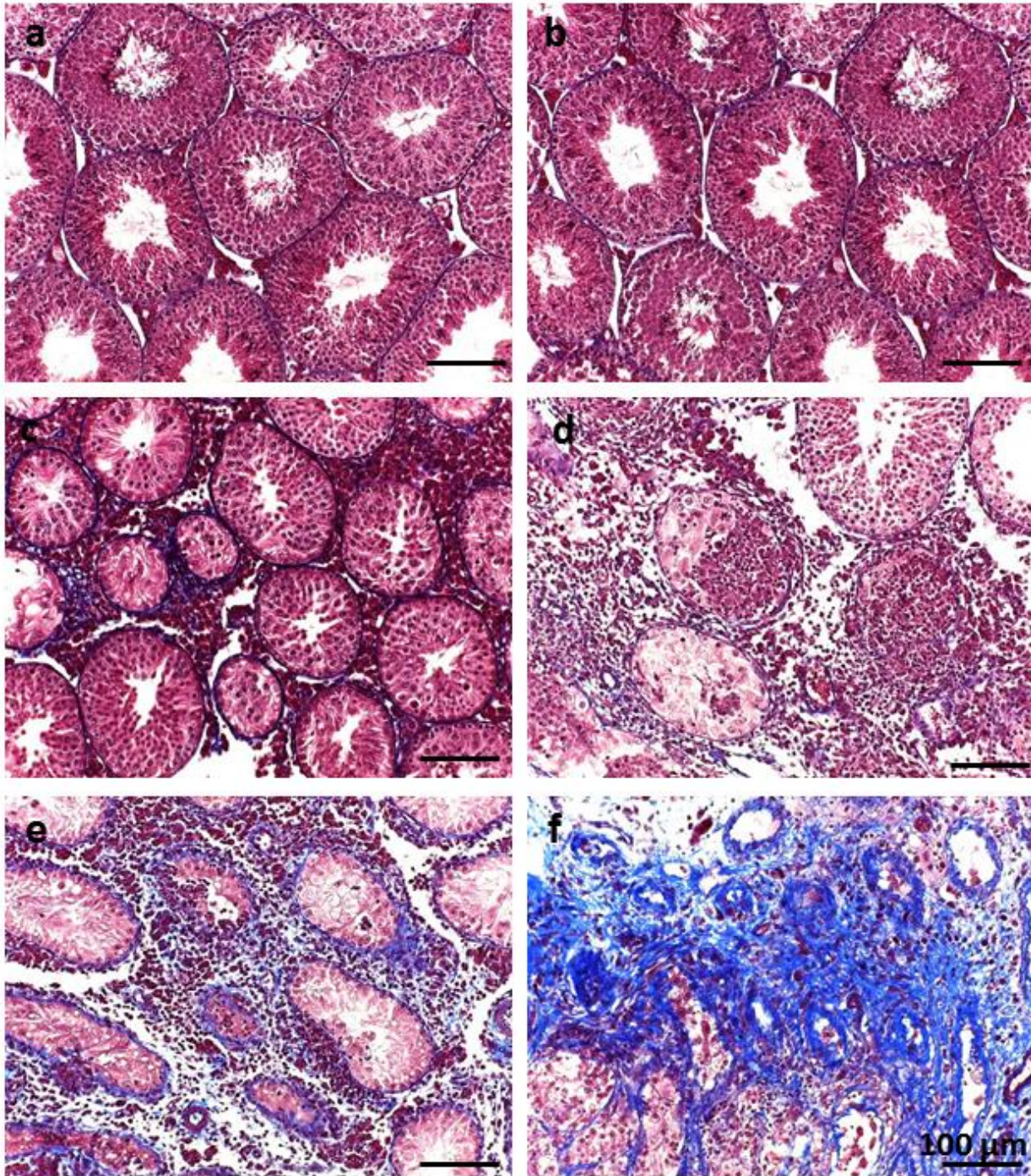
Figure 35: Fibrotic responses in EAEO testes of mice with either normal or elevated levels of follistatin.
The fibrotic response was evaluated by Masson's trichrome staining on testicular paraffin sections from TH-immunized mice (EAEO). The blue color represents the collagen fibers. Score 0 (**a**), score 1(**b**), score 2 (**c**), score 3 (**d**), score 4 (**e**), score 5 (**f**). Scale bars represent 100 μm.

Moreover, the fibrotic response was further evaluated by quantification of *Col1a1* (collagen type I, alpha 1) and *Acta2* (αSMA) mRNA expression in mice from both treatment groups (**Figure 36**) as both collagen type I, alpha 1 and αSMA are considered as fibrotic markers. Although no difference in the expression levels of these two markers was recorded between TH-immunized mice (EAEO group) and their respective untreated and adjuvant controls, it is important to mention that one of the TH-immunized mice from the EV group which developed EAEO at a score of 5 (**Fig. 36a and b**) had elevated expression of *Col1a1* by comparison with untreated and adjuvant controls, which was consistent with the histologically observed increase of collagen in its testis.
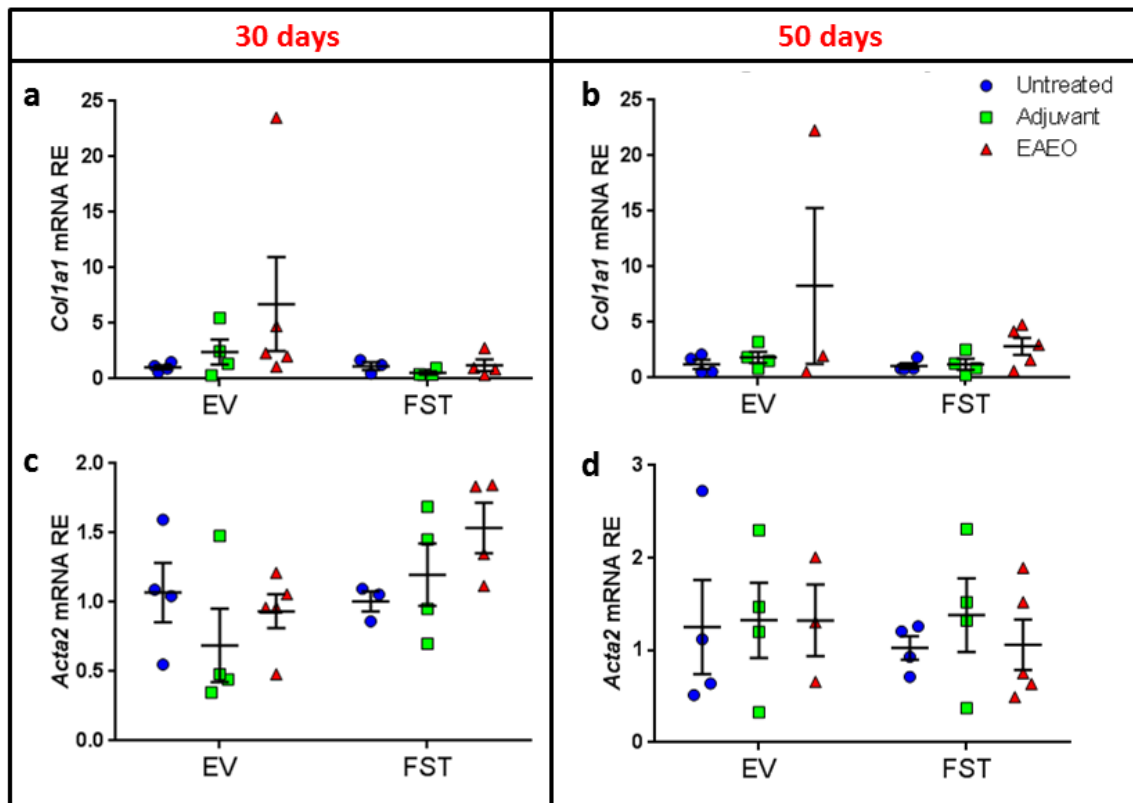
Figure 36: Expression of fibrotic markers in testes of mice with either normal or elevated levels of follistatin.
Relative mRNA expression of *Col1a1* (collagen type I alpha 1) (**a, b**) and *Acta2* (alpha smooth muscle actin) (**c, d**) in testes from untreated, adjuvant control and TH-immunized mice (EAEO) injected with empty (EV) or FST315 (FST) vector 30 (**a, c**) and 50 (**b, d**) days after the first immunization, analyzed by quantitative RT-PCR. Data are represented as a mean ± SEM of 3 - 5 animals per group. Statistical analysis was done using one-way ANOVA followed by Tukey's multiple comparisons for all treatment groups and two-way ANOVA comparing EV and FST groups followed by Sidak's multiple comparisons.

3.9. Expression of inflammatory mediators was increased in EAEO testes of mice with normal and elevated levels of follistatin

As for study I, expression levels of inflammatory mediators in testes of TH-immunized mice from study II and their untreated and adjuvant controls were quantified using quantitative RT-PCR in order to assess whether elevated circulating follistatin had an effect on development of testicular inflammation.

At 30 days after the first immunization, the mRNA expression levels of TNF (**Fig. 37a**), MCP-1 (**Fig. 37c**), IL-10 (**Fig. 37e**) and IL-6 (**Fig. 37g**) in TH-immunized groups were unchanged in all animals. At 50 days after the first immunization, mRNA levels of TNF (**Fig. 37b**) and MCP-1 (**Fig. 37d**) were significantly higher in testes of TH-immunized mice from the EV group by comparison with untreated controls, as well as by comparison with adjuvant controls for TNF (**Fig. 37b**). This elevation of the levels of TNF and MCP-1 was also seen in testes of TH-immunized mice treated with FST315 vector (FST EAEO group) compared with their untreated and adjuvant controls, although it was not significant. In contrast, IL-6 mRNA expression was significantly higher in testes of TH-immunized mice from the FST group compared with adjuvant controls (**Fig. 37h**).
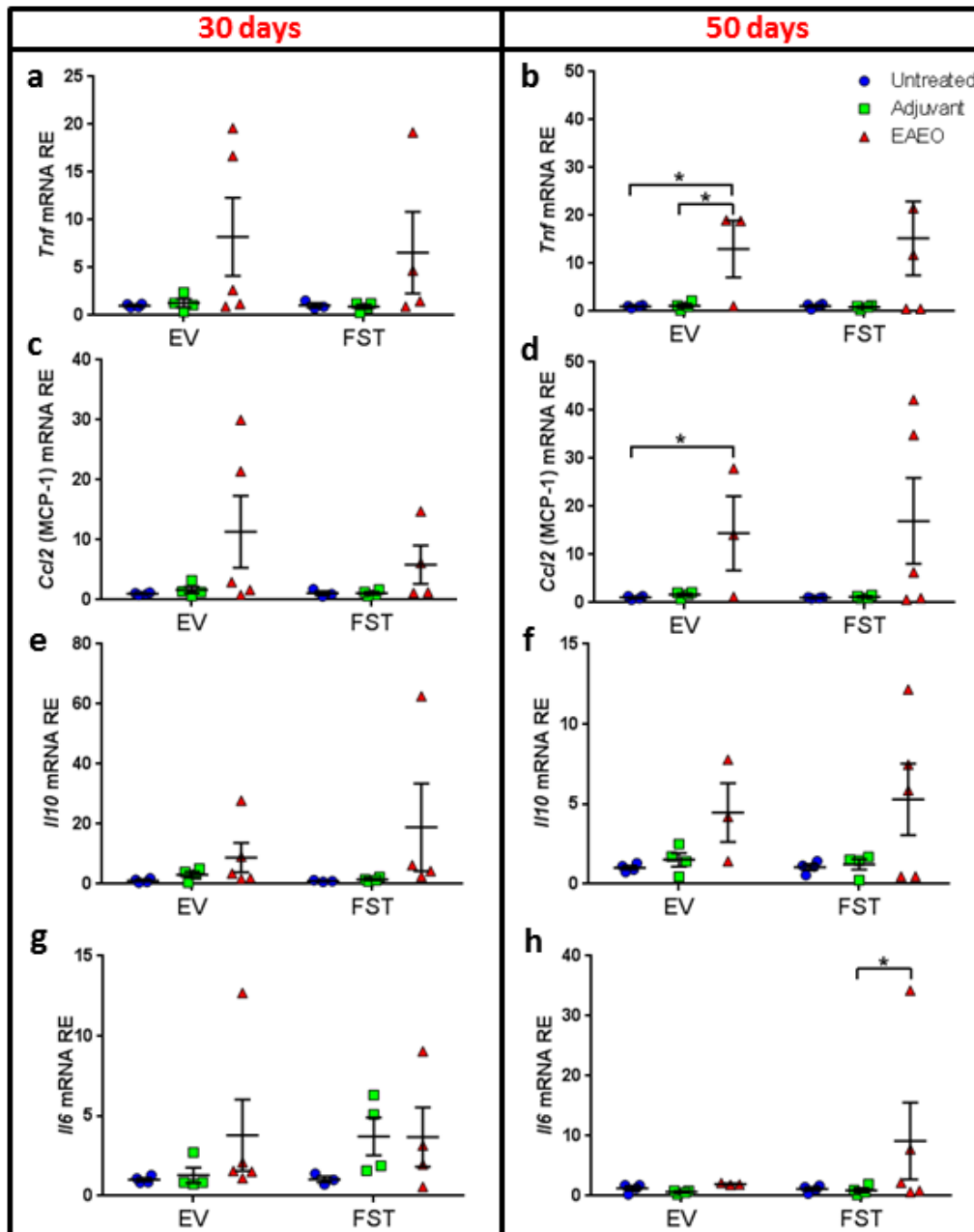
Figure 37: Expression of inflammatory mediators was elevated in EAEO testes of mice with either normal or elevated levels of follistatin.
Relative mRNA expression of *Tnf* (**a-b**), *Ccl2* (MCP-1) (**c-d**), *Il10* (**e-f**) and *Il6* (**g-h**) was measured in testes from untreated, adjuvant control and TH-immunized mice (EAEO) injected with empty (EV) or FST315 (FST) vector 30 (**a, c, e, g**) and 50 (**b, d, f, h**) days after first immunization, analyzed by quantitative RT-PCR. Data are represented as mean ± SEM (n = 3 - 5 animals per group). Statistical analysis was done using one-way ANOVA followed by Tukey's multiple comparisons for all treatment groups and two-way ANOVA comparing EV and FST groups followed by Sidak's multiple comparisons; *P<0.05, all other comparisons were not statistically significant.

3.10. Apoptotic cells were increased in EAEO testes of mice with normal and elevated levels of follistatin

Although not quantified, TUNEL staining revealed that under normal conditions, in untreated (**Fig. 38a**) and adjuvant (**Fig. 38b**) control testes a few apoptotic cells were present within the seminiferous epithelium. Similar amount of apoptotic cells was detected in testes of TH-immunized mice from both groups IV and V, which didn't develop any histological signs of EAEO, namely score 0 (**Fig. 38c**) and score 1 (**Fig. 38d**). An evident increase in the amount of apoptotic cells was visible starting from score 2 (**Fig. 38e**), particularly inside the smaller tubules. This increase was even more prominent at score 3 (**Fig. 38f**) and score 4 (**Fig. 38g**), until a complete loss of germ cells in the seminiferous epithelium at score 5 of EAEO was observed (**Fig. 38h**).
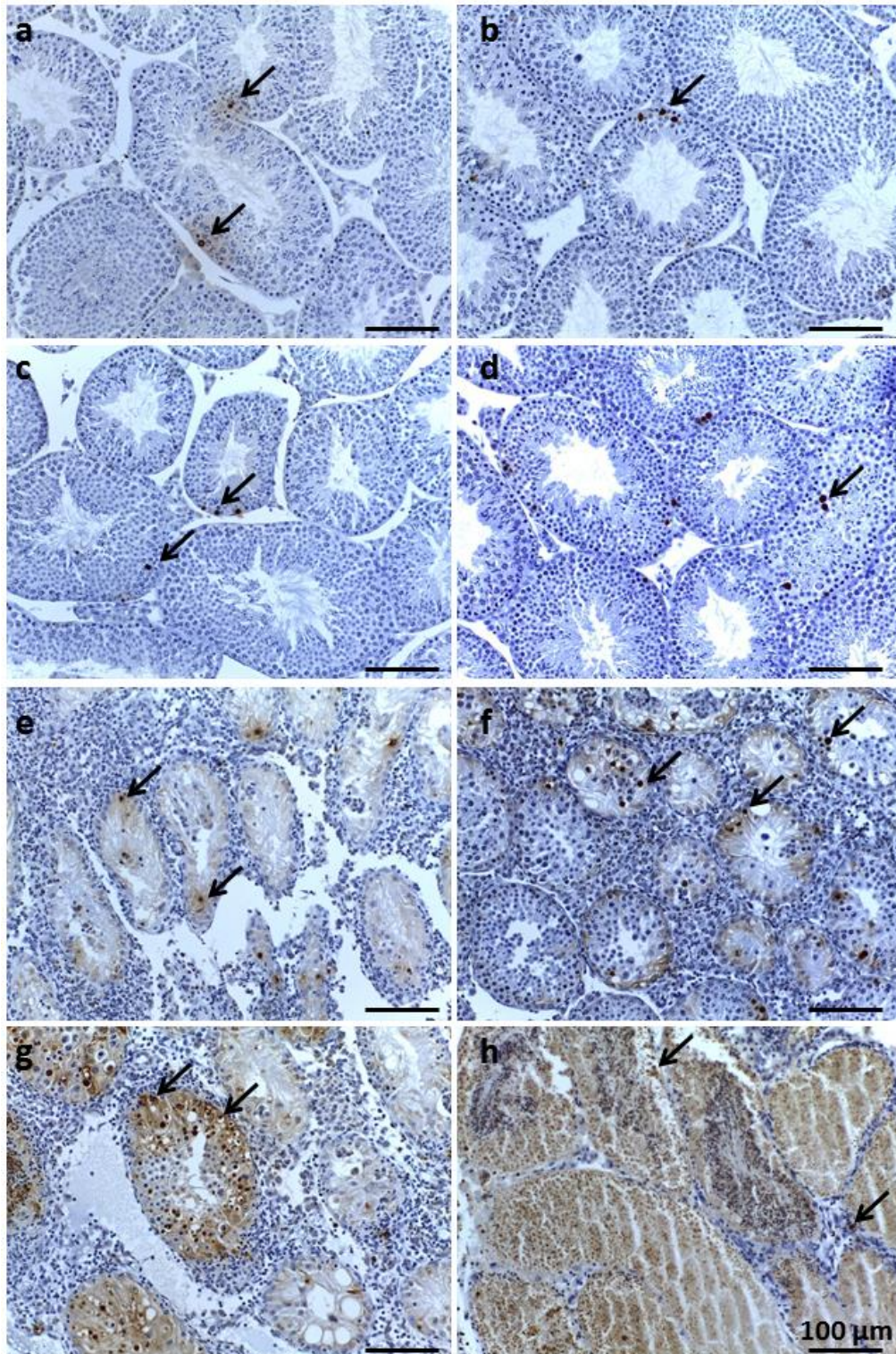
Figure 38: Increased amount of apoptotic cells in EAEO testes.
TUNEL staining on paraffin section from untreated (**a**), adjuvant control (**b**), and immunized mice testis, representing score 0 (**c**), score 1(**d**), score 2 (**e**), score 3 (**f**), score 4 (**g**) and score 5 (**h**). Arrows show apoptotic cells. Scale bars represent 100 µm.

3.11. BTB permeability was impaired in EAEO testes of mice with normal and elevated levels of follistatin

To assess BTB integrity in testes from immunized mice, a biotin tracer penetration experiment was performed. Under normal conditions, in untreated (**Fig. 39a**) and adjuvant (**Fig. 39b**) control testes, the biotin tracer was completely restricted to the interstitial space and in the basal part of the seminiferous epithelium, indicating an intact BTB. A similar observation was made in testes of TH-immunized mice from both groups IV and V representing score 0 (**Fig. 39c**) and score 1 (**Fig. 39d**). The disruption of BTB started to be visible at score 2 (**Fig. 39e**) more specifically in the areas of smaller tubules, where the tracer infiltrated into the adluminal region of the seminiferous epithelium. The disruption of the BTB integrity was evident at score 3 (**Fig. 39f**) and score 4 (**Fig. 39g**), where the tracer extensively permeated throughout the testis, including the seminiferous epithelium. The complete loss of the integrity of the BTB accompanying the complete destruction of the morphology was visible in EAEO testes representing score of 5 (**Fig. 39h**).
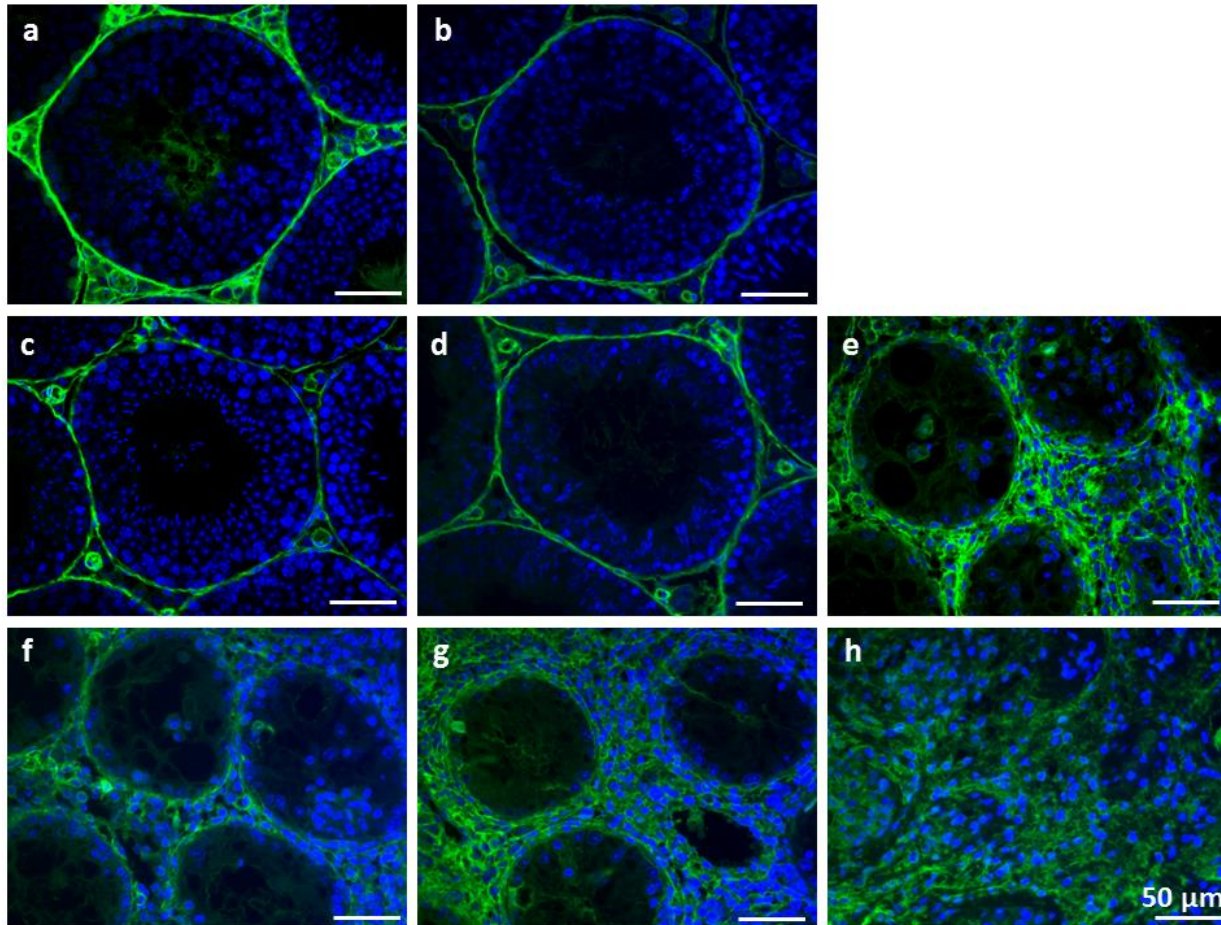
<u>Figure 39:</u> Disruption of BTB integrity in EAEO testes.
Assessment of BTB integrity using biotin tracer. The localization of the biotin tracer in testicular paraffin sections from untreated (**a**), adjuvant control (**b**), and TH-immunized mice (**c - h**) was directly visualized by florescence microscopy using streptavidin-AlexaFluor488 (green) conjugate. The images represent score 0 (**c**), score 1 (**d**), score 2 (**e**), score 3 (**f**), score 4 (**g**), score 5 (**h**). Nuclei were counterstained with DAPI. Scale bars represent 50 µm.

3.12. FSH, LH and testosterone levels in serum

The levels of gonadotropins and testosterone were analyzed in the serum of mice by RIA as shown in **Figure 40**. At 30 days after the first immunization, the levels of serum FSH were decreased in TH-immunized mice that received the FST315 vector compared with TH-immunized mice injected with an empty vector (EV) only (**Fig. 40a**). At 30 days after the first immunization, LH and testosterone levels were similar between all investigated groups, although an inter-animal biological variability was observed (**Fig. 40c and e**). At 50 days after the first immunization, serum FSH and LH levels were not changed in any group (**Fig. 40b and d**). In contrast, testosterone levels were significantly decreased in TH-immunized mice that received an empty vector compared to their untreated controls, and testosterone levels were also decreased in untreated controls with the FST315 vector compared with untreated mice with empty vector (**Fig. 40f**).
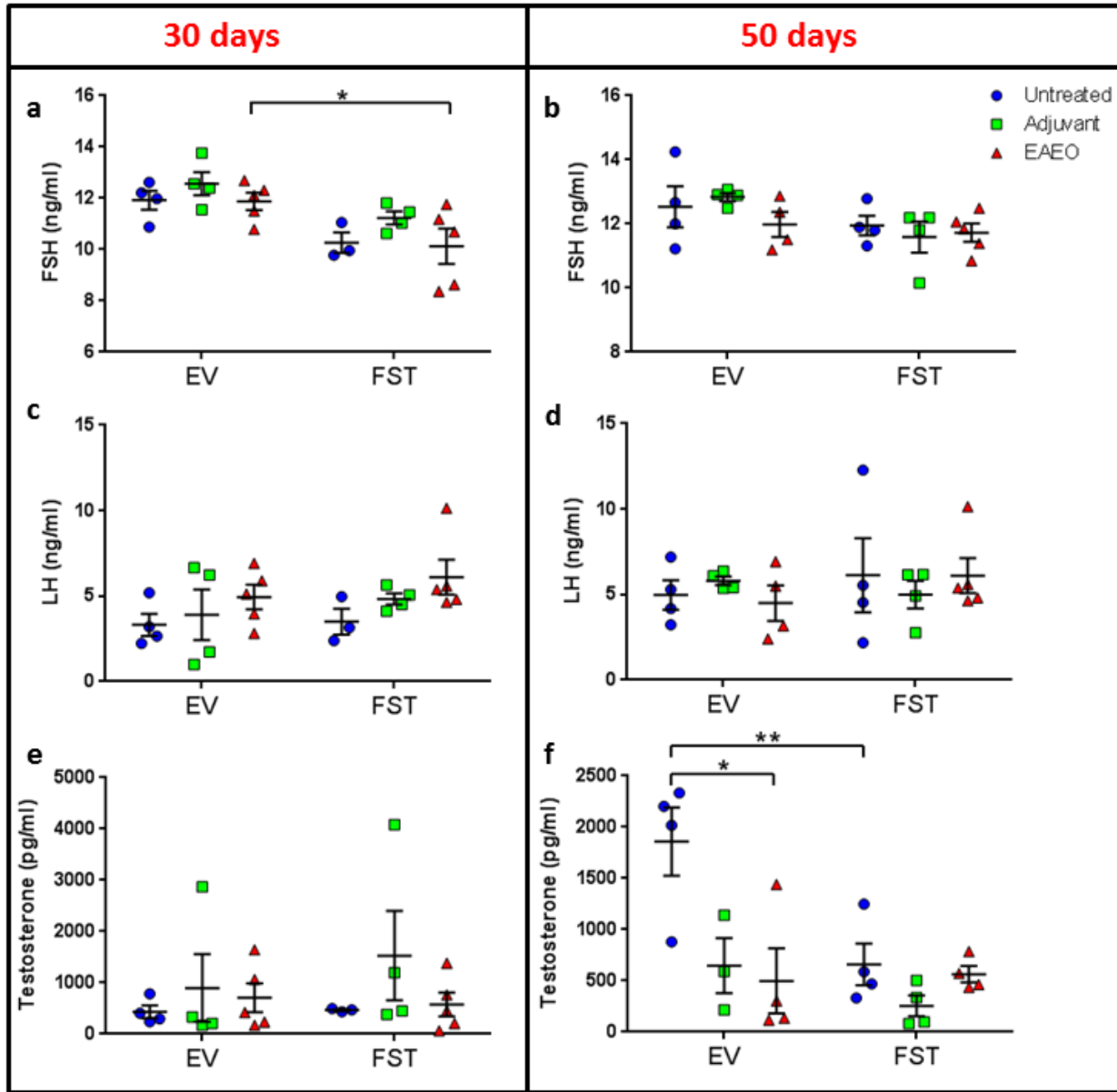
Figure 40: Levels of FSH were lower in TH-immunized mice with elevated levels of follistatin whereas levels of LH and testosterone were similar between mice with normal and elevated levels of follistatin.

FSH (**a - b**), LH (**c - d**) and testosterone (**e - f**) levels were measured in serum from untreated, adjuvant control and TH-immunized mice injected with empty (EV) or FST315 (FST) vector 30 (**a, c, e**) and 50 (**b, d, f**) days after the first immunization. Data are represented as mean ± SEM of 3 - 6 animals per group. Statistical analysis was done using one-way ANOVA followed by Tukey's multiple comparisons for all treatment groups and two-way ANOVA comparing EV and FST groups followed by Sidak's multiple comparisons; *P<0.05, **P<0.01; all other comparisons were not statistically significant.

3.13.   Expression of steroidogenic enzymes

Expression of steroidogenic regulators and enzymes in the testis was investigated by quantitative RT-PCR in order to analyze possible changes in biosynthesis of testosterone in the different experimental groups. At 30 days after the first immunizations, mRNA expression of *Star* (steroidogenic acute regulatory protein) (**Fig. 41a**) and *Hsd3b1* (hydroxy-delta-5-steroid dehydrogenase, 3 beta- and steroid delta-isomerase cluster) (**Fig. 41g**) was unchanged. In contrast, *Cyp11a1* (cytochrome P450, family 11, subfamily a, polypeptide 1) (**Fig. 41c**) and *Cyp17a1* (cytochrome P450, family 17, subfamily a, polypeptide 1) (**Fig. 41e**) mRNA transcripts were significantly decreased at 30 days in testes of TH-immunized mice (EAEO group) treated with follistatin compared with their respective untreated controls. Expression levels of *Cyp17a1* mRNA were also decreased in adjuvant control testes from the FST315 vector group compared with untreated animals. Moreover, mRNA expression of *Cyp17a1* was significantly decreased in testes of TH-immunized mice treated with follistatin compared with the EV group (**Fig. 41e**). At 50 days after the first immunization, expression of *Star* mRNA (**Fig. 41b**) was lower in adjuvant control EV and FST315 vector mice compared with their respective untreated controls. At 50 days, mRNA expression levels of *Cyp11a1* (**Fig. 41d**) were similar in testes of all mice. In the FST315 vector group, at 50 days after the first immunization, expression of *Cyp17a1* (**Fig. 41f**) and of *Hsd3b1* (**Fig. 41h**) mRNA was decreased in testes of adjuvant and TH-immunized mice compared with their untreated controls. Overall, these results show that there is a general decrease of expression of the steroidogenic enzymes and regulators in testes of mice with elevated levels of follistatin in comparison with mice with normal levels.
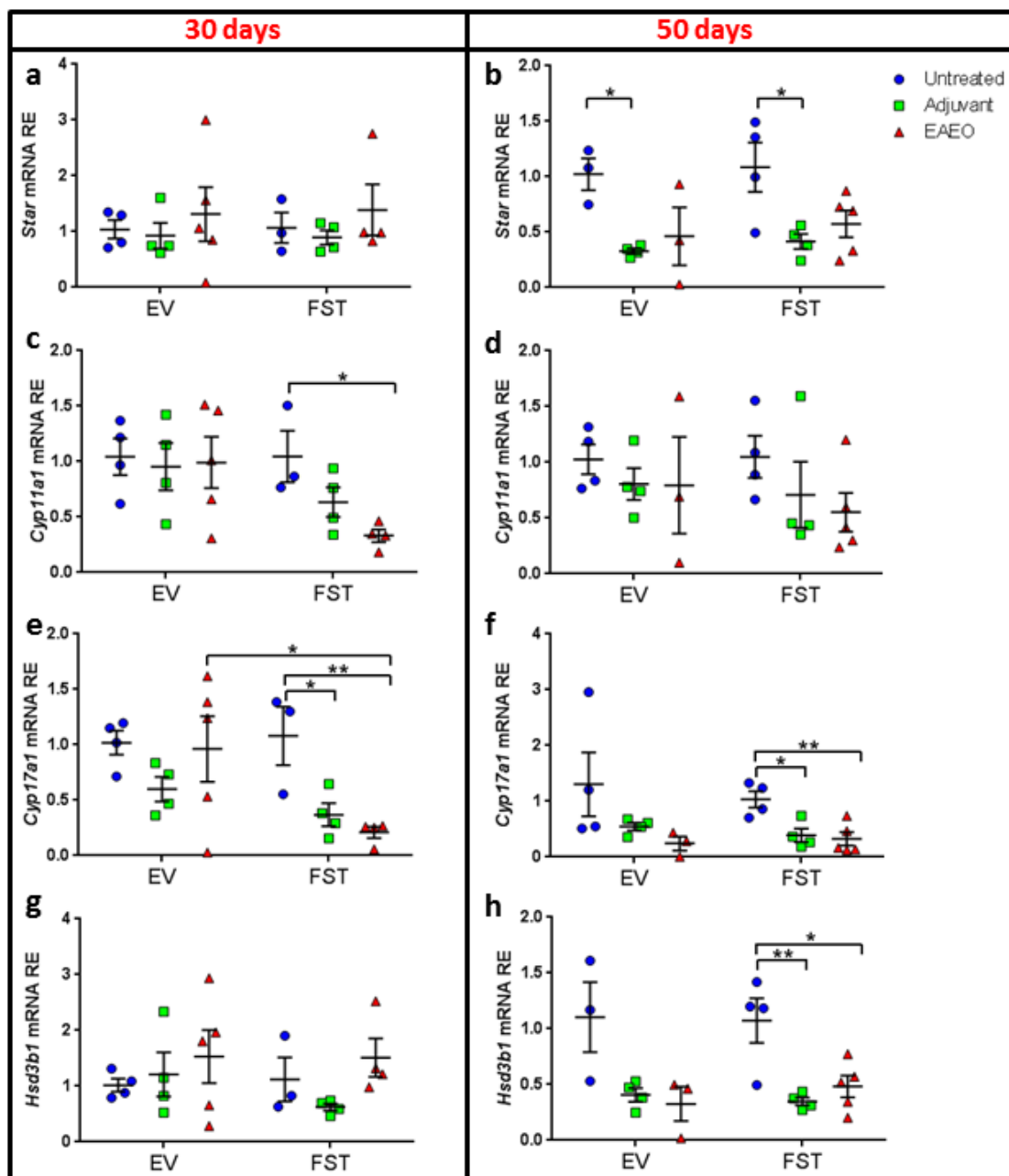
Figure 41: Decreased mRNA expression of steroidogenic enzymes *Cyp11a1*, *Cyp17a1* and *Hsd3b1* in EAEO testes.
Relative mRNA expression of *Star* (**a-b**), *Cyp11a1* (**c-d**)*, Cyp17a1* (**e-f**) and *Hsd3b1* (**g-h**) in testes from untreated, adjuvant control and TH-immunized mice (EAEO group) injected with empty (EV) or FST315 (FST) vector 30 (**a, c, e, g**) and 50 (**b, d, f, h**) days after the first immunization, analyzed by quantitative RT-PCR. Data are represented as mean ± SEM of 3 - 5 animals per group. Statistical analysis was done using one-way ANOVA followed by Tukey's multiple comparisons for all treatment groups and two-way ANOVA comparing EV and FST groups followed by Sidak's multiple comparisons; *P<0.05 and **P<0.01, all other comparisons were not statistically significant.

3.14. Expression of activin and follistatin was altered in TH-immunized mice with normal and elevated levels of follistatin

Since activin A, inhibin and activin receptor expression was regulated in the testis during EAEO (study I), their systemic and testicular expression was determined in animals from study II by protein assays (**Figures 42** and **43)** and by quantitative RT-PCR as shown in **Figures 44** and **45**.

3.14.1. Serum levels of activin A, but not inhibin were elevated in TH-immunized mice with normal and elevated levels of follistatin

Levels of activin A in serum were significantly elevated in TH-immunized mice and injected with an empty vector (EV) or the FST315 vector (FST) by comparison with untreated controls at 30 days after the first immunization (**Fig. 42a**). The levels of activin A remained increased in serum from TH-immunized FST315 vector-treated mice by comparison with untreated controls at 50 days after the first immunization (**Fig. 42b**). Serum inhibin levels were not changed in any group at 30 (**Fig. 42c**) and 50 (**Fig. 42d**) days after the first immunization.
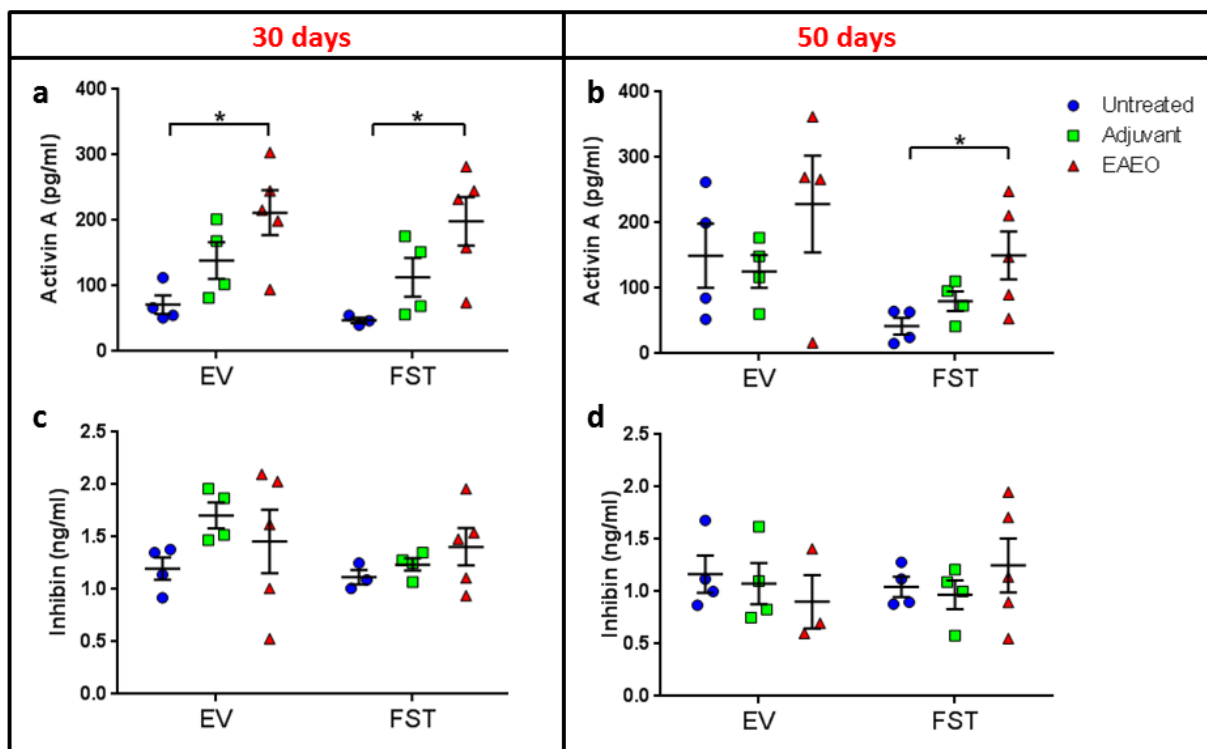
Figure 42: Elevated activin A but not inhibin serum levels in TH-immunized group 30 and 50 days after the first immunization.
Protein levels of activin A (**a, b**) and inhibin (**c, d**) were measured in serum from untreated, adjuvant control and TH-immunized mice (EAEO group) injected with empty (EV) or FST315 (FST) vector 30 (**a, c**) and 50 (**b, d**) days after the first immunization. Data are represented as mean ± SEM of 3-6 animals per group. Statistical analysis was done using one-way ANOVA followed by Tukey's multiple comparisons for all treatment groups and two-way ANOVA comparing EV and FST groups followed by Sidak's multiple comparisons; *$P<0.05$; all other comparisons were not statistically significant.

3.14.2.   Expression of activin A and inhibin in testes of mice with normal and elevated levels of follistatin

The expression of activin and inhibin at the protein (**Figure 43**) and mRNA (**Figure 44**) level was also determined in the testes.

Testicular protein and mRNA levels of activin A (**Fig. 43a** and **Fig. 44a,** respectively) and inhibin (**Fig. 43c** and **Fig. 44e,** respectively) were unchanged at 30 days after the first immunization. At 50 days after the first immunization, an increase in mRNA levels of *Inhba* was observed in testes of TH-immunized (EAEO) FST315 vector-treated mice compared with their adjuvant controls (**Fig. 44b**), although no significant changes were observed in activin A protein levels (**Fig. 43b**). Inhibin α (*Inha*) mRNA levels were

significantly decreased in testes of adjuvant control and TH-immunized mice (EAEO) in the FST315 vector-treated group compared with their untreated controls and in testes of TH-immunized mice from the FST315 vector-treated group in comparison with testes of TH-immunized mice from the EV group (**Fig. 44f**). However, no changes in inhibin protein levels were observed in testes from mice from any group at 50 days after the first immunization (**Fig. 43d**). *Inhbb* mRNA levels were similar between all groups at 30 (**Fig. 44c**) days after the first immunization. An increase of *Inhbb* mRNA expression was detected in adjuvant controls compared to untreated animals in the FST group at 50 days after the first immunization.
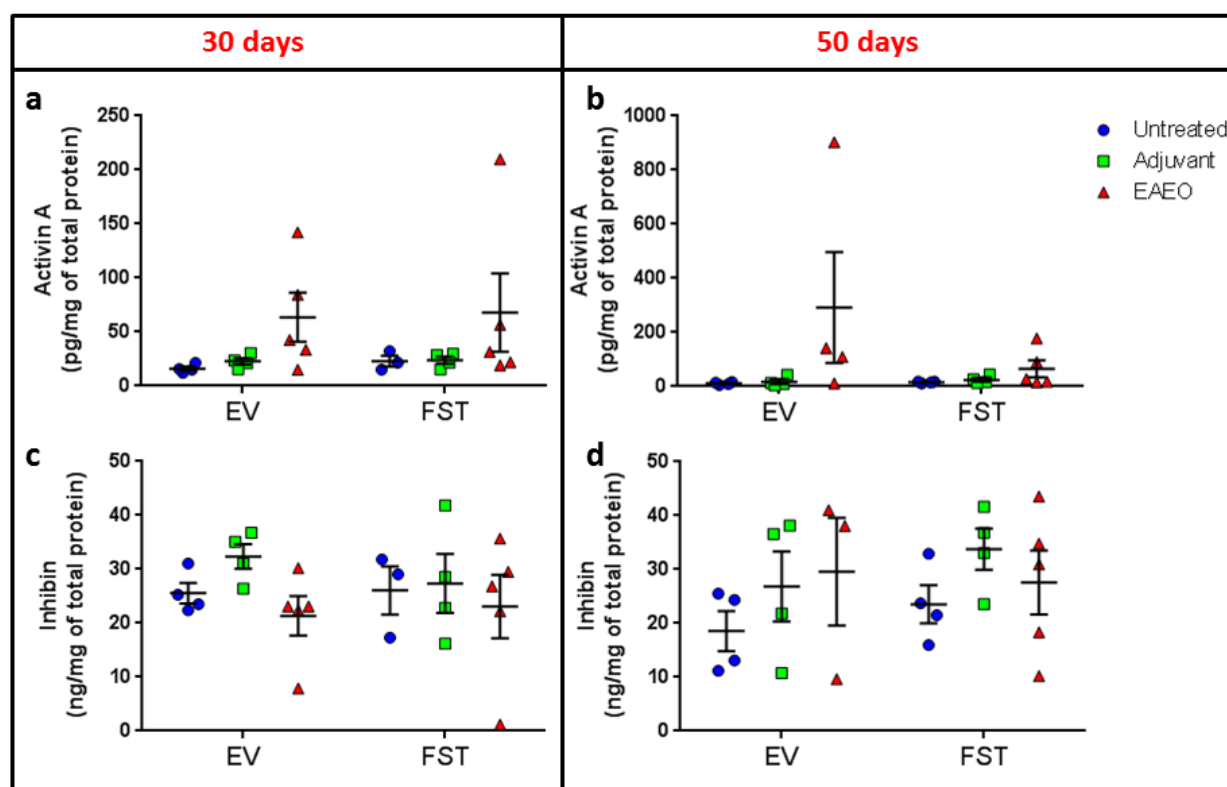
Figure 43: Expression of activin A and inhibin protein levels in the testis.
Protein levels of activin A (**a, b**) and inhibin (**c, d**) were measured in testicular homogenates from untreated, adjuvant control and TH-immunized mice (EAEO group) injected with an empty (EV) or FST315 (FST) vector, 30 (**a, c**) and 50 (**b, d**) days after the first immunization. Data are represented as mean ± SEM of 3 - 6 animals per group. Statistical analysis was done using one-way ANOVA followed by Tukey's multiple comparisons for all treatment groups and two-way ANOVA comparing EV and FST groups followed by Sidak's multiple comparisons.
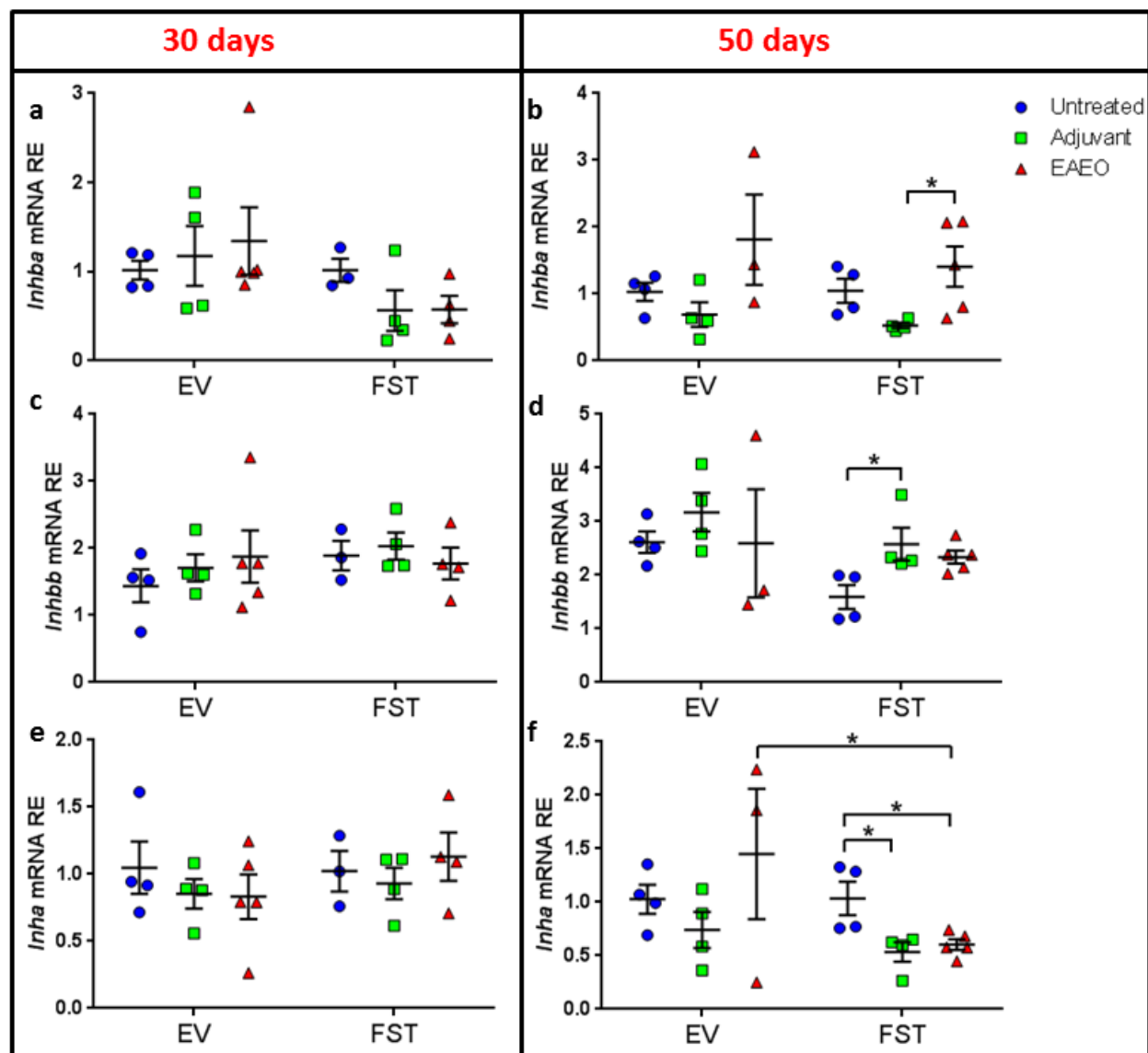
Figure 44: Activin βA (_Inhba_) subunit mRNA expression was increased and inhibin α subunit (_Inha_) mRNA expression was decreased in testes of TH-immunized mice (EAEO) with elevated levels of follistatin at 50 days after the first immunization.

Relative mRNA expression of _Inhba_ (inhibin βA) (**a-b**), _Inhbb_ (inhibin βB) (**c-d**), _Inha_ (inhibin α) (**e-f**) in testes from untreated, adjuvant control and TH-immunized mice (EAEO group) injected with empty (EV) or FST315 (FST) vector 30 (**a, c, e**) and 50 (**b, d, f**) days after the first immunization, analyzed by quantitative RT-PCR. Data are represented as mean ± SEM of 3 - 5 animals per group. Statistical analysis was done using one-way ANOVA followed by Tukey's multiple comparisons for all treatment groups and two-way ANOVA comparing EV and FST groups followed by Sidak's multiple comparisons; *P<0.05, all other comparisons were not statistically significant.

3.14.3. *Acvr1b* **(ALK4) mRNA expression was decreased in 50 day EAEO testes mice with elevated levels of follistatin**

Acvr1b (activin receptor, type IB) and *Acvr2b* (activin receptor, type IIB) mRNA expression in testes was unchanged in any group at 30 days after the first immunization (**Fig. 45a** and **c**). Likewise, *Acvr2b* mRNA *levels* at 50 days after the first immunization were similar between all groups (**Fig. 45d**). *Acvr1b* mRNA expression was significantly decreased in testes of adjuvant and TH-immunized mice by comparison with untreated controls in the FST315 vector-treated group at 50 days after the first immunization (**Fig. 45b**).
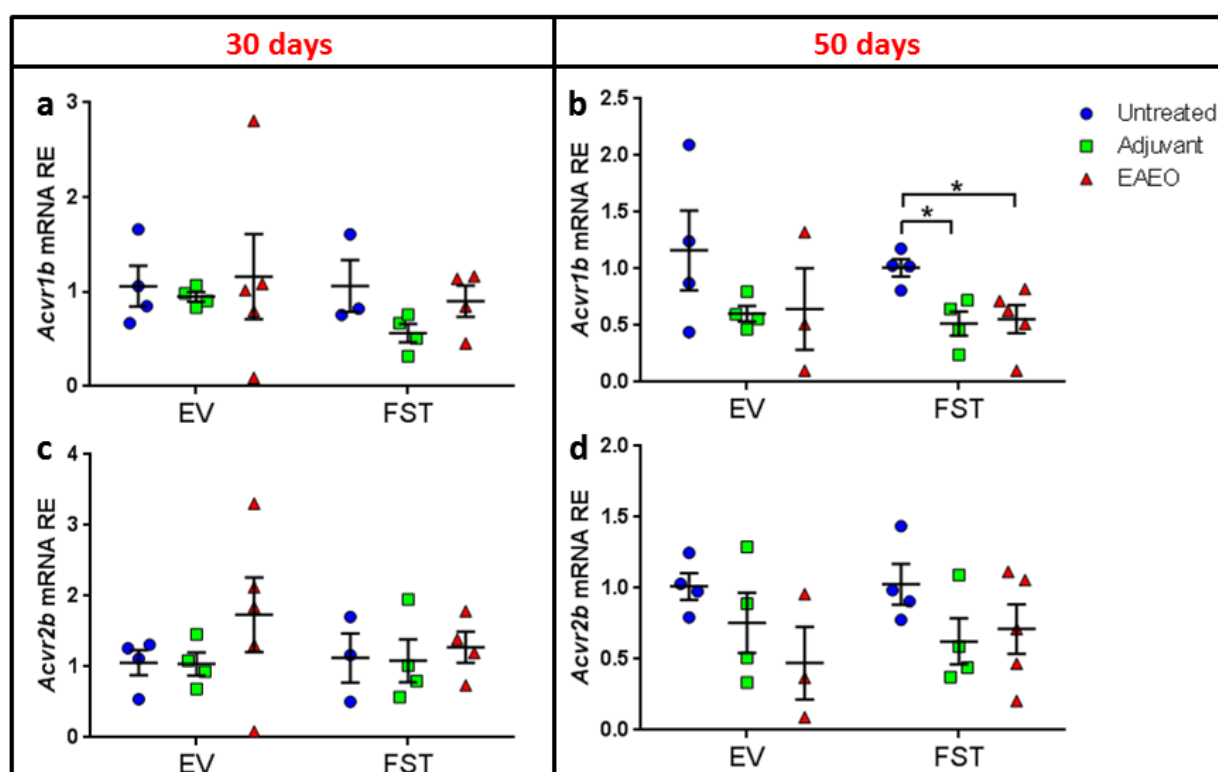
Figure 45: Decreased mRNA expression of *Acvr1b* in 50 day EAEO testes from mice with elevated levels of follistatin.
Relative mRNA expression of *Acvr1b* (activin receptor, type IB) (**a-b**) and *Acvr2b* (activin receptor, type IIB) (**c-d**) in testes from untreated, adjuvant control and TH-immunized mice (EAEO group) injected with empty (EV) or FST315 (FST) vector 30 (**a, c**) and 50 (**b, d**) days after the first immunization, analyzed by quantitative RT-PCR. Data are represented as mean ± SEM of 3 - 5 animals per group. Statistical analysis was done using one-way ANOVA followed by Tukey's multiple comparisons for all treatment groups and two-way ANOVA comparing EV and FST groups followed by Sidak's multiple comparisons; *P<0.05, all other comparisons were not statistically significant.

3.14.4. Follistatin mRNA expression was upregulated in 50 day EAEO mouse testes after follistatin treatment

At 30 days after the first immunization, protein and mRNA levels of follistatin (**Fig. 46a, c, e** and **g**) were unchanged in any group. In contrast, 50 days after the first immunization, follistatin protein levels were significantly elevated in testes of TH-immunized mice from the FST315 vector-treated group compared with untreated controls, but also by comparison with testes of TH-immunized mice from the EV group (**Fig. 46b**). However mRNA levels of total follistatin (*Fst*) (**Fig. 46d**) and the two splice variants *Fst288* (**Fig. 46f**) and *Fst315* (**Fig. 46h**) were similar in all groups at 50 days after the first immunization.
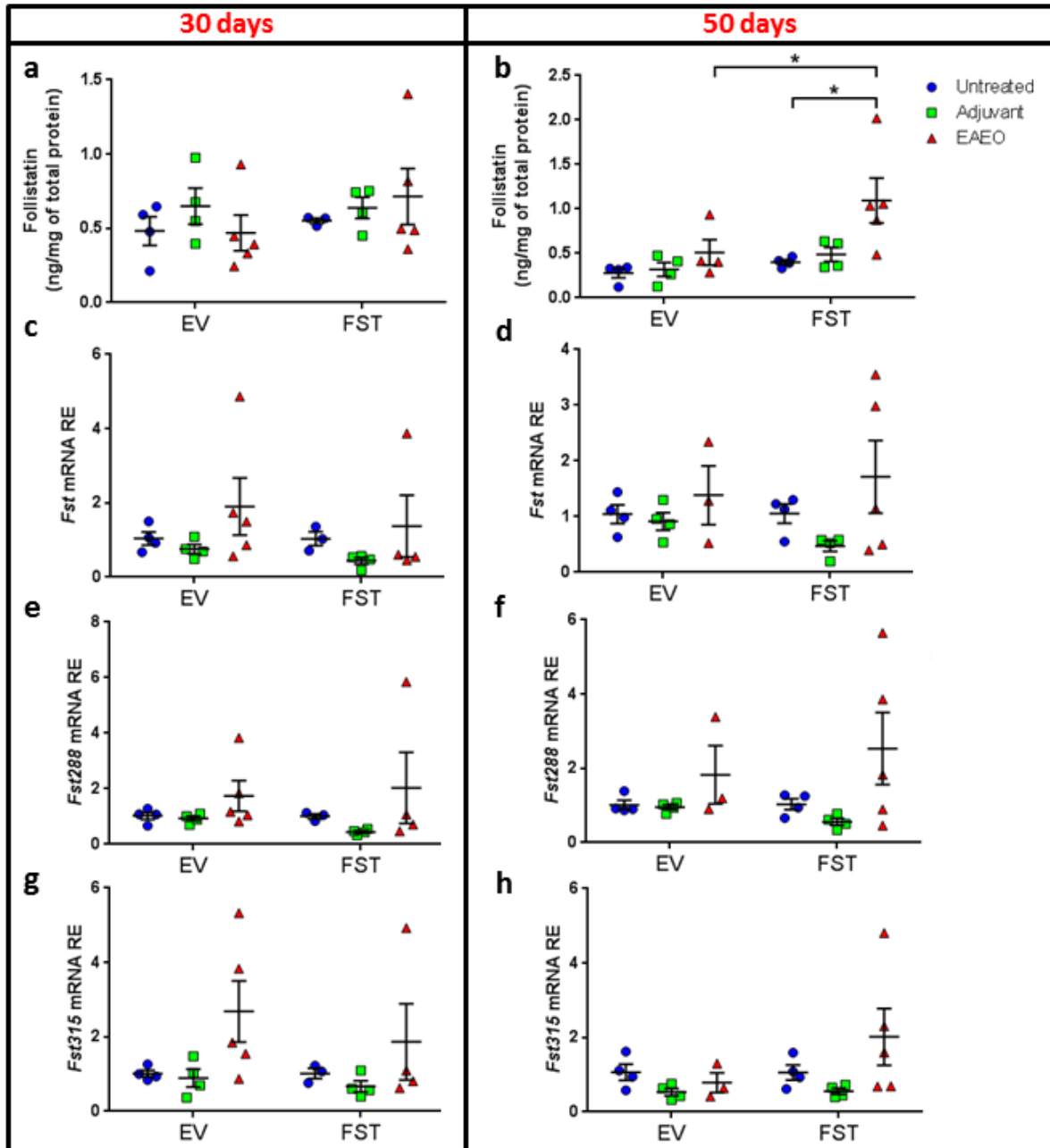
Figure 46: Elevated levels of follistatin in 50 day EAEO testes after follistatin treatment.

Protein levels of follistatin (**a-b**), and relative mRNA expression of *Fst* (**c-d**)*, Fst288* (**e-f**) and *Fst315* (**g-h**) were measured in testicular homogenates from untreated, adjuvant control and TH-immunized mice (EAEO group) injected with empty (EV) or FST315 (FST) vector 30 (**a, c, e, g**) and 50 (**b, d, f, h**) days after the first immunization. Data are represented as mean ± SEM of 3 - 5 animals per group. Statistical analysis was done using one-way ANOVA followed by Tukey's multiple comparisons for all treatment groups and two-way ANOVA comparing EV and FST groups followed by Sidak's multiple comparisons; *P<0.05, all other comparisons were not statistically significant.

3.15. Expression of activin A, follistatin and inflammatory markers showed strong correlation with EAEO score

Based on the above described results, it was relevant to perform correlations in order to elucidate if there is any causal statistical relationship between activin A expression (**Figure 47**), follistatin expression (regardless of treatment with FST315 vector) (**Figure 48**) or EAEO development (**Figure 49**).

Table 6 summarizes the most significant correlations observed between activin A and follistatin expression and EAEO score.

Table 6: **Summary of the EAEO parameters correlating with expression of testicular activin A, testicular follistatin and EAEO score.**

	Activin A			Follistatin		TNF	MCP-1	IL-10
Testicular	Testicular	mRNA	serum	Testicular	mRNA			
Activin A	+	+	+	+	no	+	no	no
Follistatin	+	+	no	+	+	+	+	+
EAEO score	+	+	+	no	no	+	+	+

+: positive correlation, no: no correlation. Analysis was done using Pearson's correlation between each two variables. Values from adjuvant control and EAEO mice injected with empty (EV) or FST315 (FST) vector, at 50 days after the first immunization were used for the statistical analysis.

Testicular activin A protein expression was positively correlated with testicular follistatin protein levels (**Fig. 47a**), as well as with activin A expression in the serum (**Fig. 47b**), with *Inhba* mRNA relative expression (**Fig. 47c**), and with the TNF mRNA levels (**Fig. 47d**). These data indicate that higher testicular activin A levels are associated with higher follistatin testicular levels, activin serum levels and TNF expression in the testis.
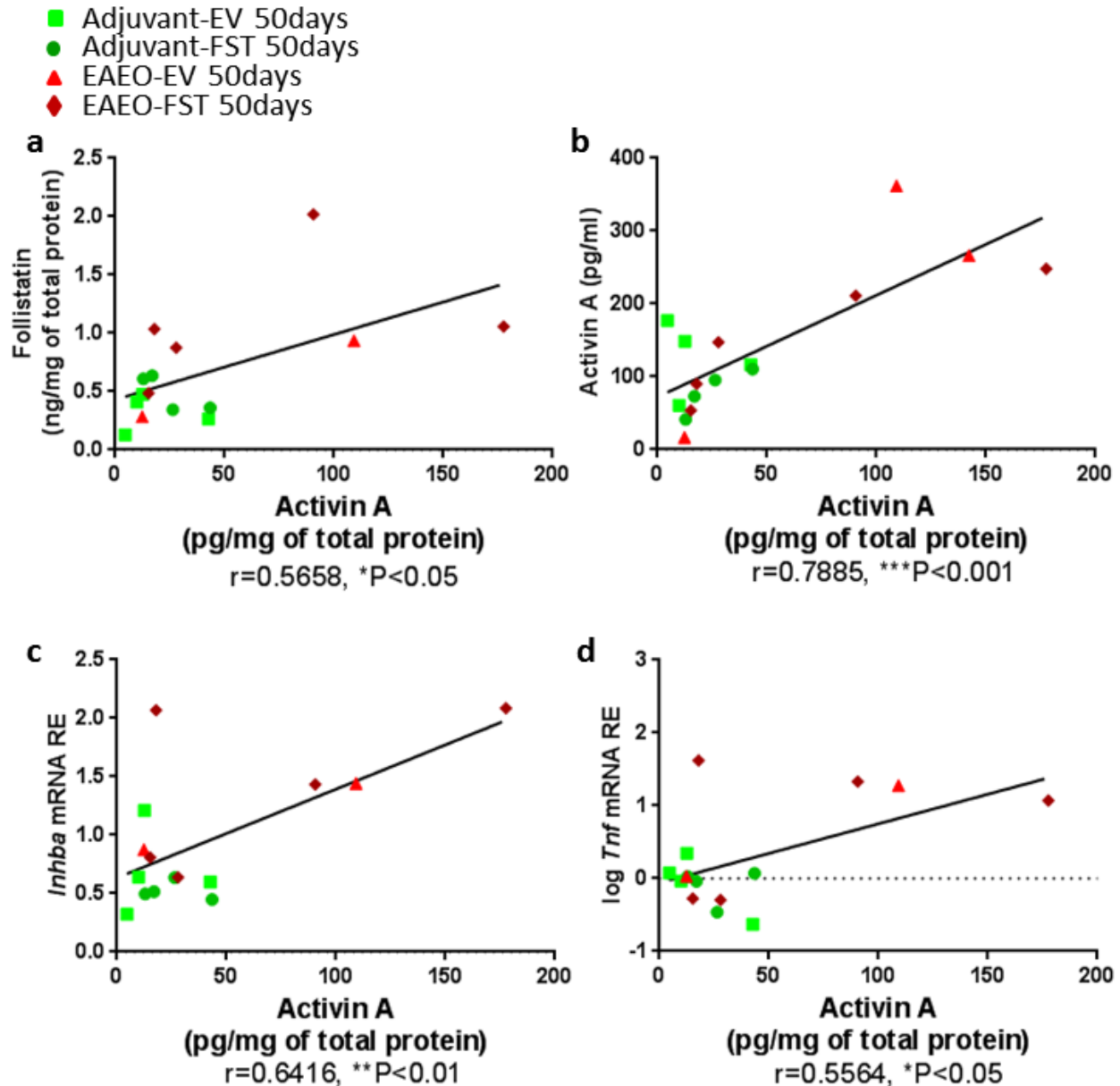
Figure 47: Testicular follistatin protein levels; serum activin A levels, *Inhba* and TNF mRNA expression were positively correlated with testicular activin A protein levels 50 days after the first immunization.
Testicular follistatin protein levels (**a**), serum activin A protein levels (**b**), *Inhba* (**b**) and TNF (**d**) mRNA levels were correlated with testicular activin A protein levels 50 days after the first immunization of adjuvant control and TH-immunized mice (EAEO group) injected with empty (EV) or FST315 (FST) vector. r represents Pearson's correlation coefficient. Pearson's correlation was considered statistically significant at *P<0.05.

Testicular follistatin protein levels were positively correlated with its own testicular mRNA expression levels (**Fig. 48a, b** and **c**), and the inflammatory mediators TNF (**Fig. 48d**), IL-10 (**Fig. 48e**) and MCP-1 (**Fig. 48f**). This means that higher follistatin levels in the testis were associated with higher expression of inflammatory mediators, such as TNF, IL-10 and MCP-1.
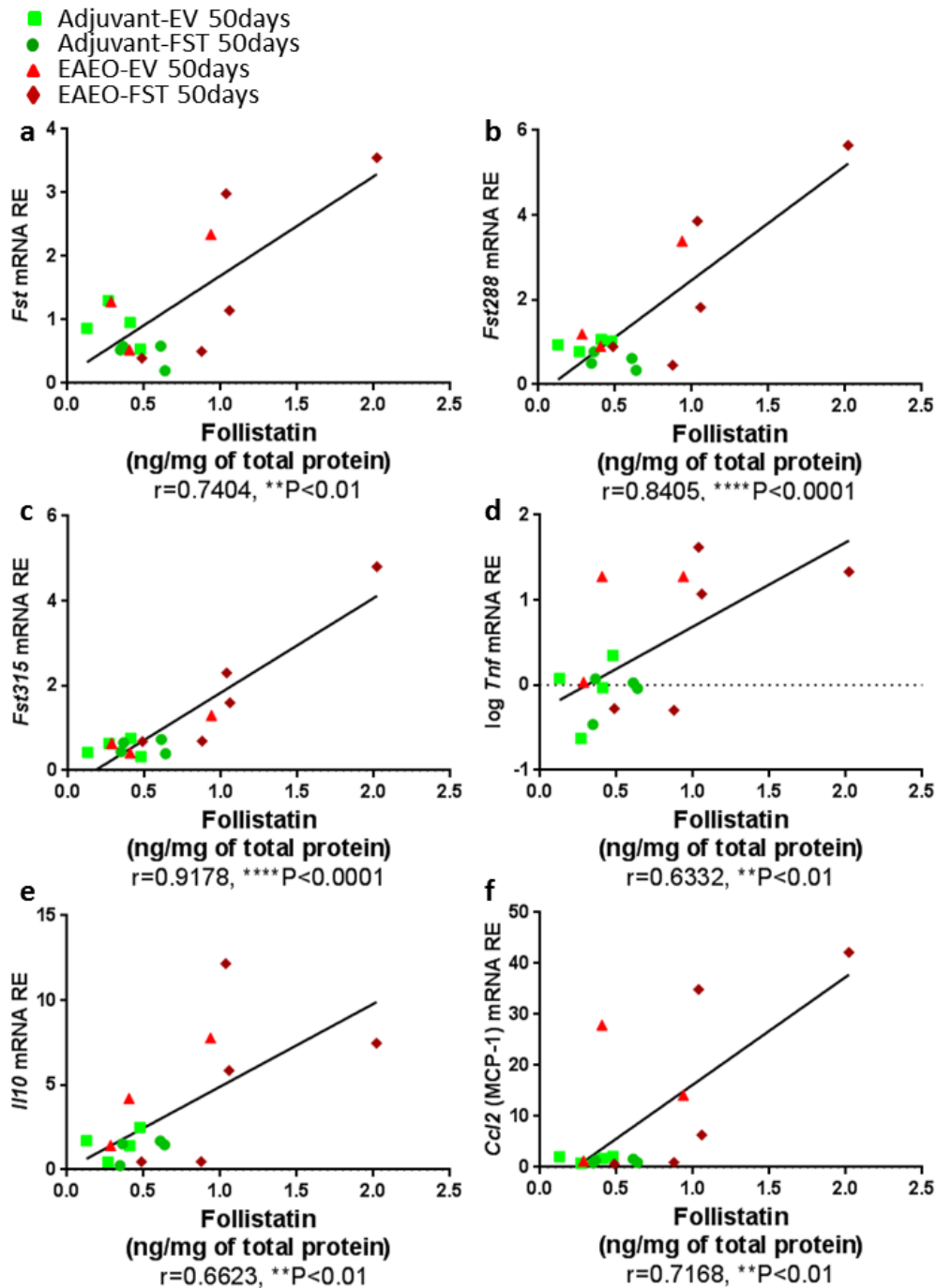
Figure 48: **Testicular follistatin, TNF, IL-10, MCP-1 mRNA levels were positively correlated with testicular follistatin protein levels, 50 days after the first immunization.**
Relative mRNA expression of *Fst* (**a**), *Fst288* (**b**), *Fst315* (**c**), TNF (**d**), IL-10 (**e**) and MCP-1 (**f**) were correlated with testicular follistatin protein levels 50 days after the first immunization of adjuvant control and TH-immunized mice (EAEO group) injected with empty (EV) or FST315 (FST) vector. r represents Pearson's correlation coefficient. Pearson's correlation was considered statistically significant at *P<0.05.

Finally, the score of EAEO was positively correlated with serum (**Fig. 49a**) and testicular activin A protein (**Fig. 49b**) and mRNA levels (**Fig. 49c**), as well as with the inflammatory mediators TNF (**Fig. 49d**), IL-10 (**Fig. 49e**) and MCP-1 (**Fig. 49f**). This means that higher levels of testicular and serum activin A are associated with higher severity of inflammation, characterized by the expression of the inflammatory mediators, such as TNF, IL-10 and MCP-1, and higher degree of development of EAEO and histological damage of the testis.
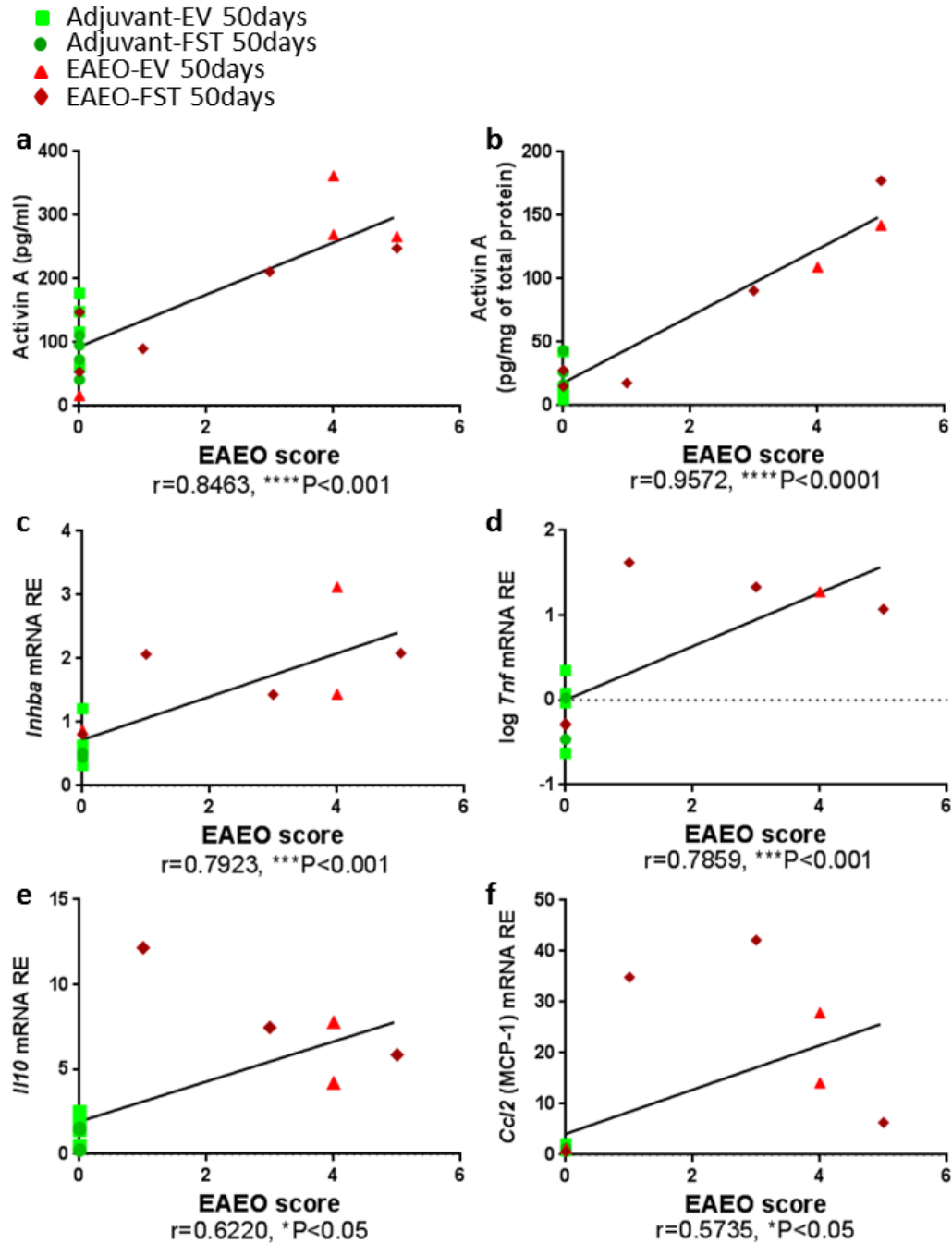
Figure 49: Serum and testicular activin A protein and mRNA levels; TNF, IL-10 and MCP-1 mRNA levels were positively correlated with EAEO score 50 days after the first immunization.

Serum activin A levels (**a**), testicular activin A protein (**b**) and mRNA (*Inhba*) levels (**c**), TNF (**d**), IL-10 (**e**) and MCP-1 (**f**) mRNA levels were positively correlated with EAEO score 50 days after the first immunization of adjuvant control and TH-immunized mice (EAEO group) injected with empty (EV) or FST315 (FST) vector. r represents Pearson's correlation coefficient. Pearson's correlation was considered statistically significant at *P<0.05.

3.16.   Expression of activin A by peritubular and Sertoli cells after treatment with inflammatory mediators

Treatment of peritubular cells with different concentrations of TNF for 24 hours (**Fig. 50a**) showed no effect on production of activin A.

Treatment of Sertoli cells with TNF for 48 hours (**Fig. 51a**) showed a dose-dependent increase in the production of activin A. The dose response from the third isolation of cells was taken as a representative result. It shows that the highest production of activin A by the Sertoli cells was obtained with a concentration of around 25 ng/ml of TNF. A 50% production of activin A by the Sertoli cells was seen at a concentration of TNF of 1 ng/ml.

Treatment of peritubular cells (**Fig. 50b**) and Sertoli cells (**Fig 51.b**) with different concentrations of recombinant activin A showed an increase of the activin A production starting at a concentration of 12.5 ng/ml treatment. The increase is proportional to the dose of recombinant activin A with which the cells were treated and that is present in the medium. The activin A detected by the assay could be the recombinant activin A used for the treatment instead of the endogenous activin A produced by the cells.
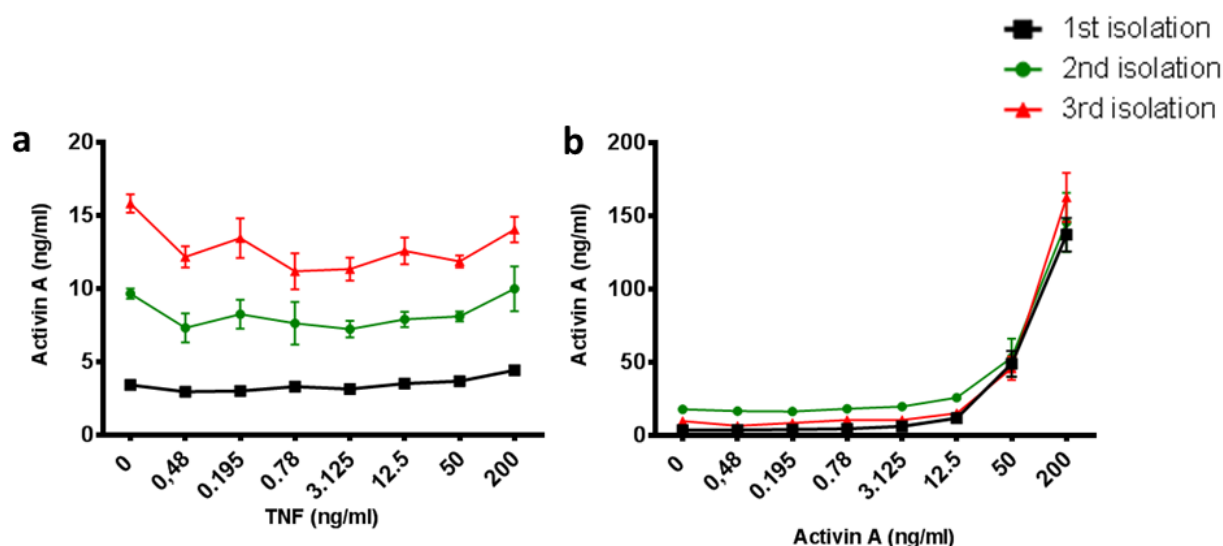
Figure 50: **Activin A production by cultured mouse peritubular cells.**
Activin A (**a-b**) was measured in the media of peritubular cells treated with recombinant TNF (**a**) or recombinant activin A (**b**) for 24 hours. Data are represented as mean ± SEM of 1 - 3 separate experiments.
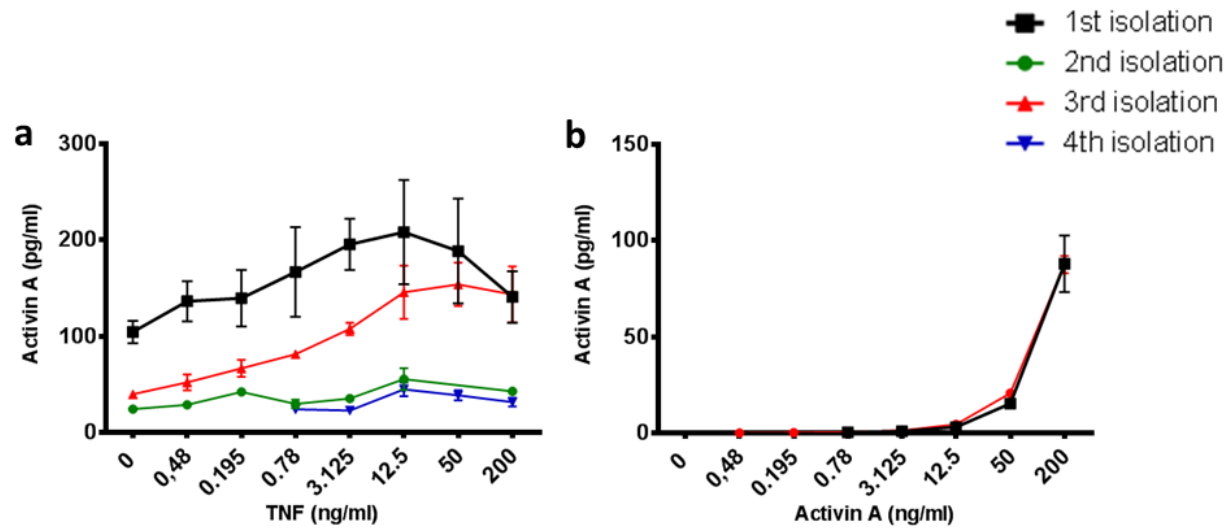
Figure 51: Activin A production by cultured mouse Sertoli cells.
Activin A (**a-b**) was measured in the media of Sertoli cells treated with recombinant TNF (**a**) or recombinant activin A (**b**) for 48 hours. Data are represented as mean ± SEM of 1 - 4 separate experiments.

4. DISCUSSION

This study provides evidence that, in a mouse model of testicular inflammation (EAEO), the levels of activin A in the testis are elevated during the course of the disease. A positive correlation between testicular activin A protein levels and the severity of the disease was found.

Furthermore, increased levels of activin A were accompanied by significantly upregulated expression of testicular follistatin during the active and chronic stages of EAEO (50 and 80 days, respectively). Moreover, the data show evidence that follistatin treatment of mice (using a FST315 vector to elevate circulating follistatin levels) before induction of EAEO, led to a slightly reduced induction rate of the disease, although there was no correlation between testicular follistatin expression and EAEO score.

In order to mimic the manifestation and symptoms of human testicular inflammation in an animal model and to transfer it to transgenic animal models in the future, C57BL/6N and J mouse strains were selected. In this study, a mouse model for induction of EAEO was utilized, mimicking some forms of human immunological infertility following a modified well-established protocol using TH in combination with adjuvants and *Bordetella pertussis* toxin ("classical" induction). This protocol has been used previously in rats and mice (Doncel et al., 1989, Fijak et al., 2005, Aslani et al., 2015, Tung et al., 1987).

Data presented here show that immunization with testicular homogenate (TH) in combination with complete Freund's adjuvant and *Bordetella pertussis* toxin leads to more severe autoimmune reaction / inflammation than immunization with TH only without adjuvants (Musha et al., 2013). Studies using different immunization protocols have proven the importance of using adjuvants and *B. pertussis* toxin for the successful induction of EAEO. Adjuvants are used in order to activate and boost the immune system, while *B. pertussis* toxin triggers inflammation as a co-adjuvant and mitogen. It also has been shown that *B. Pertussis* toxin increases the permeability of the blood-brain-barrier during the induction of another rodent model of autoimmune disease, experimental autoimmune encephalomyelitis (EAE) (Linthicum et al., 1982).

However, the toxin concentration required to induce EAE was 2-3 times higher (200-300 ng toxin per mouse), than used here for the induction of EAEO (100 ng per mouse) (Puentes et al., 2013, Prinz-Hadad et al., 2013). This concentration was far below the LD50 dose (17 µg/kg body weight) in mice (Sidey et al., 1989, Parton, 1985).

B. pertussis toxin shows pleiotropic effects on the immune system, such as triggering of T-cell mitosis and increase in cytokine production and antibodies (Morse et al., 1977, Munoz et al., 1981). In addition, microbial products like *B. Pertussis* toxin amplify the interaction between the innate and adaptive immune system. It was also reported that the toxin promotes an immune response against autoantigens in the initiation of autoimmune diseases like EAE (Hofstetter et al., 2002).

In order to analyze the induction rate, development and progression of the disease, the histopathologic and expression profiles of inflammatory mediators (TNF, IL-6, IL-10 and MCP-1), known to be involved in EAEO pathology in rats, were examined. According to the histopathological examination and immune profile of the animals, observations from this study were in line with the existing data in a rat model of EAEO, which has been the most broadly used model for studying autoimmune-based testicular inflammation (Fijak et al., 2011b, Doncel et al., 1989). The results presented here recapitulate the process of development and progression of the disease leading to degeneration of the testicular architecture in late and chronic stage of EAEO in mice during three different time points, e.g. 30, 50 and 80 days after the first immunization. Firstly, at 30 days, only a small number of the immunized mice (1 of 3 mice from study I and 2 of 5 mice from study II) showed histological symptoms of EAEO. Secondly, at 50 and 80 days all animals from study I, immunized with TH in CFA and *B. pertussis* toxin developed testicular inflammation with all the characteristics of the disease. In contrast, only 50% animals from study I, immunized with TiterMax Gold developed the disease. Induction of EAEO as performed in study II, using CFA for the first immunization and IFA for two following boost immunizations also resulted in a lower induction rate than in mice from study I injected three times with TH in CFA. These findings indicate that CFA seems to be the most effective adjuvant in inducing EAEO in C57BL/6 mouse strain. This could be due to the presence of killed Mycobacterium tuberculosis in the composition of this adjuvant.

Unfortunately, the use of CFA for the three subsequent immunizations was not possible in study II due to the local regulations of the Monash University animal Ethics committee. Moreover, the induction rate of EAEO at 50 days after the first immunization in animals from study II was of 40% for mice treated with the follistatin vector and 75% for mice injected with an empty vector. These results show that follistatin treatment has a potential effect on diminishing the induction of the disease. Furthermore, this induction rate was comparable to the induction rate mentioned in described studies in mice (e.g. 89% in C57BL/6N, 68% in B6AF1 or 92% in BALB/cBy strains) (Tung et al., 1987, Yule et al., 1988, Teuscher et al., 1985).

Even though mice treated with the follistatin vector showed a lower induction rate of EAEO compared with mice injected with the empty vector, it is important to mention that the morphological changes found in the testis during the course of the disease were similar in both studies I and II. The affected testes showed an accumulation of immune cells, disruption of the testicular morphology with a significant reduction of the diameter of the seminiferous epithelium, disruption of the BTB, which was first observed at EAEO score of 2, based on the assessment criteria described in this study, together with increased apoptosis and sloughing of germ cells and tubular atrophy leading to a significantly smaller testis size.

Apart from the different adjuvants used, another explanation for the differences in the induction rate of EAEO between the different treatment groups from study I and mice from study II with normal levels of follistatin could be due to the use of the different strains of mice (C57BL/6N and C57BL/6J). Previous studies describing induction of EAEO using one protocol, but different mouse strains suggested that the high susceptibility to the disease induction in mice seems to be also strain specific (Tokunaga et al., 1993, Teuscher et al., 1985).

The findings in this study show that the modified immunization protocol used here with CFA for three subsequent immunizations, leads to a higher induction rate of EAEO in mice (100%) compared with previously described studies (Tung et al., 1987, Yule et al.,

1988). Moreover, the results establish that CFA is the most potent adjuvant for inducing EAEO in a very severe form.

For the first time, this study shows that the observed morphological changes in EAEO testes were accompanied by a strong peritubular fibrotic response represented by an increase of collagen fibers around the seminiferous tubules. In addition to the collagen deposits, there was a change in the morphological distribution and thickening of the αSMA layer in the peritubular cells. It can be hypothesized that the inflammatory process in the testis and subsequent disruption of the testicular morphology led to a change of the function of peritubular cells and fibrotic response, as seen in human testicular biopsies from patients with impaired spermatogenesis (Mayerhofer, 2013). Adam et al., showed that peritubular cells are important players involved in the process leading to fibrotic response in the testis (Adam et al., 2011). Notably, the collagen deposits in testes from animals developing low grade EAEO (a score of 2) were less prominent as by comparison with the severe form at the later stages of the disease (score of 3 and higher). Moreover, very strong formation of collagen deposits was observed in close proximity to the areas with inflammatory infiltrates, granulomas and disturbed testicular morphology. This observation was not surprising as there is also an accumulation of mast cells in the areas with leukocytic agglomeration. In fact, mast cells are known to play a role in inducing fibrosis (Wilgus and Wulff, 2014). It is thought that mast cells have a detrimental effect in many inflammatory diseases including experimental colitis, EAE, arthritis or lung fibrosis (Wernersson and Pejler, 2014). In regard to the fibrotic response, it is also important to note that the mRNA levels of collagen I, alpha 1 (a marker of fibrosis) were highly elevated in EAEO testes at a score of 5.

The data also point to a possible involvement of immune cells in the generation of fibrotic testicular response. Observations regarding morphology and fibrotic response suggest that the active phase of EAEO starts after the third immunization period and the severe form of the disease is reached around 50 days after the first immunization, followed by the chronic form at 80 days. Fibrosis is involved in a process of tissue repair

after inflammation induced cellular destruction, however the uncontrolled fibrosis leads to serious health impairment, as occurs in idiopathic pulmonary fibrosis, cirrhosis of the liver or renal failure (reviewed in (Hedger et al., 2011). Therefore, testicular fibrosis could be leading to ill health of the organ and its function.

As EAEO is a T cell mediated disease, the findings also show the increase of the T cell population in EAEO testis with a novel characterization of the T cell subtypes. In the investigated mouse model of EAEO, an increase of the number of infiltrating leukocytes (CD45+) in the testicular interstitial space was observed consisting mainly of macrophages and T cells. A similar increase in leukocytic accumulation in inflamed testes has already been described in a rat model of EAEO (Jacobo et al., 2011). Interestingly, in rat EAEO testes, the population of CD4+ and CD8+ T effector cells was increased at the onset of the disease with a predominating population of CD4+ T cells. During the severe phase of the disease, the CD4+ T cell subset decreased, whereas CD8+ T cells were unchanged (Jacobo et al., 2009). In contrast, in the present mouse model of EAEO, highly elevated numbers of CD4+ T cells were observed, whereas the population of CD8+ T cells was significantly decreased at 50 days. The data was supported by a higher ratio of CD4+/CD8+ T cells in the testis, which was comparable to many other immune disorders and diseases. In fact, this ratio can also be used as a diagnostic tool for several inflammatory diseases such as infectious mononucleosis, chronic lymphocytic leukemia, Hodgkin disease, anemia or autoimmune neurological disorders like multiple sclerosis (Hernandez et al., 2005, Stuve et al., 2006). An increase in the number of activated T cells (CD4+CD25+) was also recorded in inflamed testes which was consistent with the increase of these cells observed in a rat model of EAEO (Guazzone et al., 2009).

Furthermore, a novel finding of the study was the detection of existence of double positive CD4+CD8+ T cells in the inflamed testis. Initially thought to be exclusively present in the thymus as an immature stage of T cell development, CD4+CD8+ cells have been identified recently in other organs (Overgaard et al., 2015). Up to now, the function of these cells in the periphery has not been very well investigated and remains

controversial. There are reports showing an increase in the number of CD4+CD8+ T cell subsets in autoimmune and chronic inflammatory disorders, namely in peripheral blood and synovium from patients with rheumatoid arthritis (Quandt et al., 2014), in fibrotic skin lesions from patients with systemic sclerosis (Parel et al., 2007), or in the liver from patients with hepatitis B and C (Nascimbeni et al., 2011). Further functional studies are necessary for deeper examination of CD4+CD8+ double positive T cells to fully elucidate their contribution to the immune response and spermatogenic damage in mouse inflamed testes.

In addition, the results show that not only the amount of macrophages is increased in EAEO testes but that the main population of macrophages possesses a pro-inflammatory M1 phenotype. In fact, under normal conditions in rodent testes, resident macrophages represent a significant population of interstitial cells (Niemi et al., 1986). Most of them are anti-inflammatory M2 macrophages that display an immunosuppressive profile, putatively are specialized in providing protection for the developing germ cells and are involved in maintaining the immune privilege of the testis (Fijak and Meinhardt, 2006, Bhushan et al., 2015). In the present mouse model of EAEO, it has been confirmed that macrophages in control testes possess mainly an M2 phenotype, as they co-express the F4/80 and CD206 markers. Under inflammatory conditions, in EAEO mouse testes, there is an evident increase in the number of macrophages, as described in an EAEO model in BALB/c and C57BL/6 mice (Yule et al., 1988) and in rats (Rival et al., 2008, Fijak et al., 2005). The majority of the macrophages in EAEO testes do not express the CD206 marker. This finding suggests that the main population of macrophages in EAEO mouse testes possesses a pro-inflammatory M1 phenotype. This is in agreement with several reports showing the inflammatory phenotype and pathogenic role of macrophages in rat EAEO (Rival et al., 2008, Guazzone et al., 2003). In this light, it is important to mention that testicular activin A could be also involved in the process of macrophage phenotype determination during inflammatory conditions by inducing transition between M1 and M2 phenotypes, knowing that M1 are pro-inflammatory and M2 are pro-fibrotic (Hedger and de Kretser, 2013).

Furthermore, TNF, a strong pro-inflammatory cytokine, was significantly increased in our models of EAEO, similar to another mouse model of testicular inflammation induced by viable germ cells alone (Terayama et al., 2011). A significant increase was also detected in testicular mRNA levels for MCP-1, a potent chemokine, involved in recruiting the macrophages to the site of inflammation (Deshmane et al., 2009). Similar findings were also reported in a rat model of EAEO (Guazzone et al., 2003, Fijak et al., 2011b). Notably, the significant increase of TNF and MCP-1 was only observed in 50 day EAEO testes of mice with normal levels of follistatin, when compared to mice treated with follistatin. The elevation of these inflammatory mediators was also observed in testes from follistatin treated mice although not significant. These data suggest that follistatin treatment could have an effect on suppressing the inflammatory response in EAEO testis. Interestingly, the testicular expression of TNF and MCP-1 was diminished at 80 days of EAEO compared to their expression at 50 days of EAEO, but was still significantly elevated by comparison with the controls.

In contrast to earlier reports in rat EAEO (Rival et al., 2006b, Fijak et al., 2011b), the mRNA levels of IL-6 were not elevated during the course of testicular inflammation in the mouse model of EAEO induced by three immunizations with CFA. Nonetheless, IL-6 mRNA levels were significantly elevated in 50 day EAEO testes of mice treated with follistatin compared with mice with normal levels of follistatin.

Moreover, this study confirms previous findings showing that activin A is located mainly within the Sertoli cells and some interstitial cells in normal testes, most likely macrophages and less prominently in the Leydig cells, as it is known that they produce activin A (Ebert et al., 2007).

As a novel finding, this study shows that, under inflammatory conditions, activin A is strongly expressed by Sertoli cells and infiltrating immune cells within the inflamed EAEO testis (50 days). Notably, in the late stage of the disease at 80 days, no significant increase in the levels of activin A either at mRNA or protein level was observed in EAEO testes. Previous reports have shown that activin A levels are elevated in numerous chronic diseases like colitis, meningitis, cancer or autoimmune based diseases like arthritis (Michel et al., 2003, Jorgensen et al., 2014, Phillips et al.,

2009, Zhang et al., 2009). The results obtained in this study have shown that testicular activin A was also elevated in a mouse model of autoimmune-based testicular inflammation with a significant increase in the severe form of the disease at 50 days. Moreover, activin A was also elevated in the serum of animals from study II developing EAEO starting from 30 days after the first immunization and the levels remained elevated at 50 days after the first immunization in the serum of animals treated with follistatin. The findings suggest that activin A may be involved in the development of autoimmune orchitis, as it has been shown to regulate inflammation and immunity in many tissues (Hedger et al., 2011). Furthermore, the increase of activin A coincided with the elevated expression of inflammatory mediators like TNF and MCP-1.

Additionally, an increase of testicular activin B and inhibin protein levels in the severe form of the disease in mice from study I was observed, but the mRNA levels of the α and βB subunit forming mainly inhibin B were decreased at 80 days. Moreover, mRNA levels of the α subunit of inhibin was also decreased in EAEO testes of mice treated with follistatin compared with their controls and with EAEO testes of mice with normal levels of follistatin. A similar observation was reported in a rat model of EAEO, demonstrating decreased levels of circulating inhibin B as well as a decreased inhibin α subunit expression in Sertoli cells (Suescun et al., 2001).

In addition, it is known from a rat model, that FSH levels are increased during EAEO (Suescun et al., 1994, Fijak et al., 2011b). This increase could be caused by the loss of inhibin production observed in the EAEO testis. LH levels were also increased in our mouse model of EAEO similarly to the rat model (Fijak et al., 2011b). Interestingly, at 30 days after the first immunization, FSH levels were significantly lower in mice treated with follistatin compared to mice with normal levels of follistatin. Knowing that activin A is involved in the HPG axis and in stimulating the production of FSH by the pituitary, it is only natural to see a decrease of FSH levels after follistatin treatment as the production of FSH by the pituitary will be indirectly inhibited through blockage of activin A and its stimulatory effect.

Moreover, testosterone circulating levels were decreased in 50 day EAEO testes of mice with normal levels of follistatin compared with their untreated controls which is in agreement with the observation seen in a rat model of the disease (Fijak et al., 2011b,

Suescun et al., 1994). A decrease in testosterone levels in untreated mice with elevated levels of follistatin was also observed compared with untreated mice with normal levels of follistatin, which could mean that follistatin treatment could have an effect on testosterone production. Additionally, an intra-animal variability of testosterone levels was observed; therefore changes in steroidogenic enzymes reflecting the function of Leydig cells in the testis were examined. A decrease in the mRNA expression of *Cyp11a1*, *Cyp17a1* and *Hsd3b1* was observed in EAEO testes compared with controls. This result was a direct indication and a confirmation of the observed decrease of testosterone levels.

Curiously, the levels of activin A receptors: ALK4 (*Acvr1b*) and the activin receptor type 2 subunit (*Acvr2b*) in the inflamed testis were significantly lower than in normal testis, while activin A levels were higher. It is likely that high activin A levels lead to a negative feedback on the receptor expression levels.

It was also shown in this study, that the increase of activin A was accompanied by an increase of follistatin expression in the inflamed testis. This observation is in line with data from the literature showing that activin A can induce expression of follistatin (Jones et al., 2000). A possible explanation for this observation would be that the increase of the follistatin levels may act to counter the effects of activin A during the disease thereby decreasing the severity of the inflammation. The present data demonstrate that higher levels of testicular follistatin at 50 days of EAEO are able to block the increase of activin A expression at 80 days. However the inhibitory function of follistatin at this stage of the disease does not lead to the resolution of inflammation at 80 days. It is likely that the positive effect of follistatin on inhibition of inflammation will be visible at later time points.

It is known that activin A causes muscle wasting and cachexia (Chen et al., 2016, Chen et al., 2014). Moreover, follistatin induces muscle hypertrophy by inhibiting the action of myostatin (Barbe et al., 2015). Nowadays, follistatin is being used as a therapy for skeletal muscle atrophy (Sepulveda et al., 2015). Therefore, it was not surprising to see

that mice that received the follistatin vector in their tibialis anterior muscle presented with muscle hypertrophy at the site of injection of the FST315 vector in mice from study II.

Furthermore, a 5-fold elevation of circulating follistatin levels in mice from study II, 30 days after the vector injection, did not lead to a change in activin A serum levels. It should be noted that the levels of activin A detected by ELISA could already be neutralized by follistatin as it is bound to activin A. Nonetheless, 30 days after the induction of EAEO, activin A serum levels were significantly higher in TH-immunized mice compared with their untreated controls regardless of follistatin treatment. This increase in activin A serum levels was still observed in TH-immunized mice compared with untreated controls even at 50 days after the first immunization, but only for mice treated with follistatin. This result shows that elevating systemic follistatin levels did not alter the levels of activin A in the serum of mice that developed EAEO, giving an additional proof that mice developing EAEO produce substantially more activin A.

Moreover, the increase of circulating follistatin levels in mice did not notably alter the testicular levels of activin A, although a slight reduction of activin A protein levels was observed EAEO testes of mice treated with follistatin compared with mice that had normal levels of follistatin at 50 days after the first immunization. This decrease of activin A levels was consistent with the significant increase of follistatin testicular levels in EAEO of mice treated with follistatin compared to their untreated controls and also to EAEO testes of mice with normal levels of follistatin. On the other hand, mRNA levels of activin A remained significantly higher in EAEO testes of mice treated with follistatin compared to their adjuvant controls at 50 days after the first immunization.

These results demonstrate that elevating follistatin circulating levels had a negative effect on activin A production in the testis and therefore led to a lower induction rate of EAEO but did not completely prevent the induction of EAEO in these mice. In fact, it was observed that mice with elevated levels of follistatin had a lower induction rate of EAEO of 40%, and higher testis weights at 50 days after the first immunization, compared with and induction rate of 75% in animals with normal levels of systemic follistatin that had significantly reduced testis weights.

Different variables such as expression of activin A, follistatin and inflammatory markers (TNF and MCP-1) were correlated with regard to EAEO development. These correlations show that, when activin A levels are elevated, there is a severe testicular inflammation, which leads to a higher EAEO score. Interestingly, the EAEO did not correlate with testicular follistatin levels, which point out that the development of the disease could be independent of testicular follistatin expression.

Therefore, data from this study suggest that treatment of EAEO by simply increasing the systemic levels of follistatin does not completely inhibit disease development, although it leads to a lower induction rate of EAEO in treated mice. Knowing the fact that testicular inflammation is a local disease, it could be speculated that a local treatment with follistatin, at the site of the inflammation directly would be more effective than elevating circulating follistatin levels.

Moreover, these observations lead to the assumption that the induction and development of orchitis requires a well-orchestrated action between activin and inflammatory mediators. In fact, each molecule, at a certain concentration, plays a role during the inflammation and its' role is dictated by the presence of the other players involved such as activins, follistatin, inflammatory markers, immune cell, fibrotic markers and others.

Finally, an *in vitro* study with primary Sertoli and peritubular cells treated with cytokines (activin A, TNF) that were elevated in the present mouse model of EAEO was undertaken, in order to mimic the inflammatory milieu in EAEO testis. Firstly, our results suggest that the optimal dose for treating SC with TNF is 25 ng/ml since the cells treated with the above mentioned concentration show the highest activin A production. Secondly, as TNF stimulates production of activin A by SC, and acts through MAPK and NFκB signaling (Takada and Aggarwal, 2004), it promotes inflammation and therefore additional activin A expression by these cells. In order to determine if treatment with activin A affects SC and PTC through activating activin signaling, it would be necessary to study the activation of the SMAD signaling in these cells by performing a SMAD Western Blot. Further *in vitro* experiments are necessary, such as treatment of cells with a mixture of the different inflammatory markers should be performed in order to pin

down the existence of a synergistic or additive effect of the cytokines on the function of the cells by evaluating the activation of the activin signaling pathway, the expression of activin receptors and the expression of fibrotic genes (αSMA and collagen type I, alpha I).

Taken together, our findings point to a pro-inflammatory role for activin A in a mouse model of testicular inflammation, having a synergistic effect with other elevated inflammatory mediators (TNF, MCP-1 and interleukins). Furthermore, detailed mechanistic and functional studies are necessary to understand the exact role of activins and their functional antagonists, inhibin and follistatin, in this process leading to severe inflammation causing infertility.

In conclusion, testicular autoimmune orchitis is a complex disease which involves multiple mechanisms for the promotion and the development of the histopathological changes observed in the testis, an immune privileged organ. These mechanisms involved in orchitis development represent a direct relation between activin and follistatin expression on one hand and factors characterizing the disease on the other hand, such as immune cell infiltration and accumulation, overexpression of inflammatory markers, loss of the BTB integrity and disruption of the immune privilege, strong fibrotic formation and apoptosis of germ cells with destruction of the seminiferous epithelium. Taken together, these different effectors work synergistically to promote orchitis and lead to irreversible infertility. Follistatin could be utilized as a potential therapeutic together with other anti-inflammatory drugs in order to diminish the severity of the disease and to restore fertility.

5. APPENDIX

5.1.   MATERIALS

5.1.1. Cell culture reagents and equipment

48 well Costar cell culture plates (#3548)	Corning, NY, USA
75cm^2 cell culture flasques (#430641)	Corning,NY, USA
Bovine serum albumin (#7030)	Sigma, St Louis, USA
CO_2 incubator HeraCell, Heraeus	Thermofischer Scientific, Waltham, MA, USA
DMEM (#10965-084)	Gibco, Grand Island, NY, USA
DMEM+GlutaMAX (#10566-016)	Gibco, Grand Island, NY, USA
DMEM/F12+GlutaMAX (#10565-042)	Gibco, Grand Island, NY, USA
Dulbecco´s PBS (1X) w/o $CaCl_2$ & $MgCl_2$ (#14190-144)	Gibco, Grand Island, NY, USA
Dulbecco´s PBS (10X) with $CaCl_2$ & $MgCl_2$ (#14080-055)	Gibco, Grand Island, NY, USA
Fetal Bovine Serum (FBS) (#16000-044)	Gibco, Grand Island, NY, USA
Laboratory water bath	Thermoline, Smithfield, NSW, Australia
L-Glutamine 200 mM (#25030-081)	Gibco, Grand Island, NY, USA
MEM Non-Essential Amino Acids (#11140-050)	Gibco, Grand Island, NY, USA
Neubauer Counting Chamber	Boeco, Hamburg, Germany
Penicillin/Streptomycin (#15140-122)	Gibco, Grand Island, NY, USA
Recombinant human/mouse/rat activin A (338-AC/CF)	R&D systems, Minneapolis, USA
Recombinant mouse CCL2/JE/MCP-1 (479-JE-010/CF)	R&D systems, Minneapolis, USA
Recombinant mouse IL-6 (406-ML-005/CF)	R&D systems, Minneapolis, USA
Recombinant mouse TNFα (aa 80-235)	R&D systems, Minneapolis, USA
Shaking water batch (RW1812)	Paton Scientific, SA, Australia
Trypan blue solution 0.4%	Sigma, St Louis, USA
TrypLE Express (#2605-028)	Gibco, Grand Island, NY, USA

5.1.2. Chemicals

Acetic acid, glacial	Merck, Darmstadt, Germany
Acid fuchsin, 1% aqueous	BDH (now Merck), Poole, UK

Agarose	Invitrogen, Karlsruhe, Germany
Ammonium solution 25%	Merck, Darmstadt, Germany
Ammonium sulfate	Merck, Darmstadt, Germany
Aniline oil (#UN1547)	VWR, Fontenay-ss-bois-France
Aniline Blue (#1279)	Merck, Darmstadt, Germany
Azocarmin G solution (#1A266)	Chroma-Gesellschaft, Stuttgart, Germany
Benzoid acid methyl ester (#6944.1)	Carl Roth, Karlsruhe, Germany
Biebrich scarlet, 1% aqueous	BDH (now Merck), Poole, UK
β-mercaptoethanol	Sigma, Saint Louis, USA
Bordetella pertussis toxin salt-free toxin (516562)	Calbiochem, Darmstadt, Germany
Bouin's Fixative Solution (#BOUN-1L)	Amber Scientific, Midvale, WA, Australia
Calcium Chloride $CaCl_2$ (#C5080-500G)	Sigma, St Louis, USA
CAS block histochemical reagent	Life technologies, Frederick, USA
Celestine blue	BDH (now Merck), Poole, UK
Citric acid (244)	Merck, Darmstadt, Germany
DPX mounting medium	Merck, Darmstadt, Germany
Entallan new mounting medium (#107961)	Merck, Darmstadt, Germany
Ethanol	Sigma, Steinheim, Germany
Ethidium bromide	Roth, Karlsruhe, Germany
Ethylene diaminetetraacetic acid disodium salt (EDTA)	Merck, Darmstadt, Germany
Eukitt Quick hardening mounting medium	Sigma-Aldrich, Saint Louis, USA
EZ-Link® Sulfo-NHS-LC-Biotin (21335)	Thermoscientific, Rockford, USA
Ferric Ammonium Sulphate	Ajax Finechem, Seven Hills, NSW, Australia
Ferric Chloride	Ajax Finechem, Tarren Point, NSW, Australia
Formaldehyde solution 37%	Merck, Darmstadt, Germany
Formalin	Trajan, Ringwood, Vic, Australia
Freund's adjuvant, complete	Sigma, Saint Louis, USA
Freund's adjuvant, incomplete	Sigma, Saint Louis, USA
Glycerin	Ajax Finechem, Taren Point, NSW, Australia

Glycine	Sigma, Steinheim, Germany
Harris Hematoxylin Solutions, Modified (#HHS16)	Sigma, St Louis, USA
Hydrochloric acid, concentrated	Merck, Munich, Germany
Hydrochloric acid 37%	Sigma, Steinheim, Germany
Hydrogen peroxide 30% (H_2O_2 30%) (#8070.1)	Carl Roth, Karlsruhe, Germany
Isopentane (#103614T)	AnalaR NORMAPUR, VWR international DBH, Fontenay-sous-bois, France
Isoflurane	Baxter, Unterschleißheim, Germany
Mayer's hematoxylin solution	Merck, Darmstadt, Germany
Methanol	Sigma, Steinheim, Germany
Orange G (#15925)	Merck, Darmstadt, Germany
Paraformaldehyde	Merck, Darmstadt, Germany
Periodic acid	Amber Scientific, Midvale, WA, Australia
Phosphotungstic acid	Ajax Finechem, Tarren Point, NSW, Australia
Picric acid	Merck, Darmstadt, Germany
Potassium chloride	Merck, Darmstadt, Germany
Protease inhibitor cocktail	Sigma, Steinheim, Germany
Protease Inhibitor Cocktail Set III, EDTA free (#539134)	Calbiochem, MA, USA
Schiff's reagent	Amber Scientific, Midvale, WA, Australia
Sodium azide (NaN_3) (#S2002)	Sigma, Steinheim, Germany
Sodium chloride (NaCl)	Sigma, Steinheim, Germany
TiterMax Gold adjuvant	Sigma, Saint Louis, USA
Toluidine Blue O	Sigma, Steinheim, Germany
Tris (4855.2)	Carl Roth, Karlsruhe, Germany
Triton X-100	Sigma, Steinheim, Germany
Tween-20	Carl Roth, Karlsruhe, Germany
Tramadol STADA 50mg Tabs	STADApharm GmbH, Bad Vilbel, Germany
VECTASHIELD antifade Mounting Medium with DAPI	Vector, Burlingame, USA

Zydol (Tramadol Hydrochloride Capsules) 50mg capsules   Aspen Pharmacare, St Leonards, NSW, Australia

5.1.3. Enzymes

Collagenase A (#C-0130)	Sigma, St Louis, USA
DNase I (#DN-25)	Sigma, St Louis, USA
Hyaluronidase, from sheep testes (# H2126)	Sigma, St Louis, USA
Soybean trypsin inhibitor (# 17075-029)	Gibco, Grand Island, NY, USA
Trypsin, from porcine pancreas (# T9201)	Sigma, St Louis, USA

5.1.4. Kits

ApopTag® Peroxidase *In Situ* Apoptosis Detection Kit	Merck, Darmstadt, Germany
iTaq Universal SYBR Green Supermix (#172-5124)	Biorad, München, Germany
Pierce BCA Protein Assay (#23227)	Thermo Scientific, Rockford, IL, USA
Liquid DAB+substrate chromogen system (#K3468)	DAKO, Carpinteria, CA, USA
Power SYBR green PCR Master Mix (4367659)	Applied Biosystems, Warrington, UK
RNase-Free DNase Set (#79254)	Qiagen, Hilden, Germany
RNeasy Mini kit	Qiagen, Hilden, Germany
Superscript III first strand Synthesis System for RT-PCR	Invitrogen, Carlsbad, USA
SYBR Green PCR Kit	Qiagen, Hilden, Germany
Testosterone kit (Immunotech IM1119)	Beckman Coulter, Prague, Czech Republic
Vectastain Elite ABC Kit-standard (#PK6100)	Vector Laboratories, Burlingame, USA

5.1.5. List of Equipment

96 well Costar plates (#3361)	Corning, NY, USA
Cell culture CO_2 incubator	Binder, Tuttlingen, Germany
Centrifuge (5424R)	Eppendorf, Hamburg, Germany
Centrifuge	Sigma, Osterode am harz, Germany
CFX touch™ Real-time PCR detection system	Biorad, München, Germany
Cold Plate for Tissue Embedding EG1150C	Leica, Mount Waverly, Australia
Cryostat CM30509	Leica, Wetzlar, Germany

Desktop centrifuge	Biofuge Fresco Heraeus, Hanau, Germany
Electronic balance SPB50	Ohaus, Giessen, Germany
Electronic balance (mettlerAE240)	Mettler Todelo, Greifensee, Switzerland
Electronic balance (Adventurer)	OHAUS, Parsippany, NJ USA
Fast Real-Time PCR system (7900HT)	Applied Biosystems, Forest city, USA
Fluorescent Microscope (Olympus IX70)	Olympus, Shinjuku, Japan
Fluorescent microscope Axioplan 2 Imaging	Carl Zeiss, Göttingen, Germany
Gel Jet Imager 2000 documentation system	Intas, Göttingen, Germany
Homogenizer (PRO200)	Proscientific, Oxford, USA
MicroAmp Optical 384-well Reaction plate	Applied biosystems, Warrington, UK
MicroAmp Optical Adhesive Film PCR compatible	Applied biosystems, Foster city, USA
Microplate ELISA reader (Multiscan RC)	Labsystems, Vantaa, Finland
Microplate reader	Berthold, Bad Wildbad, Germany
Microtome RM2255	Leica, Wetzlar, Germany
Microwave oven	Samsung, Schwalbach, Germany
Mini centrifuge Galaxy	VWR International
Mini-rocker shaker MR-1	PEQLAB, Erlangen, Germany
Mixer Mill MM 300	Retsch, Haan, Germany
MyiQTM2 Two-Color real-time PCR detection system	Bio-Rad, Munich, Germany
NanoDrop ND 2000	Promega, Mannheim, Germany
Nanodrop ND-1000 Spectrophotometer	ThermoFisher Scientific, Waltham, Mass, USA
Paraffin dispenser embedding module EG1140H	Leica, Mount Waverly, Australia
PCR thermocycler (GeneAmp PCR system 9700)	Applied Biosystems, Forest city, USA
Plate Shaker	RATEK instruments, Boronia, Australia
PCR thermocycler	Biozyme, Oldendor, Germany
PCR thermocycler	Peqlab, Erlagen, Germany
Potter S homogenizer	B. Braun, Melsungen, Germany

Power supply units	Consurs, Reiskirchen, Germany
Roller (SRT1)	Stuart Scientific, Staffordshire, UK
Stainless steel beads, 5mm (#69989)	Qiagen, Hilden, Germany
SuperFrost® Plus microscope slides	R.Langenbrinck, Emmendingen, Germany
Tips and tubes	Axygen, Union City, USA
Tissue Lyser LT (SN23.1001/05705)	Qiagen, Hilden, Germany
Vortex Mixer	RATEK instruments, Boronia, Australia

5.1.6. PCR reagents

DNA Ladder (100 bp)	Promega, Mannheim, Germany
DNase I	Qiagen, Hilden, Germany
Desoxyribonukleosidtriphosphate (dNTP) 10mM	Promega, Mannheim, Germany
iTaq Universal SYBR Green Supermix (#172-5124)	Biorad, München, Germany
Moloney Murine Leukemia Virus Reverse Transcriptase (M-MLV RT)	Promega, Mannheim, Germany
Oligo dT 15 Primer	Promega, Mannheim, Germany
Power SYBR green PCR Master Mix (4367659)	Applied Biosystems, Warrington, UK
QuantiTect SYBR Green PCR Kit	Qiagen, Hilden, Germany
Recombinant RNasine Ribonuclease inhibitor	Promega, Mannheim, Germany
Superscript III first strand Synthesis System for RT-PCR	Invitrogen, Carlsbad, USA
SYBR Green PCR Kit	Qiagen, Hilden, Germany
Taq polymerase	Promega, Mannheim, Germany

5.2.   Buffers and solutions

<u>1% aqueous acetic acid</u>

1% glacial acetic acid in distilled water

<u>0.5% acid alcohol</u>

0.5% concentrated hydrochloric acid in 70% aqueous ethanol

Aniline blue staining solution

2.5% aniline blue

2.5% glacial acetic acid in distilled water

Biebrich scarlet-acid fuchsin staining solution

0.9% Biebrich scarlet

0.1% acid fuchsin

1% glacial acetic acid in distilled water

Bouin's fixative

25% formalin

75% saturated aqueous picric acid

5% glacial acetic acid

Celestin Blue R

5% ferric ammonium sulphate

0.5% Celestin Blue in distilled water

Boil on a hot plate, cool rapidly using a magnetic stirrer and add

14% glycerin

Citrate buffer for antigen retrieval

1,92 g/l citric acid (10mM) in distilled water, pH 6,0

Munõs Buffer

25 mM Tris (MW 121.14 g/l)

0.5 M NaCl (MW 58.44 g/l)

0.017% Triton X-100 in distilled water, pH 7.6

TAE Buffer

40 mM Tris-acetate

1 mM EDTA, pH 8

TBST (Tris Buffered Saline with Tween)

10 x: 24 g/l Tris base (Molecular weight: 121.14 g/l)

88 g/l NaCl (Molecular weight: 58.4 g/l)

Distilled water

pH 7.6

1 x: 10% of 10x TBST in distilled water,

pH 7,6

0,1 % Tween20

Blocking buffer

10 % normal goat serum in TBST

Toluidine blue staining solution:

Toluidine blue stock solution: 1% toluidine blue O in 70% Ethanol

1% sodium chloride: 1 % sodium chloride in distilled water

pH 2.0 ~2.5 (Solution should be made fresh)

Toluidine Blue working solution: 10% toluidine blue stock solution in 1% sodium

chloride

pH 2.3 (Solution should be made fresh)

5% aqueous phosphotungstic acid

5% phosphotungstic acid in distilled water

Weigert's Iron Hematoxylin

Solution A: 1% of Hematoxylin powder in absolute ethanol

Solution B: 1.16% ferric chloride

1% concentrated hydrochloric acid

Distilled water

Mix solution A and B in equal parts

5.3. Buffers and solutions for cell culture

1 mg/ml DNAse

1 mg/ml DNAse in D-PBS (+)

1 mg/ml trypsin

1 mg/ml Trypsin in DMEM/F12

0.02 mg/ml DNAse

0.1 mg/ml Soybean trypsin inhibitor (SBTI)

0.1 mg/ml SBTI in D-PBS (+)

0.01 mg/ml DNAse

1 mg/ml collagenase

1 mg/ml collagenase in DMEM/F12

6 µg/ml DNAse

1 mg/ml hyaluronidase

1 mg/ml hyaluronidase in DMEM/F12

6 µg/ml DNase

DMEM/F12

0.5% L- glutamine (200 mM)

1% non-essential amino acids [100x]

1% penicillin / streptomycin (10,000 IU / 10,000 µg/ml)

Store at 4ºC

DMEM

1% non-essential amino acids [100x]

1% penicillin / streptomycin (10,000 IU / 10,000 µg/ml)

Store at 4ºC

<u>Sertoli cell culture medium</u>

0.1% BSA in DMEM

Filter sterile

<u>Peritubular cell culture medium</u>

10% FCS in DMEM

5.4.   Primary antibodies

Anti-α smooth muscle actin FITC-conjugated IgG (F3777)	Sigma, Saint Louis, USA
E4 mouse anti-activin βA	Oxford Brooks University, Oxford, UK
Mouse monoclonal anti-PCNA (M0879)	Dako, Glostrup, Denmark
Rabbit polyclonal anti-Sox9 (sc-20095)	Santa Cruz Biotechnology, Dallas, USA
Rat anti-mouse CD206 (mannose receptor) (ab64693)	Abcam, Cambridge, UK
Rat anti-mouse F4/80 (MCA497G)	AbD Serotec, Kidlington, UK

5.5.   Secondary antibodies

Streptavidin-AlexaFluor 488 (S32354)	Invitrogen (molecular probes), Eugene, USA
F(ab')2-goat anti-rabbit IgG (H+L) AlexaFluor546 (A11071)	Life Technologies, Carlsbad, USA
HRP-labeled polymer anti-rabbit (K4003)	(Dako, Glostrup, Denmark)

5.6.   Primers

Table 7: Primers used in quantitative RT-PCR experiments in this study.

Target gene	Forward primer (5'-3')	Reverse primer (5'-3')	Amplicon size (bp)	Annealing temperature (°C)	Entrez Gene ID	Catalogue number (Qiagen)
18S rRNA	TACCACATCCAAGGAAGGCAGCA	TGGAATTACCGCGGCTGCTGGCA	180	55	19791	-
Acvr1b	CCAACTGGTGGCAGAGTTAT	CTGGGACAGAGTCTTCTTGATG	119	55	11479	-
Acvr2b	ATGAGTACATGCTGCCCTTC	CTTAATCGTGGGCCTCATCTT	101	55	11481	-
Acta2 (αSMA)	CCTCCAGTTCCTTTCCAAAT	GCCAGGGCTACAAGTTAAG	106	60	11475	
B2M (β2-microglobulin)	CCGCCTCACATTGAA	TCGATCCCAGTAGACG	198	55	12010	-
actb (β-actin)	TGACAGGATGCAGAAGGAGAT	TACTCCTGCTTGCTGATCCAC	156	55	11461	-
Ccl2 (MCP-1)	QuantiTect Primer assay	Qiagen	118	55	20296	QT00167832
Ccl2 (MCP-1) (study 2)	AGGTGTCCCAAAGAAGCTGTA	ATGTCTGGACCCATTCCTTCT	85	60	20296	-
Col1a1 (Collagen I, α1)	ACGTCTGGTTTGGAGAGA	AGGAAGGTCAGCTGGATAG	298	60	12842	-
Cyp11a1 (P450scc)	CCAGTGTCCCCATGCTCAAC	TGCATGGTCCTTCCAGGTCT	74	62	13070	-
Cyp17a1 (P450c17)	GCCCAAGTCAAAGACACCTAAT	GTACCCAGGCGAAGAGAATA	159	60	13074	-
Fst (Follistatin)	AGGAGGATGTGAACGACAATAC	CACGTTCTCACACGTTTCTTTAC	95	55	14313	-
Fst288	CTCTCTCTGCGATGAGCTGTGT	GGCTCAGGTTTTACAGGCAGAT	176	55	14313	-
Fst315	CTCTCTCTGCGATGAGCTGTGT	TCTTCCTCCTCCTCCTCTTCCT	192	55	14313	-
HPRT	CTGGTAAAAGGACCTC	CTGAAGTACTCATTATAGTCAAG	110	55	15452	-
Hsd3b1	TGGACAAAGTATTCCGACCAGA	GGCACACTTGCTTGAACACAG	250	60	15492	-
Il6 (study 2)	ATGGATGCTACCAAACTGGAT	TGAAGGACTCTGGCTTTGTCT	139	60	16193	-
Il6	QuantiTect Primer assay	Qiagen	128	55	16193	QT00098875
Il10	QuantiTect Primer assay	Qiagen	109	55	16153	QT00106169
Il10 (study 2)	GGTTGCCAAGCCTTATCGGA	ACCTGCTCCACTGCCTTGCT	191	60	16153	-
Inha	GCCAAGGTGAAGGCTCTATT	AGACCTCCTGTGCATGAAAC	126	55	16322	-
Inhba	AGAACGGGTATGTGGAGATAGA	GACTCGGCAAAGGTGATGAT	97	55	16323	-
Inhbb	CTGCCAGTCGGGCAGGGTATAA	CCTTCACTCCACCAGTCATTT	110	55	16324	-
Star	TGCCCATCATTTCATTCATCCTT	AAAAGCGGTTTCTCACTCTCC	232	60	20845	-
tnf (TNF)	QuantiTect Primer assay	Qiagen	112	55	21926	QT00104006
tnf (TNF) (study 2)	CAAATTCGAGTGACAAGCCTG	GAGATCCATGCCGTTGGC	113	60	21926	-

6. SUMMARY

Experimental autoimmune epididymo-orchitis (EAEO) is a rodent model of chronic testicular inflammation that reproduces the pathology observed in some types of human infertility, characterized by elevated levels of pro-inflammatory cytokines, immune cell recruitment, germ cell loss and ultimately sub- or infertility.

Activins A and B are pro-inflammatory, pro-fibrotic cytokines, but also regulate spermatogenesis and steroidogenesis under normal conditions. The roles of activin A, B and the endogenous activin antagonists, inhibin and follistatin, were examined in EAEO. The disease was induced in adult mice by immunization with syngeneic testicular homogenate.

Age-matched untreated mice and controls showed no pathology, with activin A localized to Sertoli cells and interstitial macrophages. Immunized mice developed EAEO by 50 days (induction rate of 100%), and were characterized by a >50% reduction in testis weight, complete loss of germ cells, and a marked peritubular fibrotic response. Similar changes were also observed in biopsies from human testes with inflammatory infiltrates. Moreover, changes were accompanied by increased expression of key inflammatory mediators such as tumor necrosis factor, monocyte chemoattractant protein-1 and interleukin-10. An increase of the total CD45+ leukocytes, comprising CD3+ T cells, CD4+CD8- and CD4+CD25+ T cells, and a novel population of CD4+CD8+ double positive T cells was also detected in EAEO testes. Activin A and B protein levels were significantly increased in EAEO testes at 50 days, compared with untreated controls but not at 80 days, whereas the inhibin subunit mRNA levels (*Inha* and *Inhbb*) decreased in EAEO testes, becoming significantly lower after 80 days compared with control animals. Activin A receptor a*cvr1b* and *acvr2b* mRNA levels were also significantly decreased in EAEO testes. In contrast, testicular follistatin levels were significantly elevated at 50 and 80 days of EAEO.

These data suggest that there is a direct association between the onset of EAEO and increased activin expression. Therefore, activin may play a role in promoting inflammation and fibrosis during EAEO in mouse testis.

Consequently, the development of EAEO in a mouse model with elevated circulating levels of the activin antagonist follistatin (FST), was examined. Follistatin levels were increased by a single injection of a non-replicative recombinant adenovirus-associated viral vector carrying a gene cassette of the circulating form of follistatin (FST315). Controls received an rAAV injection with an empty cassette. EAEO was induced and testes were collected 30 and 50 days after the first immunization. Serum follistatin levels were increased 5-fold in FST315-vector injected mice compared with the control group 30 days after vector injection and remained elevated until the end of the experiment. The EAEO induction rate was 40% for the FST315-vector injected group compared with 75% for the control group. Elevated levels of inflammatory mediators and activins, recruitment of immune cells, increased fibrosis, disruption of the blood-testis-barrier, and increased apoptosis were directly proportional to the observed testicular damage in EAEO.

These data suggest that blocking activin activity alone, by increasing circulating follistatin levels before inducing EAEO, was not sufficient to inhibit the development of testicular inflammation and fibrosis.

7. ZUSAMMENFASSUNG

Die experimentelle Autoimmun-Epididymo-Orchitis (EAEO) stellt ein Nagermodell für chronische Entzündungen des Hodens dar, das besonders in der früheren Phase der Erkrankung bestimmte Formen idiopathischer, immunologisch-bedingter Infertilität des Mannes gut reproduzieren kann. Schlüsselcharakteristika bei der EAEO und entsprechenden Erkrankungen des Mannes sind erhöhte Konzentrationen pro-inflammatorischer Zytokine, die Akkumulation von Leukocyten im Organ sowie ein Verlust von Keimzellen mit nachfolgender Sub- bzw. Infertilität. Activin A und B sind pro-inflammatorische und pro-fibrotische Zytokine, die zudem eine wichtige Funktion in der Regulation der normalen Spermatogenese und Steroidogenese aufweisen. In dieser Studie wurde eine mögliche Funktion von Activin A und B sowie der endogenen Activin-Antagonisten Inhibin und Follistatin in der Pathogenese der EAEO untersucht. Die EAEO wurde durch Immunisierung mit syngenem Hodenhomogenat in adulten Mäusen ausgelöst.

Altersgleiche unbehandelte Mäuse sowie Sham-Kontrollmäuse zeigten keine pathologischen Veränderungen im Verlauf der Untersuchung, wobei Activin A immunhistochemisch in Sertoli-Zellen und interstitiellen Makrophagen gefunden wurde. Dagegen entwickelten alle immunisierten Mäuse nach 50 Tagen eine EAEO (Induktionsrate 100%) und waren durch eine mehr als 50%ige Reduktion des Hodengewichts, einem vollständigen Verlust der Keimzellen und eine deutliche fibrotische Reaktion charakterisiert. Ähnliche Veränderungen werden auch in Biopsien mit entzündlichen Infiltraten im Hoden beim Mann beobachtet. Darüber hinaus wurde die Entwicklung der EAEO durch eine erhöhte Expression entzündlicher Mediatoren wie des Tumor-Nnekrose Faktors (TNF), des Monocyte Chemoattractant Protein-1 (MCP-1) und von Interleukin-10 (IL-10) begleitet. Zusätzlich wurde eine starke Zunahme der gesamten CD45+ Leukozytenpopulation, die aus CD3+ T Zellen, CD4+CD8- und CD4+CD25+ T Zellen, sowie einer neuen Population von CD4+CD8+ doppelt positiven T Zellen besteht, beobachtet. Im Vergleich zu den Kontrolltieren waren die Proteinkonzentrationen von testikulärem Activin A und B Protein bei den EAEO-Tieren 50 Tage, nicht jedoch 80 Tagen, nach Induktion der EAEO deutlich erhöht. Dagegen sanken die testikulären mRNA Level der Inhibin Untereinheiten *Inha* und *Inhb* im Verlauf der EAEO und waren nach 80 Tagen deutlich niedriger als bei den Kontrolltieren. Auch die mRNA Level der Activinrezeptoren *acvr1b* and *acvr2b* waren in den EAEO Hoden deutlich reduziert, wogegen die testikulären Follistatin Konzentrationen in der EAEO-Gruppe sowohl nach 50 als auch nach 80 Tagen im Serum deutlich erhöht gemessen worden. Diese Ergebnisse legen nahe, dass es eine Verbindung zwischen der Entwicklung einer EAEO und erhöhter Activinexpression gibt und Activin die Entwicklung einer Hodenentzündung und –fibrose während der EAEO fördern könnte.

Die Rolle von Activin in der EAEO sollte anschließend *in vivo* in einem Mausmodell untersucht werden, in dem die Serum Follistatin-Konzentrationen experimentell durch i.m. Applikation eines nicht-replizierenden, rekombinanten adenoassoziierten Virus Vektors (rAAV), der eine Expressionskassette für die zirkulierende Follistatin Isoform (FST315) besitzt, erhöht wird. Kontrolltiere erhielten einen Vektor mit leerer

Expressionskassette. Nach Induktion einer EAEO in diesen Tieren wurden die Hoden 30 und 50 Tage nach der ersten Immunisierung entnommen. Nach 30 Tagen waren die Serum Follistatin Konzentrationen bei den FST315 überexprimierenden Mäusen 5-fach erhöht und blieben es auch bis zum Ende des Experimentes. Die EAEO Induktionsrate betrug 40% für die FST315 überexprimierenden Mäuse verglichen mit 75% in der Kontrollgruppe. Erhöhte Konzentrationen an entzündlichen Schlüsselmediatoren, Activin A und B, leukocytäre Infiltrate, eine erhöhte Fibrosierung, eine beeinträchtigte Blut-Hodenschranke und vermehrte Apoptose von Keimzellen waren direkt proportional zu pathologischen Veränderungen in der Hodenmorphologie der EAEO-Gruppe.

Diese Ergebnisse deuten darauf hin, dass eine alleinige Blockierung der Aktivinaktivität durch Erhöhung der Konzentration an zirkulierendem Follistatin vor und während der Induktion der EAEO, nicht ausreicht um die Entwicklung einer Hodenentzündung und – fibrose vollständig zu verhindern.

8. REFERENCES

ADAM, M., SCHWARZER, J. U., KOHN, F. M., STRAUSS, L., POUTANEN, M. & MAYERHOFER, A. 2011. Mast cell tryptase stimulates production of decorin by human testicular peritubular cells: possible role of decorin in male infertility by interfering with growth factor signaling. *Hum Reprod,* 26**,** 2613-25.

AHMED, E. A. & DE ROOIJ, D. G. 2009. Staging of mouse seminiferous tubule cross-sections. *Methods Mol Biol,* 558**,** 263-77.

AMOUZEGAR, A., CHAUHAN, S. K. & DANA, R. 2016. Alloimmunity and Tolerance in Corneal Transplantation. *J Immunol,* 196**,** 3983-91.

ANDERSON, R. A., EVANS, L. W., IRVINE, D. S., MCINTYRE, M. A., GROOME, N. P. & RILEY, S. C. 1998. Follistatin and activin A production by the male reproductive tract. *Hum Reprod,* 13**,** 3319-25.

ARCHAMBEAULT, D. R., TOMASZEWSKI, J., CHILDS, A. J., ANDERSON, R. A. & YAO, H. H. 2011. Testicular somatic cells, not gonocytes, are the major source of functional activin A during testis morphogenesis. *Endocrinology,* 152**,** 4358-67.

ARCHAMBEAULT, D. R. & YAO, H. H. 2010. Activin A, a product of fetal Leydig cells, is a unique paracrine regulator of Sertoli cell proliferation and fetal testis cord expansion. *Proc Natl Acad Sci U S A,* 107**,** 10526-31.

ARGUELLO, F., ALEXANDER, M., STERRY, J. A., TUDOR, G., SMITH, E. M., KALAVAR, N. T., GREENE, J. F., JR., KOSS, W., MORGAN, C. D., STINSON, S. F., SIFORD, T. J., ALVORD, W. G., KLABANSKY, R. L. & SAUSVILLE, E. A. 1998. Flavopiridol induces apoptosis of normal lymphoid cells, causes immunosuppression, and has potent antitumor activity In vivo against human leukemia and lymphoma xenografts. *Blood,* 91**,** 2482-90.

ASLANI, F., SCHUPPE, H. C., GUAZZONE, V. A., BHUSHAN, S., WAHLE, E., LOCHNIT, G., LUSTIG, L., MEINHARDT, A. & FIJAK, M. 2015. Targeting high mobility group box protein 1 ameliorates testicular inflammation in experimental autoimmune orchitis. *Hum Reprod,* 30**,** 417-31.

AUSTYN, J. M. & GORDON, S. 1981. F4/80, a monoclonal antibody directed specifically against the mouse macrophage. *Eur J Immunol,* 11**,** 805-15.

BARAKAT, B., O'CONNOR, A. E., GOLD, E., DE KRETSER, D. M. & LOVELAND, K. L. 2008. Inhibin, activin, follistatin and FSH serum levels and testicular production are highly modulated during the first spermatogenic wave in mice. *Reproduction,* 136**,** 345-59.

BARBE, C., KALISTA, S., LOUMAYE, A., RITVOS, O., LAUSE, P., FERRACIN, B. & THISSEN, J. P. 2015. Role of IGF-I in follistatin-induced skeletal muscle hypertrophy. *Am J Physiol Endocrinol Metab,* 309**,** E557-67.

BHUSHAN, S., ASLANI, F., ZHANG, Z., SEBASTIAN, T., ELSASSER, H. P. & KLUG, J. 2016. Isolation of Sertoli Cells and Peritubular Cells from Rat Testes. *J Vis Exp***,** e53389.

BHUSHAN, S. & MEINHARDT, A. 2016. The macrophages in testis function. *J Reprod Immunol*.

BHUSHAN, S., TCHATALBACHEV, S., LU, Y., FROHLICH, S., FIJAK, M., VIJAYAN, V., CHAKRABORTY, T. & MEINHARDT, A. 2015. Differential activation of

inflammatory pathways in testicular macrophages provides a rationale for their subdued inflammatory capacity. *J Immunol,* 194**,** 5455-64.

BLUESTONE, J. A., PARDOLL, D., SHARROW, S. O. & FOWLKES, B. J. 1987. Characterization of murine thymocytes with CD3-associated T-cell receptor structures. *Nature,* 326**,** 82-4.

BOBZIEN, B., YASUNAMI, Y., MAJERCIK, M., LACY, P. E. & DAVIE, J. M. 1983. Intratesticular transplants of islet xenografts (rat to mouse). *Diabetes,* 32**,** 213-6.

BRENNAN, J. & CAPEL, B. 2004. One tissue, two fates: molecular genetic events that underlie testis versus ovary development. *Nat Rev Genet,* 5**,** 509-21.

BROXMEYER, H. E., LU, L., COOPER, S., SCHWALL, R. H., MASON, A. J. & NIKOLICS, K. 1988. Selective and indirect modulation of human multipotential and erythroid hematopoietic progenitor cell proliferation by recombinant human activin and inhibin. *Proc Natl Acad Sci U S A,* 85**,** 9052-6.

BURT, T. D. 2013. Fetal regulatory T cells and peripheral immune tolerance in utero: implications for development and disease. *Am J Reprod Immunol,* 69**,** 346-58.

BUSTIN, S. A., BENES, V., GARSON, J. A., HELLEMANS, J., HUGGETT, J., KUBISTA, M., MUELLER, R., NOLAN, T., PFAFFL, M. W., SHIPLEY, G. L., VANDESOMPELE, J. & WITTWER, C. T. 2009. The MIQE guidelines: minimum information for publication of quantitative real-time PCR experiments. *Clin Chem,* 55**,** 611-22.

CARMELIET, P., DOR, Y., HERBERT, J. M., FUKUMURA, D., BRUSSELMANS, K., DEWERCHIN, M., NEEMAN, M., BONO, F., ABRAMOVITCH, R., MAXWELL, P., KOCH, C. J., RATCLIFFE, P., MOONS, L., JAIN, R. K., COLLEN, D. & KESHERT, E. 1998. Role of HIF-1alpha in hypoxia-mediated apoptosis, cell proliferation and tumour angiogenesis. *Nature,* 394**,** 485-90.

CARVAJAL MONROY, P. L., GREFTE, S., KUIJPERS-JAGTMAN, A. M., HELMICH, M. P., WAGENER, F. A. & VON DEN HOFF, J. W. 2015. Fibrosis impairs the formation of new myofibers in the soft palate after injury. *Wound Repair Regen,* 23**,** 866-73.

CHEN, J. L., WALTON, K. L., QIAN, H., COLGAN, T. D., HAGG, A., WATT, M. J., HARRISON, C. A. & GREGOREVIC, P. 2016. Differential effects of interleukin-6 and activin A in the development of cancer-associated cachexia. *Cancer Res.*

CHEN, J. L., WALTON, K. L., WINBANKS, C. E., MURPHY, K. T., THOMSON, R. E., MAKANJI, Y., QIAN, H., LYNCH, G. S., HARRISON, C. A. & GREGOREVIC, P. 2014. Elevated expression of activins promotes muscle wasting and cachexia. *Faseb j,* 28**,** 1711-23.

DAI, Z., NASR, I. W., REEL, M., DENG, S., DIGGS, L., LARSEN, C. P., ROTHSTEIN, D. M. & LAKKIS, F. G. 2005. Impaired recall of CD8 memory T cells in immunologically privileged tissue. *J Immunol,* 174**,** 1165-70.

DATTA-MANNAN, A., YADEN, B., KRISHNAN, V., JONES, B. E. & CROY, J. E. 2013. An engineered human follistatin variant: insights into the pharmacokinetic and pharmacodynamic relationships of a novel molecule with broad therapeutic potential. *J Pharmacol Exp Ther,* 344**,** 616-23.

DE CESARIS, P., FILIPPINI, A., CERVELLI, C., RICCIOLI, A., MUCI, S., STARACE, G., STEFANINI, M. & ZIPARO, E. 1992. Immunosuppressive molecules

produced by Sertoli cells cultured in vitro: biological effects on lymphocytes. *Biochem Biophys Res Commun,* 186**,** 1639-46.

DE KRETSER, D. M. 1997. Male infertility. *Lancet,* 349**,** 787-90.

DE KRETSER, D. M., LOVELAND, K. L., MEEHAN, T., O'BRYAN, M. K., PHILLIPS, D. J. & WREFORD, N. G. 2001. Inhibins, activins and follistatin: actions on the testis. *Mol Cell Endocrinol,* 180**,** 87-92.

DE WINTER, J. P., VANDERSTICHELE, H. M., VERHOEVEN, G., TIMMERMAN, M. A., WESSELING, J. G. & DE JONG, F. H. 1994. Peritubular myoid cells from immature rat testes secrete activin-A and express activin receptor type II in vitro. *Endocrinology,* 135**,** 759-67.

DESHMANE, S. L., KREMLEV, S., AMINI, S. & SAWAYA, B. E. 2009. Monocyte chemoattractant protein-1 (MCP-1): an overview. *J Interferon Cytokine Res,* 29**,** 313-26.

DOHLE, G. R., COLPI, G. M., HARGREAVE, T. B., PAPP, G. K., JUNGWIRTH, A. & WEIDNER, W. 2005. EAU guidelines on male infertility. *Eur Urol,* 48**,** 703-11.

DONCEL, G. F., DI PAOLA, J. A. & LUSTIG, L. 1989. Sequential study of the histopathology and cellular and humoral immune response during the development of an autoimmune orchitis in Wistar rats. *Am J Reprod Immunol,* 20**,** 44-51.

DOYLE, T. J., KAUR, G., PUTREVU, S. M., DYSON, E. L., DYSON, M., MCCUNNIFF, W. T., PASHAM, M. R., KIM, K. H. & DUFOUR, J. M. 2012. Immunoprotective properties of primary Sertoli cells in mice: potential functional pathways that confer immune privilege. *Biol Reprod,* 86**,** 1-14.

DUFOUR, J. M., HAMILTON, M., RAJOTTE, R. V. & KORBUTT, G. S. 2005. Neonatal porcine Sertoli cells inhibit human natural antibody-mediated lysis. *Biol Reprod,* 72**,** 1224-31.

EBERT, S., ZERETZKE, M., NAU, R. & MICHEL, U. 2007. Microglial cells and peritoneal macrophages release activin A upon stimulation with Toll-like receptor agonists. *Neurosci Lett,* 413**,** 241-4.

FIJAK, M., BHUSHAN, S. & MEINHARDT, A. 2011a. Immunoprivileged sites: the testis. *Methods Mol Biol,* 677**,** 459-70.

FIJAK, M., IOSUB, R., SCHNEIDER, E., LINDER, M., RESPONDEK, K., KLUG, J. & MEINHARDT, A. 2005. Identification of immunodominant autoantigens in rat autoimmune orchitis. *J Pathol,* 207**,** 127-38.

FIJAK, M. & MEINHARDT, A. 2006. The testis in immune privilege. *Immunol Rev,* 213**,** 66-81.

FIJAK, M., SCHNEIDER, E., KLUG, J., BHUSHAN, S., HACKSTEIN, H., SCHULER, G., WYGRECKA, M., GROMOLL, J. & MEINHARDT, A. 2011b. Testosterone replacement effectively inhibits the development of experimental autoimmune orchitis in rats: evidence for a direct role of testosterone on regulatory T cell expansion. *J Immunol,* 186**,** 5162-72.

FILLION, C., TAHRI-JOUTEI, A., HUGUES, J. N., ALLEVARD, A. M., TAIB, N. & POINTIS, G. 1994. Presence in mouse Sertoli cell-conditioned medium of a factor that expresses AVP-like inhibition of steroidogenesis by mouse Leydig cells in long-term culture. *Mol Cell Endocrinol,* 99**,** 25-30.

FRANCA, L. R., HESS, R. A., DUFOUR, J. M., HOFMANN, M. C. & GRISWOLD, M. D. 2016. The Sertoli cell: one hundred fifty years of beauty and plasticity. *Andrology,* 4**,** 189-212.

FREUND, J., LIPTON, M. M. & THOMPSON, G. E. 1953. Aspermatogenesis in the guinea pig induced by testicular tissue and adjuvants. *J Exp Med,* 97**,** 711-26.

FREUND, J., LIPTON, M. M. & THOMPSON, G. E. 1954. Impairment of spermatogenesis in the rat after cutaneous injection of testicular suspension with complete adjuvants. *Proc Soc Exp Biol Med,* 87**,** 408-11.

GAVRIELI, Y., SHERMAN, Y. & BEN-SASSON, S. A. 1992. Identification of programmed cell death in situ via specific labeling of nuclear DNA fragmentation. *J Cell Biol,* 119**,** 493-501.

GUAZZONE, V. A., JACOBO, P., THEAS, M. S. & LUSTIG, L. 2009. Cytokines and chemokines in testicular inflammation: A brief review. *Microsc Res Tech,* 72**,** 620-8.

GUAZZONE, V. A., RIVAL, C., DENDUCHIS, B. & LUSTIG, L. 2003. Monocyte chemoattractant protein-1 (MCP-1/CCL2) in experimental autoimmune orchitis. *J Reprod Immunol,* 60**,** 143-57.

HAGG, A., COLGAN, T. D., THOMSON, R. E., QIAN, H., LYNCH, G. S. & GREGOREVIC, P. 2016. Using AAV vectors expressing the beta2-adrenoceptor or associated Galpha proteins to modulate skeletal muscle mass and muscle fibre size. *Sci Rep,* 6**,** 23042.

HALL, P. A., LEVISON, D. A., WOODS, A. L., YU, C. C., KELLOCK, D. B., WATKINS, J. A., BARNES, D. M., GILLETT, C. E., CAMPLEJOHN, R., DOVER, R. & ET AL. 1990. Proliferating cell nuclear antigen (PCNA) immunolocalization in paraffin sections: an index of cell proliferation with evidence of deregulated expression in some neoplasms. *J Pathol,* 162**,** 285-94.

HARDY, C. L., NGUYEN, H. A., MOHAMUD, R., YAO, J., OH, D. Y., PLEBANSKI, M., LOVELAND, K. L., HARRISON, C. A., ROLLAND, J. M. & O'HEHIR, R. E. 2013. The activin A antagonist follistatin inhibits asthmatic airway remodelling. *Thorax,* 68**,** 9-18.

HAVERFIELD, J. T., MEACHEM, S. J., NICHOLLS, P. K., RAINCZUK, K. E., SIMPSON, E. R. & STANTON, P. G. 2014. Differential permeability of the blood-testis barrier during reinitiation of spermatogenesis in adult male rats. *Endocrinology,* 155**,** 1131-44.

HEAD, J. R., NEAVES, W. B. & BILLINGHAM, R. E. 1983. Immune privilege in the testis. I. Basic parameters of allograft survival. *Transplantation,* 36**,** 423-31.

HEDGER, M. P. 1997. Testicular leukocytes: what are they doing? *Rev Reprod,* 2**,** 38-47.

HEDGER, M. P. 2002. Macrophages and the immune responsiveness of the testis. *J Reprod Immunol,* 57**,** 19-34.

HEDGER, M. P. 2013. *The Immunophysiology of Male Reproduction.*

HEDGER, M. P. & DE KRETSER, D. M. 2013. The activins and their binding protein, follistatin-Diagnostic and therapeutic targets in inflammatory disease and fibrosis. *Cytokine Growth Factor Rev,* 24**,** 285-95.

HEDGER, M. P. & WINNALL, W. R. 2012. Regulation of activin and inhibin in the adult testis and the evidence for functional roles in spermatogenesis and immunoregulation. *Mol Cell Endocrinol,* 359**,** 30-42.

HEDGER, M. P., WINNALL, W. R., PHILLIPS, D. J. & DE KRETSER, D. M. 2011. The regulation and functions of activin and follistatin in inflammation and immunity. *Vitam Horm,* 85**,** 255-97.

HEINZ, M., NIEDERLEITHNER, H. L., PUUJALKA, E., SOLER-CARDONA, A., GRUSCH, M., PEHAMBERGER, H., LOEWE, R. & PETZELBAUER, P. 2015. Activin A is anti-lymphangiogenic in a melanoma mouse model. *J Invest Dermatol,* 135**,** 212-21.

HERNANDEZ, O., OWEITY, T. & IBRAHIM, S. 2005. Is an increase in CD4/CD8 T-cell ratio in lymph node fine needle aspiration helpful for diagnosing Hodgkin lymphoma? A study of 85 lymph node FNAs with increased CD4/CD8 ratio. *Cytojournal,* 2**,** 14.

HOEK, A., ALLAERTS, W., LEENEN, P. J., SCHOEMAKER, J. & DREXHAGE, H. A. 1997. Dendritic cells and macrophages in the pituitary and the gonads. Evidence for their role in the fine regulation of the reproductive endocrine response. *Eur J Endocrinol,* 136**,** 8-24.

HOFSTETTER, H. H., SHIVE, C. L. & FORSTHUBER, T. G. 2002. Pertussis toxin modulates the immune response to neuroantigens injected in incomplete Freund's adjuvant: induction of Th1 cells and experimental autoimmune encephalomyelitis in the presence of high frequencies of Th2 cells. *J Immunol,* 169**,** 117-25.

HONG, Y., HAN, Y. Q., WANG, Y. Z., GAO, J. R., LI, Y. X., LIU, Q. & XIA, L. Z. 2016. Paridis Rhizoma Sapoinins attenuates liver fibrosis in rats by regulating the expression of RASAL1/ERK1/2 signal pathway. *J Ethnopharmacol.*

HUME, D. A., ROBINSON, A. P., MACPHERSON, G. G. & GORDON, S. 1983. The mononuclear phagocyte system of the mouse defined by immunohistochemical localization of antigen F4/80. Relationship between macrophages, Langerhans cells, reticular cells, and dendritic cells in lymphoid and hematopoietic organs. *J Exp Med,* 158**,** 1522-36.

IOSUB, R., KLUG, J., FIJAK, M., SCHNEIDER, E., FROHLICH, S., BLUMBACH, K., WENNEMUTH, G., SOMMERHOFF, C. P., STEINHOFF, M. & MEINHARDT, A. 2006. Development of testicular inflammation in the rat involves activation of proteinase-activated receptor-2. *J Pathol,* 208**,** 686-98.

ITMAN, C., MENDIS, S., BARAKAT, B. & LOVELAND, K. L. 2006. All in the family: TGF-beta family action in testis development. *Reproduction,* 132**,** 233-46.

ITOH, M., DE ROOIJ, D. G., JANSEN, A. & DREXHAGE, H. A. 1995. Phenotypical heterogeneity of testicular macrophages/dendritic cells in normal adult mice: an immunohistochemical study. *J Reprod Immunol,* 28**,** 217-32.

ITOH, M., HIRAMINE, C. & HOJO, K. 1991. A new murine model of autoimmune orchitis induced by immunization with viable syngeneic testicular germ cells alone. I. Immunological and histological studies. *Clin Exp Immunol,* 83**,** 137-42.

JACOBO, P., GUAZZONE, V. A., JARAZO-DIETRICH, S., THEAS, M. S. & LUSTIG, L. 2009. Differential changes in CD4+ and CD8+ effector and regulatory T

lymphocyte subsets in the testis of rats undergoing autoimmune orchitis. *J Reprod Immunol,* 81**,** 44-54.

JACOBO, P., PEREZ, C. V., THEAS, M. S., GUAZZONE, V. A. & LUSTIG, L. 2011. CD4+ and CD8+ T cells producing Th1 and Th17 cytokines are involved in the pathogenesis of autoimmune orchitis. *Reproduction,* 141**,** 249-58.

JAISWAL, M. K., KATARA, G. K., MALLERS, T., CHAOUAT, G., GILMAN-SACHS, A. & BEAMAN, K. D. 2014. Vacuolar-ATPase isoform a2 regulates macrophages and cytokine profile necessary for normal spermatogenesis in testis. *J Leukoc Biol,* 96**,** 337-47.

JANEWAY, C. A. J. T. P. W. M. S. M. J. 2001. *Immunobiology, The Immune System in Health and Disease. 5th edition,* New York, Garland Science.

JONES, K. L., BRAUMAN, J. N., GROOME, N. P., DE KRETSER, D. M. & PHILLIPS, D. J. 2000. Activin A release into the circulation is an early event in systemic inflammation and precedes the release of follistatin. *Endocrinology,* 141**,** 1905-8.

JORGENSEN, A., YOUNG, J., NIELSEN, J. E., JOENSEN, U. N., TOFT, B. G., RAJPERT-DE MEYTS, E. & LOVELAND, K. L. 2014. Hanging drop cultures of human testis and testis cancer samples: a model used to investigate activin treatment effects in a preserved niche. *Br J Cancer,* 110**,** 2604-14.

JUNGWIRTH, A., GIWERCMAN, A., TOURNAYE, H., DIEMER, T., KOPA, Z., DOHLE, G. & KRAUSZ, C. 2012. European Association of Urology guidelines on Male Infertility: the 2012 update. *Eur Urol,* 62**,** 324-32.

KALLIOKOSKI, S., PIQUERAS, V. O., FRIAS, R., SULIC, A. M., MAATTA, J. A., KAHKONEN, N., VIIRI, K., HUHTALA, H., PASTERNACK, A., LAURILA, K., SBLATTERO, D., KORPONAY-SZABO, I. R., MAKI, M., CAJA, S., KAUKINEN, K. & LINDFORS, K. 2016. Transglutaminase 2-specific coeliac disease autoantibodies induce morphological changes and signs of inflammation in the small-bowel mucosa of mice. *Amino Acids.*

KIKUI, Y. & MIKI, A. 1995. A differential staining method for adenohypophyseal cells. *Arch Histol Cytol,* 58**,** 375-8.

KNIGHT, P. G., MUTTUKRISHNA, S. & GROOME, N. P. 1996. Development and application of a two-site enzyme immunoassay for the determination of 'total' activin-A concentrations in serum and follicular fluid. *J Endocrinol,* 148**,** 267-79.

KOHNO, S., MUNOZ, J. A., WILLIAMS, T. M., TEUSCHER, C., BERNARD, C. C. & TUNG, K. S. 1983. Immunopathology of murine experimental allergic orchitis. *J Immunol,* 130**,** 2675-82.

KOOPMAN, P., MUNSTERBERG, A., CAPEL, B., VIVIAN, N. & LOVELL-BADGE, R. 1990. Expression of a candidate sex-determining gene during mouse testis differentiation. *Nature,* 348**,** 450-2.

LE BRAS, G. F., LOOMANS, H. A., TAYLOR, C. J., REVETTA, F. L. & ANDL, C. D. 2014. Activin A balance regulates epithelial invasiveness and tumorigenesis. *Lab Invest,* 94**,** 1134-46.

LEBRUN, J. J. & VALE, W. W. 1997. Activin and inhibin have antagonistic effects on ligand-dependent heteromerization of the type I and type II activin receptors and human erythroid differentiation. *Mol Cell Biol,* 17**,** 1682-91.

LERCH, T. F., SHIMASAKI, S., WOODRUFF, T. K. & JARDETZKY, T. S. 2007. Structural and biophysical coupling of heparin and activin binding to follistatin isoform functions. *J Biol Chem,* 282**,** 15930-9.

LETO, G., INCORVAIA, L., BADALAMENTI, G., TUMMINELLO, F. M., GEBBIA, N., FLANDINA, C., CRESCIMANNO, M. & RINI, G. 2006. Activin A circulating levels in patients with bone metastasis from breast or prostate cancer. *Clin Exp Metastasis,* 23**,** 117-22.

LEWIS, K. A., GRAY, P. C., BLOUNT, A. L., MACCONELL, L. A., WIATER, E., BILEZIKJIAN, L. M. & VALE, W. 2000. Betaglycan binds inhibin and can mediate functional antagonism of activin signalling. *Nature,* 404**,** 411-4.

LI, N., LIU, Z., ZHANG, Y., CHEN, Q., LIU, P., CHENG, C. Y., LEE, W. M., CHEN, Y. & HAN, D. 2015. Mice lacking Axl and Mer tyrosine kinase receptors are susceptible to experimental autoimmune orchitis induction. *Immunol Cell Biol,* 93**,** 311-20.

LING, N., YING, S. Y., UENO, N., SHIMASAKI, S., ESCH, F., HOTTA, M. & GUILLEMIN, R. 1986. Pituitary FSH is released by a heterodimer of the beta-subunits from the two forms of inhibin. *Nature,* 321**,** 779-82.

LINTHICUM, D. S., MUNOZ, J. J. & BLASKETT, A. 1982. Acute experimental autoimmune encephalomyelitis in mice. I. Adjuvant action of Bordetella pertussis is due to vasoactive amine sensitization and increased vascular permeability of the central nervous system. *Cell Immunol,* 73**,** 299-310.

LIVAK, K. J. & SCHMITTGEN, T. D. 2001. Analysis of relative gene expression data using real-time quantitative PCR and the 2(-Delta Delta C(T)) Method. *Methods,* 25**,** 402-8.

LOGAN, T. T., VILLAPOL, S. & SYMES, A. J. 2013. TGF-beta superfamily gene expression and induction of the Runx1 transcription factor in adult neurogenic regions after brain injury. *PLoS One,* 8**,** e59250.

LUDLOW, H., PHILLIPS, D. J., MYERS, M., MCLACHLAN, R. I., DE KRETSER, D. M., ALLAN, C. A., ANDERSON, R. A., GROOME, N. P., HYVONEN, M., DUNCAN, W. C. & MUTTUKRISHNA, S. 2009. A new 'total' activin B enzyme-linked immunosorbent assay (ELISA): development and validation for human samples. *Clin Endocrinol (Oxf),* 71**,** 867-73.

LYON, K. R., BOSSEBOEUF, E. & VOGL, A. W. 2015. An Alternative Model of Tubulobulbar Complex Internalization During Junction Remodeling in the Seminiferous Epithelium of the Rat Testis. *Biol Reprod,* 93**,** 12.

MAHI-BROWN, C. A., YULE, T. D. & TUNG, K. S. 1987. Adoptive transfer of murine autoimmune orchitis to naive recipients with immune lymphocytes. *Cell Immunol,* 106**,** 408-19.

MARTINEZ, F. O. & GORDON, S. 2014. The M1 and M2 paradigm of macrophage activation: time for reassessment. *F1000Prime Rep,* 6**,** 13.

MATHER, J. P., MOORE, A. & LI, R. H. 1997. Activins, inhibins, and follistatins: further thoughts on a growing family of regulators. *Proc Soc Exp Biol Med,* 215**,** 209-22.

MAYERHOFER, A. 2013. Human testicular peritubular cells: more than meets the eye. *Reproduction,* 145**,** R107-16.

MCCABE, M. J., ALLAN, C. M., FOO, C. F., NICHOLLS, P. K., MCTAVISH, K. J. & STANTON, P. G. 2012. Androgen initiates Sertoli cell tight junction formation in the hypogonadal (hpg) mouse. *Biol Reprod,* 87**,** 38.

MCGAHON, A., BISSONNETTE, R., SCHMITT, M., COTTER, K. M., GREEN, D. R. & COTTER, T. G. 1994. BCR-ABL maintains resistance of chronic myelogenous leukemia cells to apoptotic cell death. *Blood,* 83**,** 1179-87.

MEINHARDT, A. & HEDGER, M. P. 2011. Immunological, paracrine and endocrine aspects of testicular immune privilege. *Mol Cell Endocrinol,* 335**,** 60-8.

MEINHARDT, A., O'BRYAN, M. K., MCFARLANE, J. R., LOVELAND, K. L., MALLIDIS, C., FOULDS, L. M., PHILLIPS, D. J. & DE KRETSER, D. M. 1998. Localization of follistatin in the rat testis. *J Reprod Fertil,* 112**,** 233-41.

MENDIS, S. H., MEACHEM, S. J., SARRAJ, M. A. & LOVELAND, K. L. 2011. Activin A balances Sertoli and germ cell proliferation in the fetal mouse testis. *Biol Reprod,* 84**,** 379-91.

MENG, J., HOLDCRAFT, R. W., SHIMA, J. E., GRISWOLD, M. D. & BRAUN, R. E. 2005. Androgens regulate the permeability of the blood-testis barrier. *Proc Natl Acad Sci U S A,* 102**,** 16696-700.

MENIRU, G. 2001. *Cambridge guide to infertility management and assisted reproduction*, Cambridge University Press.

MICHEL, U., GERBER, J., A, E. O. C., BUNKOWSKI, S., BRUCK, W., NAU, R. & PHILLIPS, D. J. 2003. Increased activin levels in cerebrospinal fluid of rabbits with bacterial meningitis are associated with activation of microglia. *J Neurochem,* 86**,** 238-45.

MICHEL, V., DUAN, Y., STOSCHEK, E., BHUSHAN, S., MIDDENDORFF, R., YOUNG, J. M., LOVELAND, K. A., KRETSER, D. M., HEDGER, M. P. & MEINHARDT, A. 2016. Uropathogenic Escherichia coli cause fibrotic remodelling of the epididymis. *J Pathol.*

MIESCHER, G. C., SCHREYER, M. & MACDONALD, H. R. 1989. Production and characterization of a rat monoclonal antibody against the murine CD3 molecular complex. *Immunol Lett,* 23**,** 113-8.

MITHRAPRABHU, S., MENDIS, S., MEACHEM, S. J., TUBINO, L., MATZUK, M. M., BROWN, C. W. & LOVELAND, K. L. 2010. Activin bioactivity affects germ cell differentiation in the postnatal mouse testis in vivo. *Biol Reprod,* 82**,** 980-90.

MORAIS DA SILVA, S., HACKER, A., HARLEY, V., GOODFELLOW, P., SWAIN, A. & LOVELL-BADGE, R. 1996. Sox9 expression during gonadal development implies a conserved role for the gene in testis differentiation in mammals and birds. *Nat Genet,* 14**,** 62-8.

MORSE, J. H., KONG, A. S., LINDENBAUM, J. & MORSE, S. I. 1977. The mitogenic effect of the lymphocytosis promoting factor from Bordetella pertussis on human lymphocytes. *J Clin Invest,* 60**,** 683-92.

MUKASA, A., HIROMATSU, K., MATSUZAKI, G., O'BRIEN, R., BORN, W. & NOMOTO, K. 1995. Bacterial infection of the testis leading to autoaggressive immunity triggers apparently opposed responses of alpha beta and gamma delta T cells. *J Immunol,* 155**,** 2047-56.

MUNOZ, J. J., ARAI, H., BERGMAN, R. K. & SADOWSKI, P. L. 1981. Biological activities of crystalline pertussigen from Bordetella pertussis. *Infect Immun,* 33**,** 820-6.

MUSHA, M., HIRAI, S., NAITO, M., TERAYAMA, H., QU, N., HATAYAMA, N. & ITOH, M. 2013. The effects of adjuvants on autoimmune responses against testicular antigens in mice. *J Reprod Dev,* 59**,** 139-44.

MYLLARNIEMI, M., TIKKANEN, J., HULMI, J. J., PASTERNACK, A., SUTINEN, E., RONTY, M., LEPPARANTA, O., MA, H., RITVOS, O. & KOLI, K. 2014. Upregulation of activin-B and follistatin in pulmonary fibrosis - a translational study using human biopsies and a specific inhibitor in mouse fibrosis models. *BMC Pulm Med,* 14**,** 170.

NAITO, M., HIRAI, S., TERAYAMA, H., QU, N., KUERBAN, M., MUSHA, M., KITAOKA, M., OGAWA, Y. & ITOH, M. 2012. Postinflammation stage of autoimmune orchitis induced by immunization with syngeneic testicular germ cells alone in mice. *Med Mol Morphol,* 45**,** 35-44.

NAKAMURA, T., ASASHIMA, M., ETO, Y., TAKIO, K., UCHIYAMA, H., MORIYA, N., ARIIZUMI, T., YASHIRO, T., SUGINO, K., TITANI, K. & ET AL. 1992. Isolation and characterization of native activin B. *J Biol Chem,* 267**,** 16385-9.

NAKAMURA, T., TAKIO, K., ETO, Y., SHIBAI, H., TITANI, K. & SUGINO, H. 1990. Activin-binding protein from rat ovary is follistatin. *Science,* 247**,** 836-8.

NASCIMBENI, M., POL, S. & SAUNIER, B. 2011. Distinct CD4+ CD8+ double-positive T cells in the blood and liver of patients during chronic hepatitis B and C. *PLoS One,* 6**,** e20145.

NASR, I. W., WANG, Y., GAO, G., DENG, S., DIGGS, L., ROTHSTEIN, D. M., TELLIDES, G., LAKKIS, F. G. & DAI, Z. 2005. Testicular immune privilege promotes transplantation tolerance by altering the balance between memory and regulatory T cells. *J Immunol,* 174**,** 6161-8.

NIAKANI, A., FARROKHI, F. & HASANZADEH, S. 2013. Decapeptyl ameliorates cyclophosphamide-induced reproductive toxicity in male Balb/C mice: histomorphometric, stereologic and hormonal evidences. *Iran J Reprod Med,* 11**,** 791-800.

NICHOLLS, P. K., STANTON, P. G., CHEN, J. L., OLCORN, J. S., HAVERFIELD, J. T., QIAN, H., WALTON, K. L., GREGOREVIC, P. & HARRISON, C. A. 2012. Activin signaling regulates Sertoli cell differentiation and function. *Endocrinology,* 153**,** 6065-77.

NIEMI, M., SHARPE, R. M. & BROWN, W. R. 1986. Macrophages in the interstitial tissue of the rat testis. *Cell Tissue Res,* 243**,** 337-44.

O'BRIEN, D. A., GABEL, C. A., ROCKETT, D. L. & EDDY, E. M. 1989. Receptor-mediated endocytosis and differential synthesis of mannose 6-phosphate receptors in isolated spermatogenic and sertoli cells. *Endocrinology,* 125**,** 2973-84.

O'CONNOR, A. E., MCFARLANE, J. R., HAYWARD, S., YOHKAICHIYA, T., GROOME, N. P. & DE KRETSER, D. M. 1999. Serum activin A and follistatin concentrations during human pregnancy: a cross-sectional and longitudinal study. *Hum Reprod,* 14**,** 827-32.

OAKBERG, E. F. 1956. Duration of spermatogenesis in the mouse and timing of stages of the cycle of the seminiferous epithelium. *Am J Anat,* 99**,** 507-16.

OKUMA, Y., O'CONNOR, A. E., HAYASHI, T., LOVELAND, K. L., DE KRETSER, D. M. & HEDGER, M. P. 2006. Regulated production of activin A and inhibin B throughout the cycle of the seminiferous epithelium in the rat. *J Endocrinol,* 190**,** 331-40.

OKUMA, Y., O'CONNOR, A. E., MUIR, J. A., STANTON, P. G., DE KRETSER, D. M. & HEDGER, M. P. 2005. Regulation of activin A and inhibin B secretion by inflammatory mediators in adult rat Sertoli cell cultures. *J Endocrinol,* 187**,** 125-34.

ORTH, J. M. 1982. Proliferation of Sertoli cells in fetal and postnatal rats: a quantitative autoradiographic study. *Anat Rec,* 203**,** 485-92.

OVERGAARD, N. H., JUNG, J. W., STEPTOE, R. J. & WELLS, J. W. 2015. CD4+/CD8+ double-positive T cells: more than just a developmental stage? *J Leukoc Biol,* 97**,** 31-8.

PARADOWSKA-GORYCKA, A., PAWLIK, A., ROMANOWSKA-PROCHNICKA, K., HALADYJ, E., MALINOWSKI, D., STYPINSKA, B., MANCZAK, M. & OLESINSKA, M. 2016. Relationship between VEGF Gene Polymorphisms and Serum VEGF Protein Levels in Patients with Rheumatoid Arthritis. *PLoS One,* 11**,** e0160769.

PAREL, Y., AURRAND-LIONS, M., SCHEJA, A., DAYER, J. M., ROOSNEK, E. & CHIZZOLINI, C. 2007. Presence of CD4+CD8+ double-positive T cells with very high interleukin-4 production potential in lesional skin of patients with systemic sclerosis. *Arthritis Rheum,* 56**,** 3459-67.

PAREL, Y. & CHIZZOLINI, C. 2004. CD4+ CD8+ double positive (DP) T cells in health and disease. *Autoimmun Rev,* 3**,** 215-20.

PARTON, R. 1985. Effect of prednisolone on the toxicity of Bordetella pertussis for mice. *J Med Microbiol,* 19**,** 391-400.

PATELLA, S., PHILLIPS, D. J., TCHONGUE, J., DE KRETSER, D. M. & SIEVERT, W. 2006. Follistatin attenuates early liver fibrosis: effects on hepatic stellate cell activation and hepatocyte apoptosis. *Am J Physiol Gastrointest Liver Physiol,* 290**,** G137-44.

PEREZ, C. V., SOBARZO, C. M., JACOBO, P. V., PELLIZZARI, E. H., CIGORRAGA, S. B., DENDUCHIS, B. & LUSTIG, L. 2012. Loss of occludin expression and impairment of blood-testis barrier permeability in rats with autoimmune orchitis: effect of interleukin 6 on Sertoli cell tight junctions. *Biol Reprod,* 87**,** 122.

PHILLIPS, D. J., DE KRETSER, D. M. & HEDGER, M. P. 2009. Activin and related proteins in inflammation: not just interested bystanders. *Cytokine Growth Factor Rev,* 20**,** 153-64.

PRINZ-HADAD, H., MIZRACHI, T., IRONY-TUR-SINAI, M., PRIGOZHINA, T. B., ARONIN, A., BRENNER, T. & DRANITZKI-ELHALEL, M. 2013. Amelioration of autoimmune neuroinflammation by the fusion molecule Fn14.TRAIL. *J Neuroinflammation,* 10**,** 36.

PROCACCINI, C., SANTOPAOLO, M., FAICCHIA, D., COLAMATTEO, A., FORMISANO, L., DE CANDIA, P., GALGANI, M., DE ROSA, V. & MATARESE,

G. 2016. Role of metabolism in neurodegenerative disorders. *Metabolism,* 65**,** 1376-90.

PUENTES, F., DICKHAUT, K., HOFSTATTER, M., FALK, K. & ROTZSCHKE, O. 2013. Active suppression induced by repetitive self-epitopes protects against EAE development. *PLoS One,* 8**,** e64888.

QUANDT, D., ROTHE, K., SCHOLZ, R., BAERWALD, C. W. & WAGNER, U. 2014. Peripheral CD4CD8 double positive T cells with a distinct helper cytokine profile are increased in rheumatoid arthritis. *PLoS One,* 9**,** e93293.

RAMHORST, R. E., GIRIBALDI, L., FRACCAROLI, L., TOSCANO, M. A., STUPIRSKI, J. C., ROMERO, M. D., DURAND, E. S., RUBINSTEIN, N., BLASCHITZ, A., SEDLMAYR, P., GENTI-RAIMONDI, S., FAINBOIM, L. & RABINOVICH, G. A. 2012. Galectin-1 confers immune privilege to human trophoblast: implications in recurrent fetal loss. *Glycobiology,* 22**,** 1374-86.

REBOURCET, D., O'SHAUGHNESSY, P. J., MONTEIRO, A., MILNE, L., CRUICKSHANKS, L., JEFFREY, N., GUILLOU, F., FREEMAN, T. C., MITCHELL, R. T. & SMITH, L. B. 2014. Sertoli cells maintain Leydig cell number and peritubular myoid cell activity in the adult mouse testis. *PLoS One,* 9**,** e105687.

RIVAL, C., GUAZZONE, V. A., VON WULFFEN, W., HACKSTEIN, H., SCHNEIDER, E., LUSTIG, L., MEINHARDT, A. & FIJAK, M. 2007. Expression of co-stimulatory molecules, chemokine receptors and proinflammatory cytokines in dendritic cells from normal and chronically inflamed rat testis. *Mol Hum Reprod,* 13**,** 853-61.

RIVAL, C., LUSTIG, L., IOSUB, R., GUAZZONE, V. A., SCHNEIDER, E., MEINHARDT, A. & FIJAK, M. 2006a. Identification of a dendritic cell population in normal testis and in chronically inflamed testis of rats with autoimmune orchitis. *Cell Tissue Res,* 324**,** 311-8.

RIVAL, C., THEAS, M. S., GUAZZONE, V. A. & LUSTIG, L. 2006b. Interleukin-6 and IL-6 receptor cell expression in testis of rats with autoimmune orchitis. *J Reprod Immunol,* 70**,** 43-58.

RIVAL, C., THEAS, M. S., SUESCUN, M. O., JACOBO, P., GUAZZONE, V., VAN ROOIJEN, N. & LUSTIG, L. 2008. Functional and phenotypic characteristics of testicular macrophages in experimental autoimmune orchitis. *J Pathol,* 215**,** 108-17.

ROBERTSON, D. M., HAYWARD, S., IRBY, D., JACOBSEN, J., CLARKE, L., MCLACHLAN, R. I. & DE KRETSER, D. M. 1988. Radioimmunoassay of rat serum inhibin: changes after PMSG stimulation and gonadectomy. *Mol Cell Endocrinol,* 58**,** 1-8.

RODINO-KLAPAC, L. R., HAIDET, A. M., KOTA, J., HANDY, C., KASPAR, B. K. & MENDELL, J. R. 2009. Inhibition of myostatin with emphasis on follistatin as a therapy for muscle disease. *Muscle Nerve,* 39**,** 283-96.

ROMANI, L. 2004. Immunity to fungal infections. *Nat Rev Immunol,* 4**,** 1-23.

ROWE, P., COMHAIRE, F., HARGREAVE, T. & MAHMOUD, A. 2000. *WHO Manual for the Standardized Investigation and Diagnosis of the Infertile Male,* Cambridge, UK, Cambridge University Press.

SAKAGUCHI, S., MIYARA, M., COSTANTINO, C. M. & HAFLER, D. A. 2010. FOXP3+ regulatory T cells in the human immune system. *Nat Rev Immunol,* 10**,** 490-500.

SCHMITZ, G. G., WALTER, T., SEIBL, R. & KESSLER, C. 1991. Nonradioactive labeling of oligonucleotides in vitro with the hapten digoxigenin by tailing with terminal transferase. *Anal Biochem,* 192**,** 222-31.

SCHUPPE, H. C. & BERGMANN, M. 2013. *Inflammatory conditions of the testis. In: Atlas of the human testis.,* London, Springer.

SCHUPPE, H. C. & MEINHARDT, A. 2005. Immune privilege and inflammation of the testis. *Chem Immunol Allergy,* 88**,** 1-14.

SCHUPPE, H. C., MEINHARDT, A., ALLAM, J. P., BERGMANN, M., WEIDNER, W. & HAIDL, G. 2008. Chronic orchitis: a neglected cause of male infertility? *Andrologia,* 40**,** 84-91.

SEPULVEDA, P. V., LAMON, S., HAGG, A., THOMSON, R. E., WINBANKS, C. E., QIAN, H., BRUCE, C. R., RUSSELL, A. P. & GREGOREVIC, P. 2015. Evaluation of follistatin as a therapeutic in models of skeletal muscle atrophy associated with denervation and tenotomy. *Sci Rep,* 5**,** 17535.

SHIMASAKI, S., KOGA, M., ESCH, F., COOKSEY, K., MERCADO, M., KOBA, A., UENO, N., YING, S. Y., LING, N. & GUILLEMIN, R. 1988. Primary structure of the human follistatin precursor and its genomic organization. *Proc Natl Acad Sci U S A,* 85**,** 4218-22.

SIDEY, F. M., FURMAN, B. L. & WARDLAW, A. C. 1989. Effect of hyperreactivity to endotoxin on the toxicity of pertussis vaccine and pertussis toxin in mice. *Vaccine,* 7**,** 237-41.

SMITH, L. B., O'SHAUGHNESSY, P. J. & REBOURCET, D. 2015. Cell-specific ablation in the testis: what have we learned? *Andrology,* 3**,** 1035-49.

SMITH, T. D., TSE, M. J., READ, E. L. & LIU, W. F. 2016. Regulation of macrophage polarization and plasticity by complex activation signals. *Integr Biol (Camb)*.

SOLER PALACIOS, B., ESTRADA-CAPETILLO, L., IZQUIERDO, E., CRIADO, G., NIETO, C., MUNICIO, C., GONZALEZ-ALVARO, I., SANCHEZ-MATEOS, P., PABLOS, J. L., CORBI, A. L. & PUIG-KROGER, A. 2015. Macrophages from the synovium of active rheumatoid arthritis exhibit an activin A-dependent pro-inflammatory profile. *J Pathol,* 235**,** 515-26.

SOLOMOS, A. C. & RALL, G. F. 2016. Get It through Your Thick Head: Emerging Principles in Neuroimmunology and Neurovirology Redefine Central Nervous System "Immune Privilege". *ACS Chem Neurosci,* 7**,** 435-41.

STUVE, O., MARRA, C. M., BAR-OR, A., NIINO, M., CRAVENS, P. D., CEPOK, S., FROHMAN, E. M., PHILLIPS, J. T., ARENDT, G., JEROME, K. R., COOK, L., GRAND'MAISON, F., HEMMER, B., MONSON, N. L. & RACKE, M. K. 2006. Altered CD4+/CD8+ T-cell ratios in cerebrospinal fluid of natalizumab-treated patients with multiple sclerosis. *Arch Neurol,* 63**,** 1383-7.

SUESCUN, M. O., CALANDRA, R. S. & LUSTIG, L. 1994. Alterations of testicular function after induced autoimmune orchitis in rats. *J Androl,* 15**,** 442-8.

SUESCUN, M. O., RIVAL, C., THEAS, M. S., CALANDRA, R. S. & LUSTIG, L. 2003. Involvement of tumor necrosis factor-alpha in the pathogenesis of autoimmune orchitis in rats. *Biol Reprod,* 68**,** 2114-21.

SUESCUN, M. O., SUESCUN, M. O., LUSTIG, L., CALANDRA, R. S., CALANDRA, R. S., GROOME, N. P. & CAMPO, S. 2001. Correlation between inhibin secretion

and damage of seminiferous tubules in a model of experimental autoimmune orchitis. *J Endocrinol,* 170**,** 113-20.

TAKADA, Y. & AGGARWAL, B. B. 2004. TNF activates Syk protein tyrosine kinase leading to TNF-induced MAPK activation, NF-kappaB activation, and apoptosis. *J Immunol,* 173**,** 1066-77.

TANIMOTO, Y., TANIMOTO, K., SUGIYAMA, F., HORIGUCHI, H., MURAKAMI, K., YAGAMI, K. & FUKAMIZU, A. 1999. Male sterility in transgenic mice expressing activin betaA subunit gene in testis. *Biochem Biophys Res Commun,* 259**,** 699-705.

TERAYAMA, H., NAITO, M., QU, N., HIRAI, S., KITAOKA, M., OGAWA, Y. & ITOH, M. 2011. Intratesticular expression of mRNAs of both interferon gamma and tumor necrosis factor alpha is significantly increased in experimental autoimmune orchitis in mice. *J Reprod Dev,* 57**,** 296-302.

TEUSCHER, C., SMITH, S. M., GOLDBERG, E. H., SHEARER, G. M. & TUNG, K. S. 1985. Experimental allergic orchitis in mice. I. Genetic control of susceptibility and resistance to induction of autoimmune orchitis. *Immunogenetics,* 22, 323-33.

TOKUNAGA, Y., HIRAMINE, C. & HOJO, K. 1993. Genetic susceptibility to the induction of murine experimental autoimmune orchitis (EAO) without adjuvant. II. Analysis on susceptibility to EAO induction using F1 hybrid mice and adoptive transfer system. *Clin Immunol Immunopathol,* 66**,** 248-53.

TOMPKINS, A. B., HUTCHINSON, P., DE KRETSER, D. M. & HEDGER, M. P. 1998. Characterization of lymphocytes in the adult rat testis by flow cytometry: effects of activin and transforming growth factor beta on lymphocyte subsets in vitro. *Biol Reprod,* 58**,** 943-51.

TUNG, K. S. & TEUSCHER, C. 1995. Mechanisms of autoimmune disease in the testis and ovary. *Hum Reprod Update,* 1**,** 35-50.

TUNG, K. S., YULE, T. D., MAHI-BROWN, C. A. & LISTROM, M. B. 1987. Distribution of histopathology and Ia positive cells in actively induced and passively transferred experimental autoimmune orchitis. *J Immunol,* 138**,** 752-9.

VALE, W., RIVIER, J., VAUGHAN, J., MCCLINTOCK, R., CORRIGAN, A., WOO, W., KARR, D. & SPIESS, J. 1986. Purification and characterization of an FSH releasing protein from porcine ovarian follicular fluid. *Nature,* 321**,** 776-9.

WADA, M., SHINTANI, Y., KOSAKA, M., SANO, T., HIZAWA, K. & SAITO, S. 1996. Immunohistochemical localization of activin A and follistatin in human tissues. *Endocr J,* 43**,** 375-85.

WANG, S. Y., TAI, G. X., ZHANG, P. Y., MU, D. P., ZHANG, X. J. & LIU, Z. H. 2008. Inhibitory effect of activin A on activation of lipopolysaccharide-stimulated mouse macrophage RAW264.7 cells. *Cytokine,* 42**,** 85-91.

WERNERSSON, S. & PEJLER, G. 2014. Mast cell secretory granules: armed for battle. *Nat Rev Immunol,* 14**,** 478-94.

WIJAYARATHNA, R. & DE KRETSER, D. M. 2016. Activins in reproductive biology and beyond. *Hum Reprod Update*.

WILGUS, T. A. & WULFF, B. C. 2014. The Importance of Mast Cells in Dermal Scarring. *Adv Wound Care (New Rochelle),* 3**,** 356-365.

WINBANKS, C. E., WEEKS, K. L., THOMSON, R. E., SEPULVEDA, P. V., BEYER, C., QIAN, H., CHEN, J. L., ALLEN, J. M., LANCASTER, G. I., FEBBRAIO, M. A.,

HARRISON, C. A., MCMULLEN, J. R., CHAMBERLAIN, J. S. & GREGOREVIC, P. 2012. Follistatin-mediated skeletal muscle hypertrophy is regulated by Smad3 and mTOR independently of myostatin. *J Cell Biol,* 197**,** 997-1008.

WINNALL, W. R., WU, H., SARRAJ, M. A., ROGERS, P. A., DE KRETSER, D. M., GIRLING, J. E. & HEDGER, M. P. 2013. Expression patterns of activin, inhibin and follistatin variants in the adult male mouse reproductive tract suggest important roles in the epididymis and vas deferens. *Reprod Fertil Dev,* 25**,** 570-80.

WU, J., LONG, Z., CAI, H., DU, C., LIU, X., YU, S. & WANG, Y. 2016. High expression of WISP1 in colon cancer is associated with apoptosis, invasion and poor prognosis. *Oncotarget.*

XING, Y. & HOGQUIST, K. A. 2012. T-cell tolerance: central and peripheral. *Cold Spring Harb Perspect Biol,* 4.

YADEN, B. C., CROY, J. E., WANG, Y., WILSON, J. M., DATTA-MANNAN, A., SHETLER, P., MILNER, A., BRYANT, H. U., ANDREWS, J., DAI, G. & KRISHNAN, V. 2014. Follistatin: a novel therapeutic for the improvement of muscle regeneration. *J Pharmacol Exp Ther,* 349**,** 355-71.

YANAGIMACHI, R. 1994. Fertility of mammalian spermatozoa: its development and relativity. *Zygote,* 2**,** 371-2.

YANG, Y., ZHANG, N., CROMBRUGGEN, K. V., LAN, F., HU, G., HONG, S. & BACHERT, C. 2015. Differential Expression and Release of Activin A and Follistatin in Chronic Rhinosinusitis with and without Nasal Polyps. *PLoS One,* 10**,** e0128564.

YOUNG, J. C., WAKITANI, S. & LOVELAND, K. L. 2015. TGF-beta superfamily signaling in testis formation and early male germline development. *Semin Cell Dev Biol,* 45**,** 94-103.

YULE, T. D., MONTOYA, G. D., RUSSELL, L. D., WILLIAMS, T. M. & TUNG, K. S. 1988. Autoantigenic germ cells exist outside the blood testis barrier. *J Immunol,* 141**,** 1161-7.

ZEYSE, D., LUNENFELD, E., BECK, M., PRINSLOO, I. & HULEIHEL, M. 2000. Induction of interleukin-1alpha production in murine Sertoli cells by interleukin-1. *Biol Reprod,* 62**,** 1291-6.

ZHANG, Y. Q., RESTA, S., JUNG, B., BARRETT, K. E. & SARVETNICK, N. 2009. Upregulation of activin signaling in experimental colitis. *Am J Physiol Gastrointest Liver Physiol,* 297**,** G768-80.

ZHAO, Y. T., QI, Y. W., HU, C. Y., CHEN, S. H. & LIU, Y. 2016. Advanced glycation end products inhibit testosterone secretion by rat Leydig cells by inducing oxidative stress and endoplasmic reticulum stress. *Int J Mol Med,* 38**,** 659-65.

http://www.majordifferences.com/2013/06/difference-between-spermatogenesis-and.html#.V7G8Xfl97IU

9. ACKNOWLEDGEMENTS

The experimental work for this dissertation was performed at the Institute of Anatomy and Cell Biology at the Justus Liebig University Giessen, Germany, under the direction of Prof. Dr. Andreas Meinhardt to whom I am very thankful; and in the Centre of Reproductive Health in the Hudson Institute of Medical Research at Monash University, Melbourne, Australia, under the supervision of A. Prof. Mark Hedger.

First and foremost, I would like to thank my supervisor Dr. Monika Fijak for giving me the chance to work on her project, providing me with both scientific and technical guidance, for patiently correcting my writing and financially supporting my research. I would like to express my deepest gratitude for your enormous support, caring, patience and trust that you provided me in order to grow as a researcher.

I would equally like to extend my gratitude to my co-supervisor A. Prof. Mark Hedger for having me in my host lab in Australia. Thank you for you excellent scientific support and advice, for your kindness and guidance.

I also appreciate the scientific discussions and input from Prof. Kate Loveland, Prof. David de Kretser and Dr. Sudhanshu Bhushan.

I am also grateful for the assistance, help and support from Dr. Vera Michel, Dr. Jörg Klug, Dr. Florian Eisel, Dr. Magdalena Walecki, Ewa Wahle, Tao Lei, Christine Kleinert, Rukmali Wijayarathna, Ming Wang, Tim Sebastian, Miguel Keidel, Julia Kautz, Zhengguo Zhang, Pawel Szczesniak, Farhad Khosravi, Vera Stadler, Pradeep Kudipudi, Susan Hayward, Rosemary Genovese, Rajini Sreenivasan, Adnan Sali, Dr. Justin Chen, Prof. Perter Stanton, Dr. Sarah Meachem and Prof. Ralf Middendorff.

I extend my warmest wishes to my dear friends Dr. Ferial Aslani, Britta Klein and Elke Stoschek for their kindness, generosity and unconditional support. Moreover, special thanks go to Suada Fröhlich for always brining a smile and joy to the lab, to Julie Muir for being such a beautiful person and for your enormous technical support; and to Pia Jürgens for her substantial administrative help and unlimited support.

Lastly, I cannot express the gratitude and love I have for my wonderful parents, brother and family and friends who have always supported me and been by my side. I cannot have done this without you.

10. OWN PUBLICATIONS

a) Publications originally from this thesis
- N. Nicolas, V. Michel, S. Bhushan, E. Wahle, S. Hayward, H. Ludlow, D.M. de Kretser, K.L. Loveland, H-C. Schuppe, A. Meinhardt, M.P. Hedger and M. Fijak. Testicular activin and follistatin levels are elevated during the course of experimental autoimmune epididymo–orchitis in mice. *Scientific reports,* 2017 Feb 13;7:42391.
- N. Nicolas, D.M. de Kretser, K.L. Loveland, S. Bhushan, A. Meinhardt, M.Fijak and M.P. Hedger. Induction of experimental autoimmune epididymo–orchitis in mice with elevated levels of follistatin. *Repdroduction*. (**Under revision**).

b) Other publications
- M. Fijak, A. Pilatz, M.P. Hedger, N. Nicolas. S. Bhushan, V. Michel, K.S. Tung, A. Meinhardt. Infectious, inflammatory and „autoimmune" male factor infertility: how do animal models inform clinical practice? *HRU.* (**Under revision**).
- N. Synhaeve, S. Musilli, J. Stefani, N. Nicolas, O. Delissen, I. Dublineau and J-M. Bertho. Immune System Modifications Induced in a Mouse Model of Chronic Exposure to (90)Sr. *Radiat Res.* 2016 Mar;185(3):267-84.
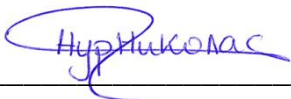
c) Conference abstracts
- **9th International Giessen Graduate Centre for the Life Sciences (GGL) Conference** (20-21 September 2016) Giessen, Germany. Induction of experimental autoimmune epididymo–orchitis in mice with elevated levels of follistatin. [Oral presentation]
- **19th European Testis Workshop** (11-15 June 2016) Saint Malo, France. Involvement of activin A and follistatin in the inflammatory response of autoimmune orchitis in mice. [Oral presentation].
- **Victorian Infection and Immunity Network Conference** (17-19 February 2016) Lorne, Australia. Testicular activin A and its binding protein, follistatin are increased during experimental autoimmune epididymo-orchitis in mice. [Poster presentation].
- **Melbourne's Men's Health Symposium** (28 November 2015) Clayton, Australia. Testicular activin A during the development of autoimmune orchitis in mice. [Poster presentation].
- **Annual Scientific Meeting of the Endocrine Society of Australia (ESA) and the Society of Reproductive Biology (SRB)** (23-26 August 2015) Adelaide, Australia. Testicular activin A during the development of autoimmune orchitis in mice. [Poster presentation].
- **26th Annual Meeting of the German Society of Andrology (DGA) (18-20 September 2014) Giessen, Germany.** Role of activin and follistatin in chronic testicular inflammation in mice. [Poster presentation].
- **7th GGL Conference** (17-18 September 2014) Giessen, Germany. Role of activin and follistatin in chronic testicular inflammation in mice. [Poster presentation].
- **18th European Testis Workshop** (13-17 May 2014) Helsingor, Denmark. Role of activin and follistatin in chronic testicular inflammation in mice. [Oral presentation].

11. EHRENWÖRTLICHE ERKLÄRUNG

Ich erkläre: Ich habe die vorgelegte Dissertation selbständig und ohne unerlaubte fremde Hilfe und nur mit den Hilfen angefertigt, die ich in der Dissertation angegeben habe. Alle Textstellen, die wörtlich oder sinngemäß aus veröffentlichten oder nicht veröffentlichten Schriften entnommen sind, und alle Angaben, die auf mündlichen Auskünften beruhen, sind als solche kenntlich gemacht. Bei den von mir durchgeführten und in der Dissertation erwähnten Untersuchungen habe ich die Grundsätze guter wissenschaftlicher Praxis, wie sie in der „Satzung der Justus-Liebig-Universität Giessen zur Sicherung guter wissenschaftlicher Praxis" niedergelegt sind, eingehalten.

I declare that I have completed this dissertation single-handedly without the unauthorized help of a second party and only with the assistance acknowledged therein. I have appropriately acknowledged and referenced all text passages that are derived literally from or are based on the content of published or unpublished work of others, and all information that relates to verbal communications. I have abided by the principles of good scientific conduct laid down in the charter of the Justus Liebig University of Giessen in carrying out the investigations described in the dissertation.

Giessen, den

_____

Nour Nicolas